A Comparison of Drought Indices in CMIP6 Climate Projections

Master Thesis of

Lukas Ruhe

2725124

University of Bremen
Institute of Environmental Physics
Department of Climate Modelling

February 28, 2022

Supervised by:

Prof. Dr Veronika Eyring
University of Bremen, Climate Modelling

Prof. Dr Gerrit Lohmann
Alfred Wegner Institute, Paleoclimate Dynamics

Abstract

Droughts are harmful for humans for example through their impact on agriculture and freshwater resources. Monitoring and projecting of these natural hazards is realized using different drought indices dependent on which drought type is addressed. In this thesis four drought indices are compared in their abilities to identify the changes of droughts in a changing climate. The standard precipitation index (SPI) is based on precipitation only, the Standardized Precipitation Evapotranspiration Index (SPEI) as well as the Palmer Drought Severity Index (PDSI) and the scaled PDSI (SC-PDSI) are indices that include the Potential Evapotranspiration (PET) and are therefore influenced by the thermodynamic state of the atmosphere. For these analyses all four indices are calculated based on variables from seven Earth System Models (ESM), which are part of the Coupled Model Intercomparison Project Phase 6 (CMIP6) for a historical simulation (1900-2014) and two future scenarios (2014-2100). The changes of detected droughts are analysed based on trends of the four drought indices as well as the frequency, duration, and mean index of moderate and extreme droughts. SPEI and SC-PDSI, which are spatially comparable on a global scale, have been chosen for a closer comparison of the two future scenarios based on two Shared Socioeconomic Pathways, SSP2-4.5 and SSP5-8.5, with different forcing level. Compared to the other indices, SPI shows more regions with an increasing trend, i.e. fewer droughts and smaller absolute trends where they are decreasing. This indicates an underestimation of the change of droughts, because thermodynamic processes are not considered for SPI. PDSI and SC-PDSI show a high temporal correlation for most regions when applied to the same data set. It is known that a global applicability of the PDSI is limited, therefore only the SC-PDSI is analysed in detail in this study for future changes. For SPEI and SC-PDSI, a shift towards more frequent droughts is found for most parts of the globe. This result agrees well with recent findings about changes of agricultural drought severity in the IPCC AR6. Trends and changes of future drought characteristics differ strongly between regions. The strongest negative trends and largest differences between the indices are found in arid regions (North Africa, Middle East, and Central Asia), which is linked to the influence of increasing PET in the future. The characteristics based on SC-PDSI show similar, but less pronounced, features compared to the SPEI. In general, PET and hence thermodynamic processes have a larger influence on SPEI than on SC-PDSI. For both indices, the differences between SSP5-8.5 and SSP2-4.5 are small in relation to the changes from the historical to the future periods, and significantly more extreme droughts are found in the SSP5-8.5 scenario. Overall, an increase of droughts is found to be governed by changes of thermodynamic processes, which increases with warming climate leading to more severe droughts in the future in arid regions. This is in agreement with findings in the recent IPCC AR6.

ACKNOWLEDGEMENT

To begin with, I would like to thank my first thesis supervisor Prof. Dr Veronika Eyring of the Climate Modelling Group at the University of Bremen. Her significant contributions to ongoing climate science are an inspiration for me and have drawn my interest to the field of climate modelling. Furthermore, she gave me the opportunity to do research in this important field of science and allowed me to choose the main objectives and methods used in this thesis, while also steering me into the right direction, when needed.

I would like to thank Prof. Dr Gerrit Lohmann of the Alfred-Wegner-Institute as the second supervisor of this thesis. I am gratefully indebted to his short-term willingness to grade this thesis.

Special acknowledgement is given to Dr Katja Weigel. She was consistently supportive and helpful. I was able to turn to her with any concern, whether it was organisational, technical or scientific. Therefore, as well as the corrections she and and Dr Birgit Hassler have given me to improve this thesis I am thankful.

Finally, I must express my very profound gratitude to my parents and to my partner for providing me with unfailing support and continuous encouragement throughout my years of study and through the process of researching and writing this thesis. This accomplishment would not have been possible without them.

Thank you.

Contents

List of Figures

List of Tables

1. Introduction

The availability of water is an essential requirement for human life, as it is crucial for several sectors including food production, freshwater supply and industry. Droughts are dangerous and complex natural hazards. Changes of their characteristics and their impacts in a changing climate are still not fully understood. Despite these changes it can affect more people than most other natural disasters (Hagman et al. 1984; Wilhite 2000).

A drought occurs when the demand of water exceeds the supply over a period of time, i.e. due to the lack of precipitation as one of the primary freshwater sources. Considering a drought as an exceptional dry event requires some normal climatic conditions as reference, which is just one of the challenges of defining droughts. The definition further depends on the field of application and can be roughly clustered into the following categories. A decline or absence of precipitation for several days to months is defined as a meteorological drought. The agricultural drought as another drought category primarily depends on soil moisture and typically appears on larger time scales. If a drought persists long enough, it may turn into a hydrological drought, whose primary indicators are run-off and a decreasing water level of lakes, rivers and groundwater (Wilhite 2000). The sixths Assessment Report (AR6) of the Intergovernmental Panel on Climate Change (IPCC)(AR6) found an agreement in recent scientific research with at least medium confidence in an increase of agricultural droughts for several regions of the world (IPCC 2021; Seneviratne et al. 2021). This change is more significant than in meteorological droughts and may implicate serious consequences for humans. The overarching aim of this thesis is to contribute to the understanding of the reasons for changes in the characteristics of droughts in a changing climate on a global scale. Increase of temperature leads to an increase of Atmospheric Evaporative Demand (AED) or Potential Evapo-Transpiration (PET), which is an indicator for one of the physical processes involved in the creation of agricultural droughts. The evaluation of the impact of changing PET is part of this thesis. To asses changes in drought indices climate model simulations from the Coupled Model Intercomparison Project Phase 6 (CMIP6; Eyring et al. 2016a) are used. For the future two scenarios are chosen, based on two different Shared Socioeconomic Pathways (SSPs; O'Neill et al. 2016).

For several decades efforts have been made to quantify severities and magnitudes of droughts using indices derived from observable or predictable physical variables. Nowadays, many of such indices have been proposed

for different types of droughts, fields of application, and research topics. Some of them are designed for monitoring droughts in specific regions. One of the earliest and widely used drought indices is the Palmer Drought Severity Index (PDSI; Palmer 1965). It is based on a simple water balance, that makes use of PET. Due to a lack of spatial comparability (Karl 1983; Alley 1984; Heddinghaus and Sabol 1991; Guttman 1998), the self calibrating PDSI (SC-PDSI) have been developed in 2004 by Wells, Goddard, and Hayes as a modern derivative. The accounting for the PET, however, may qualify this indices for being applied in climate change research using model predictions. The PDSI and SC-PDSI are compared to the widely used precipitation based Standardized Precipitation Index (SPI; McKee, Doesken, and Kleist 1993) and its derivative the Standardized Precipitation Evapotranspiration Index (SPEI). To archive this, corresponding diagnostics have been developed to calculate PDSI and SC-PDSI values for the Earth System Model Validation Tool (ESMValTool; Righi et al. 2019; Eyring et al. 2020; Lauer et al. 2020; Weigel et al. 2021) Version 2 (v2).

Further, methods are elaborated to systematically apply widely used drought indices, i.e. PDSI, SC-PDSI, SPI and SPEI, to climate projections. The comparison and understanding of the different drought indices is the first specific objective of this thesis. The second objective is to find and highlight differences in long term changes of agricultural droughts between the SSP2-4.5 and SSP5-5.8 future scenarios. The central pathway SSP2-4.5 assumes a continuation of historical trends resulting in a forcing level of 4.5 Wm^{-2}. For the SSP5-8.5 scenario a rapid growth of a fossil-based economy is assumed leading to a forcing level of 8.5 Wm^{-2} at the end of this century. Both scenarios are part of the CMIP6 ScenarioMIP (Tebaldi et al. 2021).

This master thesis is structured as follows. Section 2 describes the different categories of droughts and the indices used to quantify them. It explains the physical background of processes related to agricultural droughts and provides an insight to the current state of related research. In Section 3 the approximation method of PET is discussed (3.1) and the primary steps for calculation of the used indices are given (3.2). Applied metrics and methods including characteristics of events, trends and correlation are described in Section 3.4. Most of the methods have been embedded into, or directly rely on, the software framework of the ESMValTool v2, which is introduced in Section 4.1. Section 4.2 gives an overview of ScenarioMIP and lists the models, whose contributions have been used. The results in Section 5, produced in the scope of this thesis, are separated into two parts: The first part, Section 5.1, starts with an exemplarily discussion of the calculated PDSI and SC-PDSI values and compares PDSI, SC-PDSI, SPI and SPEI based on their agreement in time series based on the same input data and multi-model mean trends and event characteristics. To address the second objective of the thesis, the assessment of changes in drought indices in the two different

future scenarios, the occurrence of moderate and extreme droughts and the statistical distribution of SPEI and SC-PDSI are evaluated in Section 5.2. The SPI and PDSI have been omitted for this part, since they are not expected to be spatial comparable and consider thermodynamic processes at the same time. The results are discussed in Section 6 with respect to their reliability and scientific relevance. Finally, the primary results of this work are summarized and an outlook towards further research questions on this topic are given in Section 7.

2. Scientific Background

2.1 Drought Types

A drought describes a deficit of water availability. An exact definition can only be given for a specific application or impact considering the respective regional climate. A single precise universally accepted definition of drought does not exist (Wilhite 2000). Wilhite and Glantz (1985) analysed 150 existing definitions of droughts and clustered them into four types: meteorological, agricultural, hydrological and socioeconomic droughts.

Meteorological Droughts appear already on short periods as an absence of precipitation over days or months. Counting consecutive dry days or calculating statistical precipitation deficits are common methods to identify droughts of this type.

Agricultural droughts are defined by the impact of meteorological conditions on crop yield and typically appear on time scales of multiple months or years. Properties of the soil and the atmosphere also affect the transpiration and therefore the water stress of the crops. Besides the meteorological variables (i.e. soil moisture, precipitation and PET) the water demand of crop also depends on their biological properties, which can vary with the type of crop and the state of growth. Meteorological droughts can turn into, or overlap, with agricultural droughts, but they do not necessarily coincide. (Wilhite and Glantz 1985)

Hydrological Droughts might establish if a drought persists long enough. Its primary indicators are run-off and a decreasing water level of lakes, rivers and groundwater. (Wilhite 2000)

Socioeconomic Droughts are usually associated with the supply and demand of economic goods. Their features can incorporate with those from other drought types. An agricultural drought can also be treated as a socio-economic drought by considering the demand of crop yield. (Wilhite and Glantz 1985)

Besides these different still conceptual definitions, droughts are difficult to pinpoint in time and space, as they can have different causes and affect large areas over long duration (Burton, Kates, and White 1978). For an agricultural drought to establish different circumstances (i.e. missing

precipitation and high evapotranspiration) have to accumulate over a certain period of time. The actual start of the drought is not trivial to link to a threshold of any observable variable. The indices discussed in sections 2.3 and 3.2 are approaches to substantiate the conceptual definitions to an operational level where thresholds of numerical values can be used to define start and end of a drought. Because of regional differences and different fields of applications many of this indices have been developed in the last decades.

2.2 Mechanisms and Drivers of Agricultural Droughts

Figure 2.1 shows some of the main processes in the hydrological cycle relevant for understanding the establishment of droughts and impacts of climate change. The main driver of the cycle is evaporation over the oceans. It is the largest source for the atmospheric moisture. Atmospheric uptake of water is the strongest in the tropics and subtropics, while precipitation dominates evaporation in higher latitudes. Moist air is transported through the atmosphere and part of its water content is depleted over land. On the land surface water can directly run-off and flow through a network of rivers into lakes or back to the ocean. A part of the depleted water, depending on surface conditions, is infiltrated into the soil and can be taken up again by plants or flows into reservoirs.

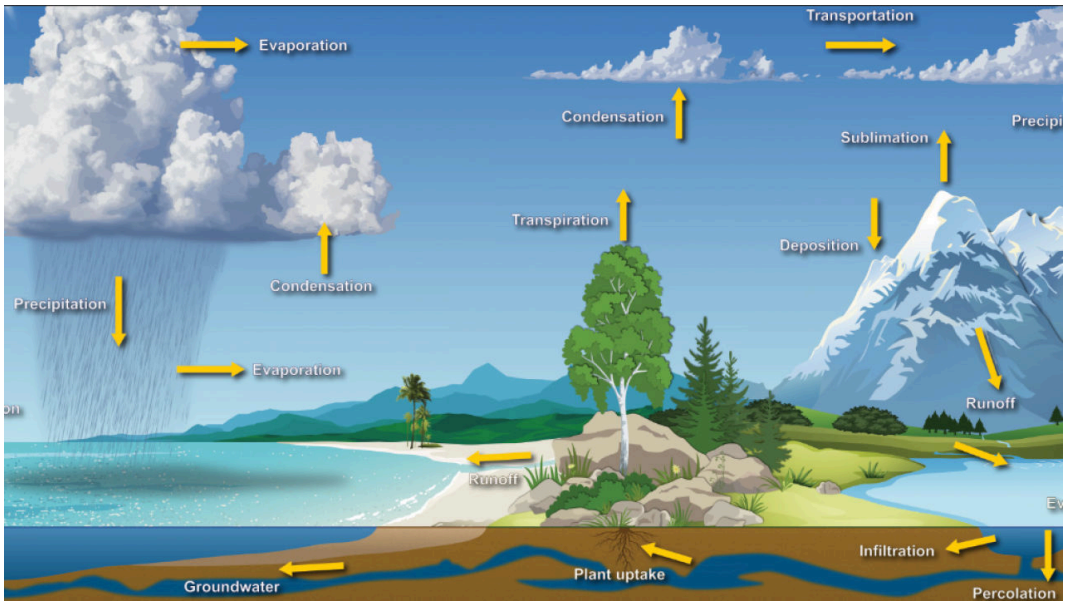

Figure 2.1: Schematic of a hydrological cycle focusing on processes, that are relevant for understanding droughts. Figure taken from Dennis (2019). Original Caption: The water cycle.

Evaporation is not limited to water surfaces. It also happens at land surfaces and can directly reduce soil moisture. An additional process of the water cycle, that primarily occurs on land surface, is transpiration. Plants can take up water from deeper soil layers and transport it upwards utilizing capillary action. Their water supply and CO_2 exchange is controlled by biological processes depending on water vapour pressure difference and temperature (Schulze et al. 1973). Due to plant coverage of a significant part of global land surface, plants provide an additional interface for moisture exchange on the surface layer. The sum of transpiration by plants and direct surface evaporation is often referred to as actual evapotranspiration (ET).

Both processes, evaporation and transpiration, depend on relative humidity, temperature and surface wind speed. These atmospheric properties can be combined to the Potential Evapo-Transpiration (PET), which includes only atmospheric properties that impact the actual evaporation and is therefore also referred to as Atmospheric Evaporative Demand (AED). Actual evaporation further depends on physical properties of the surface including availability of water, and additionally depends on physical and biological properties of the plant. Atmospheric properties such as temperature, humidity and precipitation are widely available in observations and future projections. One method to approximate the PET from atmospheric properties, recommended by the FAO, is given in section 3.1. Less physical approaches of estimating PET, that are based only on precipitation (i.e. Hargreaves and Samani 1985, Thornthwaite 1948), tend to overestimate PET (Seneviratne et al. 2021). Under agricultural drought conditions ET is usually low compared to the PET, because of limited water availability.

2.3 Drought Indicators and Indices

Different atmospheric variables play a role in dynamic and thermodynamic processes of the atmosphere, which leads to the establishment of droughts. This includes precipitation, temperature, radiation and wind speed. Hydrological variables like soil moisture, groundwater level and streamflow can be closer linked indicators for agricultural droughts, but are more difficult to observe or estimate. Variables that can be used to describe drought properties such as magnitude, duration, severity and spatial extend are also called drought indicators (Hayes, Cavalcanti, and Steinemann 2005). Multiple drought indicators can be synthesized into a single drought index.

Drought indices are numerical representations of the magnitude or severity of droughts, whose exact definition may vary, and thus their operational or scientific meaning (Hayes, Cavalcanti, and Steinemann 2005). They are usually complex multi-scalar functions of one or more of the named indicators (McKee, Doesken, and Kleist 1993). A drought index is not necessarily a

value with physical units, but instead often represents an assignment to labels on a statistical or arbitrarily derived quantitative scale (Redmond 2002). This makes it difficult to compare different indices in a pure mathematical sense without a discussion about their application. Which index is the most suitable depends on the field of application, the type of drought and the availability of data.

The currently existing indices for drought monitoring can be derived in two broad groups. The first group contains the indices based on water balance calculation (i.e. PDSI and SC-PDSI) and the second group are the indices that are derived from statistics of a time series (i.e. SPI and SPEI) (Peters 2014). For methods involving a water balance additional physical variables are required (i.e. Available Water Capacity (AWC) for the PDSI). In the IPCC AR6 the SPI has been considered in the assessment of meteorological and SPEI, PDSI and soil moisture in the assessment of agricultural droughts (Seneviratne et al. 2021). The derived information is primarily based on indices and their trends calculated for observational data and model projections (Seneviratne et al. 2021). PET plays a crucial role for the development and has important influence on the intensity of drought events (Masson-Delmotte et al. 2021; García-Herrera et al. 2019a; Otkin et al. 2016).

The four indices used in thesis are widely used in different fields of drought research. And some of their limitations have already been shown. The SPI does solely depend on precipitation. It is used to highlight the impact of PET in the results by comparison with other indices. The SPEI does account for PET but not for actual water availability on the surface and overestimates drought intensities for arid regions (Rehana and Monish 2021). One of the first indices involving PET was the PDSI. Even if the index itself can be applied to wet spells in the same way as to droughts, it has been developed for drought monitoring. The wet spells predicted by the PDSI are not designed to detect floods. It was criticized a lot for not being spatially comparable (Karl 1983; Alley 1984; Heddinghaus and Sabol 1991; Guttman 1998). To overcome this issue the self calibrating PDSI (SC-PDSI) has been developed in 2004 by Wells, Goddard, and Hayes as a modern derivative, that can be used globally. While the SC-PDSI includes some mechanisms that make it applicable for climate change studies, others are still missing. The simple two-layered water balance model does not account for snow melt, ice cover, run-off or changes in land-use and vegetation or human interactions like irrigations (Dai, Trenberth, and Qian 2004; Hayes, Cavalcanti, and Steinemann 2005).

2.4 Droughts in a Changing Climate

The IPCC AR6 concludes, that changes in climate and extreme events can be substantial on local and regional scales (IPCC 2021; Seneviratne et al. 2021). Trends of drought indices can have different signs for specific regions and differ considerably from global means (Fischer, Beyerle, and Knutti 2013; Chen et al. 2021).

For previous publications of the IPCC various sets of geographical regions are proposed, to properly analyse the emergent climate change signal across. Suitable shapes and size of such regions depend on the climate variable, process and feedback of interest (Chen et al. 2021). To analyse the impact of a changing climate to extreme events such as droughts, the Land-subset of the IPCC AR6 WG1 reference regions is used in this thesis. Their shapes are shown in Figure 2.2 (Iturbide et al. 2020).

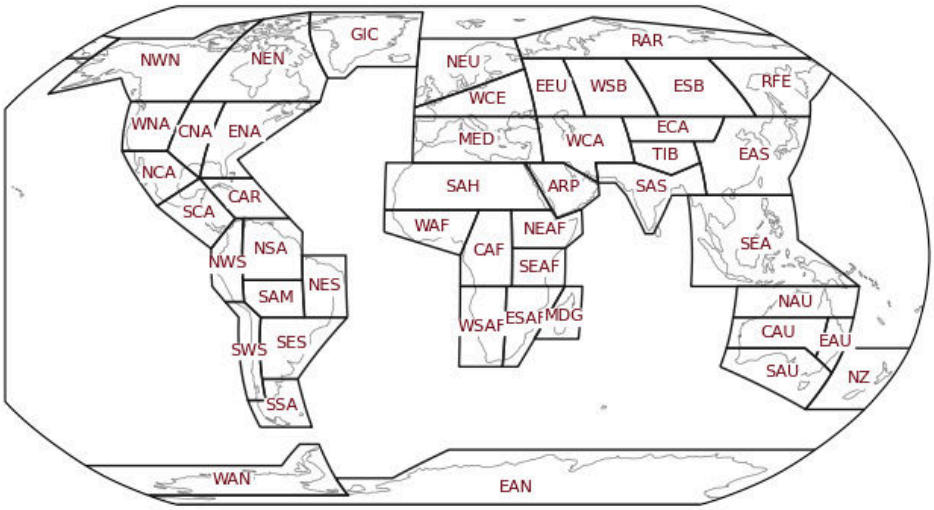

Figure 2.2: IPCC WG1 reference regions (v4) land masked. This figure has been generated using the regionmask package by Hauser et al. (2021). Abbreviations and names of the regions: North America: NWN (North-Western North America, NEN (North-Eastern North America), WNA (Western North America), CNA (Central North America), ENA (Eastern North America), Central America: NCA (Northern Central America), SCA (Southern Central America), CAR (Caribbean), South America: NWS (North-Western South America), NSA (Northern South America), NES (North-Eastern South America), SAM (South American Monsoon), SWS (South-Western South America), SES (South-Eastern South America), SSA (Southern South America), Europe: GIC (Greenland/Iceland), NEU (Northern Europe), WCE (Western and Central Europe), EEU (Eastern Europe), MED (Mediterranean), Africa: MED (Mediterranean), SAH (Sahara), WAF (Western Africa), CAF (Central Africa), NEAF (North Eastern Africa), SEAF (South Eastern Africa), WSAF (West Southern Africa), ESAF (East Southern Africa), MDG (Madagascar), Asia: RAR (Russian Arctic), WSB (West Siberia), ESB (East Siberia), RFE (Russian Far East), WCA (West Central Asia), ECA (East Central Asia), TIB (Tibetan Plateau), EAS (East Asia), ARP (Arabian Peninsula), SAS (South Asia), SEA (South East Asia), Australasia: NAU (Northern Australia), CAU (Central Australia), EAU (Eastern Australia), SAU (Southern Australia), NZ (New Zealand), Small Islands: CAR (Caribbean), PAC (Pacific Small Islands)

In the IPCC AR6, assessments about different types of droughts have been made for each of these regions for the period 1950 to present (Seneviratne et al. 2021). Changes in meteorological drought are estimated based on precipitation-based indices including SPI. The estimation of changes in agricultural and ecological droughts is based on SPEI, PDSI. A stronger increase in frequency and severity of agricultural compared to meteorological droughts, might be caused by the contribution of PET (Seneviratne et al. 2021; García-Herrera et al. 2019b; Williams et al. 2020). The synthesis from several studies (Greve et al. 2014; Dai and Zhao 2017; Spinoni et al. 2019; Padrón et al. 2020) of observed changes in agricultural and ecological

drought are shown in Figure 2.3 (Masson-Delmotte et al. 2021). The complete list of references is given in Table 11.9 of the IPCC AR6 (Seneviratne et al. 2021). Beside the SPEI and PDSI, different drought indicators including total and surface soil moisture, water-balance estimates (precipitation minus ET) have been taken into account for the assessment. An agreement with at least medium confidence in an increase of agricultural and ecological droughts since 1950 have been found for four regions in Africa, (WAF, CAF, WSAF, ESAF), three in Asia (WCA, ECA, EAS), two in Europe (WCE, MED) and one each in North (WNA) and South America (NES) and Australasia (SAU). Drought decrease can be found in just one region (NAU) with at least medium confidence. All other regions have low agreement or limited data and/or literature (GIC, SAH, ARP, PAC). There is no high confidence for any region linking the general trends of drought severity to human contributions, but for the impact of greenhouse gas emission to thermodynamic changes (Masson-Delmotte et al. 2021). However, the moisture exchange between surface and atmosphere is complex and depends on dynamic processes, which can only be linked to human contributions with low confidence (Gulev et al. 2021).

In future projections of CMIP5 simulations an increase in frequency of extreme droughts in subtropical regions is found in several studies (Dai and Zhao 2017; Touma et al. 2015; Hunt 2011; Martin 2018). For the deep tropics studies discovered a wetting trend in future projections until 2100 (Martin 2018; Collins et al. 2013). More recent studies, some of them including CMIP6 models, allow a more robust assessment of drought changes, for the regions specified in Figure 2.2 (Seneviratne et al. 2021). Following some of these studies (Greve, Gudmundsson, and Seneviratne 2018; Wartenburger et al. 2017; Xu, Chen, and Zhang 2019), an increase in drought frequency and intensity can be found as a function of global warming for several regions. The probability of drought hazards is also rising with increasing forcing levels of different future scenarios (Seneviratne et al. 2021).

Balting et al. (2021) recently published a study, to exhibit an increase of summer droughts for the northern hemisphere in CMIP6 future projections. The most significant intensification is found for arid regions. Based on the SPEI from multi-model simulations for three different socioeconomic pathways (SSP1-2.6, SSP2-4.5, SSP5-8.5), a doubling of the concurrence rate between SSP1-2.6 and SSP5-8.5 is shown for sub-tropical regions (Balting et al. 2021).

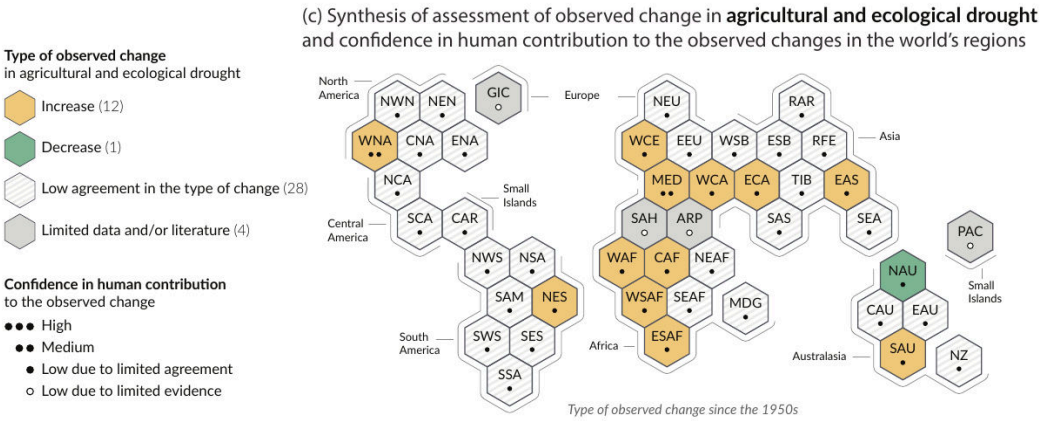

Figure 2.3: The IPCC AR6 WGI inhabited regions are displayed as hexagons with identical size in their approximate geographical location. All assessments are made for each region as a whole and for the 1950s to the present. The colours in each panel represent the four outcomes of the assessment on observed changes. Striped hexagons (white and light-grey) are used where there is low agreement in the type of change for the region as a whole, and grey hexagons are used when there is limited data and/ or literature that prevents an assessment of the region as a whole. Other colours indicate at least medium confidence in the observed change. [...] Agricultural and ecological droughts are assessed based on observed and simulated changes in total column soil moisture, complemented by evidence on changes in surface soil moisture, water balance (precipitation minus evapotranspiration) and indices driven by precipitation and atmospheric evaporative demand. Yellow hexagons indicate regions where there is at least medium confidence in an observed increase in this type of drought, and green hexagons indicate regions where there is at least medium confidence in an observed decrease in agricultural and ecological drought. Panel c from Figure SPM.3 published in Masson-Delmotte et al. 2021.

3. Methods

3.1 Potential Evapo-Transpiration

The PET is a required input variable for the SC-PDSI, PDSI and SPEI. It combines evaporation and transpiration, which is water released from plants to the atmosphere. PET depends on several environmental parameters (i.e. radiation, temperature and humidity). Transpiration and evaporation generally happen at the same time, but the ratio of their potential values highly depends on the surface type (Allen et al. 1998). However, for the drought indices only the easier to predict combined PET is of interest. Some of the models participating in CMIP6 already provide the PET through a variable called *evspblpot*, but it is neither a standard variable, nor is its calculation documented in detail for any model. To make the climate indices applicable to a wider range of models and the performance of indices less dependent on the internal land-surface components of the respective model, a mathematical approximation for this value is calculated and used for all analysed models.

Over the last century a variety of methods to approximate the PET has been developed. Thornthwaite (1948) proposed a method based on daytime length and daily temperature. 15 years later Hamon (1963) came up with an equation, that includes the saturation vapour pressure. Both approximations are not reliable under changing climate conditions (Shaw and Riha 2011). In contrast, the Penman-Monteith (PM) method (Monteith 1965; Penman 1948) provides a more complex combination of parameters (Equation 3.1) to approximate PET with a closer link to the underlying physical processes. It includes several variables like the soil heat flux density G , mean daily air temperature at 2m T_d, wind speed at 2m u_2, the psychometric constant γ, saturation and actual vapour pressure e_s and e_a. Δ is the slope of the vapour pressure curve (Allen et al. 1998).

$$PET_{pm} = \frac{0.408\Delta(R_n - G) + \gamma \frac{900}{T+273} u_2 (e_s - e_a)}{\Delta + \gamma(1 + 0.34u_2)} \tag{3.1}$$

PET approximations which are solely based on air temperature exist as well (Hargreaves and Samani 1985; Thornthwaite 1948), but the PM-method shown in Equation 3.1 is more adequate and recommended by the Food and Agriculture Organization of the United Nations (FAO), and therefore some-

times referred to as FAO-56 Penman-Monteith equation (Pereira et al. 2015). Allen et al. (1998) and Zotarelli et al. (2010) provide instructions how to calculate the psychometric constant and how to approximate variables that may not be available in observational or model data. Equation 3.1 is used in the SPEI R package (Beguería et al. 2014) and through this in the SPEI diagnostics of the ESMValTool (Adeniyi 2019). Additional approximation methods have been developed since then (Oudin et al. 2005).

3.2 Calculation of Indices

In the following the methods are described that have been used to calculate the indices. Some mathematical details, which are relevant for the analysis and parameters, required to reproduce the results are given. The calculation for PDSI and SC-PDSI is described step by step to support the understanding of the diagnostics developed for the ESMValTool during this thesis.

3.2.1 Standardized Precipitation Index

The SPI categorizes droughts based on the deficit between observed or predicted precipitation and a standardized probability to observe such precipitation (Guttman 1998). Since precipitation is not normally distributed probability functions other than gauss functions might represent measurements better. In this thesis a gamma distribution is used to locally describe normal climate conditions for a historical reference period of 115 years (1900-2014).

By cumulating monthly precipitation, the SPI can be calculated for any time scale of interest (McKee, Doesken, and Kleist 1993). Typical choices of this smoothing windows are 1, 3, 6, 12, 24 or 48 months (McEvoy et al. 2012; McKee, Doesken, and Kleist 1993). SPI calculated on short time scales can be related to soil moisture, while larger time scales are used to analyse impacts on ground water or other reservoirs. For this month a scale of six months is chosen which is expected to be relatable to agricultural impacts and shows the smallest time lag to the PDSI (Guttman 1998).

The probability of the averaged precipitation over the chosen time scale can be derived from the probability function (i.e. a gamma-distribution), which has been fitted to match the percentiles given in Table 3.1 (Guenang and Kamga 2014). A detailed description of the computational process can be found in publications (McKee, Doesken, and Kleist 1993; Guenang and Kamga 2014).

Table 3.1: Mapping of SPI and SPEI values to their category and occurrence. These probabilities are used to fit the probability function used by the SPI or SPEI (Le et al. 2019; Vicente-Serrano, Beguería, and López-Moreno 2010). SPI values between 0 and -1 for the SPI have originally been labelled as mild droughts, but are considered as normal for simplification (McKee, Doesken, and Kleist 1993).

SPI/SPEI	**Label**	**Occurrence**
$2.0 \leq$ SPI	Extreme wet	2.3%
$1.5 \leq$ SPI $<$ 2.0	Severe wet	4.4%
$1.0 \leq$ SPI $<$ 1.5	Moderate wet	9.2%
-1.0 $<$ SPI $<$ 1.0	Normal	68.2%
-1.5 $<$ SPI $\leq$ -1.0	Moderate dry	9.2%
-2.0 $<$ SPI $\leq$ -1.5	Severe dry	4.4%
SPI $\leq$ -2.0	Extreme dry	2.3%

3.2.2 Standardized Precipitation Evapotranspiration Index

In contrast to the classical SPI, which is solely based on precipitation, the Standardized Precipitation Evapotranspiration Index (SPEI; Vicente-Serrano, Beguería, and López-Moreno 2010) includes additional atmospheric variables through PET. The difference between precipitation and PET is used as a simple climatic water balance. While the proposed SPEI uses a PET approximation method that only requires monthly temperature data (Thornthwaite 1948), in this thesis the more complex Penman-Monteith approximation is used. A description of the approximation method is provided in Section 3.1 and further details on calculation of the SPEI can be found in (Vicente-Serrano, Beguería, and López-Moreno 2010). The scale of the SPEI is the same as the one for SPI given in Table 3.1. As probability function for the SPEI a log-Logistic distribution is used with a time scale of nine months.

3.2.3 Palmer Drought Severity Index

One of the first and most widely used drought indices is the PDSI proposed by Palmer (1965). The Index is calculated using a simple water balance model to find the climatically appropriate precipitation P_c, based on AWC, PET and precipitation P_c. A moisture anomaly index Z is calculated by comparing P and P_c and used to recursively calculate three drought indices with different limitations. The final PDSI is one of these three indices, chosen based on the establishment of a drought or wet spell. In the following, the mentioned steps are described in detail, based on published guidelines (Palmer 1965); Alley 1984; Guttman 1998).

Step 1: Hydrological Accounting from Water Balance

The first step of calculating PDSI is to find the climatically appropriate precipitation P_c, which can then be compared to the actual measured or predicted precipitation. In analogy to a simple water balance model (where precipitation is the sum of run-off RO, recharge R, evapotranspiration ET and change in moisture $-L$) the balance for P_c is defined by Palmer (1965) as

$$P_c = \alpha PET + \beta PR + \gamma PRO - \delta PL \tag{3.2}$$

In this equation PR is potential recharge, PRO potential run-off and PL potential loss or potential change of soil moisture. The coefficients (α, β, γ, δ) are ratios of long-term mean quantities of actual to potential values (Alley 1984). They are calculated for each month of the year $j = 1, \ldots, 12$ to finally provide $P_{c,j}$ accounting for seasonal variability:

$$\alpha_j = \frac{\bar{ET}_j}{\bar{PET}_j} \quad \beta_j = \frac{\bar{R}_j}{\bar{PR}_j} \quad \gamma_j = \frac{\bar{RO}_j}{\bar{PRO}_j} \quad \delta_j = \frac{\bar{L}_j}{\bar{PL}_j} \tag{3.3}$$

The exchange of water between soil and atmosphere is limited by the availability of water close to the surface. Palmer divided the soil in two layers and assumed the upper (surface) layer has a capacity of 25 mm water column. The amount of water stored in this layer is referred to as S_s. The underlying layer has an actual amount of S_u and its maximum storage is defined by the given Available Water Capacity (AWC). The AWC refers to the combination of both layers. The assumptions that the surface layer needs to be completely dry (or wet) before water is transferred between the layers and that the evapotranspiration takes place at the potential rate, lead to the expressions for the loss of each layer $L_s = min(S_s, PET - P)$ and $L_u = (PET - P - L_s)\, S_u / AWC$. Considering no run-off unless $S_s + S_u > PET$, potential values can be defined as:

$$PR = AWC - (S_s + S_u) \tag{3.4}$$

$$PRO = S_s + S_u = AWC - PR \tag{3.5}$$

$$PL = min(PE, S_s) + (PE - min(PE, S_s))\, S_u / AWC \tag{3.6}$$

Step 2: Moisture Anomaly

The monthly moisture anomaly is the difference between the observed precipitation P and P_c. Scaling the anomaly by a standardizing factor K to make it comparable between different months and regions, leads to the moisture anomaly index Z.

$$Z = K(P - P_c) = K(P - \alpha PET - \beta PR - \gamma PRO + \delta PL) \tag{3.7}$$

A given deficit of rain has stronger influence on the PDSI (larger K) in an arid region rather than in a humid region. The standardizing factor K (also referred to as climate characteristic) is an refinement of Palmers general climate characteristics approximation K':

$$K'_i = 1.5 \log_1 0 \left(\frac{\frac{\bar{PE}_i + \bar{R}_i + \bar{RO}_i}{\bar{P}_i + \bar{L}_i} + 2.8}{\bar{D}_i} \right) + 0.5 \tag{3.8}$$

$$K_j = \frac{17.67 K'_j}{\sum_{i=1}^{12} \bar{D}_i K'_i} \tag{3.9}$$

The parameter $\tau_j = \frac{\bar{PE}_j + \bar{R}_j + \bar{RO}_j}{\bar{P}_j + \bar{L}_j}$, can be interpreted as the ratio between demand and supply of moisture (Alley 1984).

Step 3: Recursive PDSI Calculation

The Palmer Drought Index PDI for month t is then calculated by the following equation:

$$PDI_t = 0.897 PDI_{t-1} + 0.333 Z_t \tag{3.10}$$

Equation (3.10) is empirically determined to fulfil the assignments of Table 3.2 for the historically driest periods in nine locations in the USA (Kansas, Iowa, North Dakota, Ohio, Pennsylvania, Tennessee central Iowa and western Kansas and three locations in Texas) observed before 1965, which limits its applications to regions with climate similar to this nine locations. Calculating an index as defined in Equation (3.10) poses the problem of finding

Table 3.2: Mapping of PDSI values to their category. The labels have been assigned by Palmer (1965) based on observations.

PDSI Range	**Label**
PDSI $>$ 4.0	Extremely wet
4.0 $\geq$ PDSI $>$ 3.0	Very wet
3.0 $\geq$ PDSI $>$ 2.0	Moderately wet
2.0 $\geq$ PDSI $>$ 1.0	Slightly wet
1.0 $\geq$ PDSI $>$ 0.5	Incipient wet spell
0.5 $>$ PDSI $>$ -0.5	Near normal
-0.5 $>$ PDSI $\geq$ -1.0	Incipient drought
-1.0 $>$ PDSI $\geq$ -2.0	Mild dry spell
-2.0 $>$ PDSI $\geq$ -3.0	Moderate drought
-3.0 $>$ PDSI $>$ -4.0	Severe drought
-4.0 $\geq$ PDSI	Extreme drought

exact start or end dates for a dry or wet spell, which is crucial to describe the severity of a drought. The PDI_t is highly influenced by the PDI of the previous months (t_{-1}, t_{-2}, ...). Therefore, long periods of dry conditions can retain a low PDI, even if the precipitation of one or two months should have ended the drought.

Palmer solved this issue by calculating three indices $PDI_{1,t}$, $PDI_{2,t}$ and $PDI_{3,t}$, where $PDI_{1,t} \geq 0$ tracks a wet spell that is becoming established, while $PDI_{2,t} \leq 0$ tracks establishing droughts accordingly. A drought (or wet spell) is considered to be established for $PDI \leq -1$ (or $PDI \geq 1$) after the previous established event ended. The end of such an event can either be designated by the respective PDI reaching near normal conditions ($-0.5 <$ PDI < 0.5) or the received moisture reaching the amount required to end a wet or dry spell. How these amounts are determined is described by Alley (1984). $PDI_{3,t}$ tracks both types of events, by setting $PDI_{3,t} = PDI_{1,t}$ (or $PDI_{3,t} = PDI_{2,t}$) whenever a new drought or wet spell becomes established. The final PDSI will be assigned to one (non-zero) of these PDIs. However, different situations, including the common case of two non-zero PDIs, require additional rules for these assignments. Palmer provides a whole set of rules, which in some cases require information about the end of the event. It is one of the main limitations for real time application of this index, that it is not able to provide the final index continuously for ongoing events.

Table 3.2 shows the mapping of PDSI values to the drought categories Palmer used. The assignments follow the arbitrary definition of an extreme drought having an index value of -4.

3.2.4 Self-Calibrating PDSI

To overcome some of the PDSIs limitations, Wells, Goddard, and Hayes (2004) introduced a method to replace the parameters, which have been derived from observational data of a few locations, by dynamically calculated values. In particular the climate characteristic K and the duration factors p and q are calculated from historical reference data at the specific location. p and q replace the constants 0.897 and 0.333 in Equation 3.10. When the original PDSI has been developed in 1965, the required reference data and computational power was not available (Wells, Goddard, and Hayes 2004).

Adjusting Climate Characteristics

The given climate characteristic from Equation 3.9 contains the empirical value 17.67, which is the accumulated yearly moisture anomaly averaged over the nine locations named in Section 3.2.3. The equation is therefore a ratio of the expected and observed yearly moisture anomaly. Since the PDSI is based on the accumulated moisture anomaly, the new spatially dependent climate characteristic $\tilde{K}$ could be estimated by calibrating

$$\tilde{K} = \frac{\text{expected PDSI}}{\text{oberved PDSI}}. \tag{3.11}$$

Since the PDSI is centralized at zero its tails are more suited for calibration. Therefore the frequency of extreme events f_e is used to calibrate $\tilde{K}$, considering the driest 2% (wettest 2%) of the reference time belongs to Indices below -4 (above 4):

$$\tilde{K} = \begin{cases} K'(-4.00/\text{2nd percentile}), & \text{if } d < 0 \\ K'(4.00/\text{98th percentile}), & \text{if } d \geq 0 \end{cases} \tag{3.12}$$

To apply the calibration the PDSI is calculated once using a first order approximation of $Z = dK'$, where Equation 3.8 defines K'.

Calculate Duration Factors

As one can see in Equation 3.10 the PDI and therefore the PDSI is a recursive Index, where each value is the weighted sum of the previous value (represents the climate trend) and the current moisture anomaly (represents the contribution by the current month). These experimentally determined

weights will be replaced by the duration factors p and q, which are calculated dynamically for the SC-PDSI, to define the sensitivity to precipitation and the lack thereof (Wells, Goddard, and Hayes 2004). Further, Equation 3.10 can be written as

$$X_i = pX_{i-1} + qZ_i \tag{3.13}$$

The duration factors calculated similar to the PDSI from the linearisation of cumulated moisture anomaly $\hat{Z} = \sum_i^t Z_i$ vs time periods t:

$$p = \left(1 - \frac{m}{m+b}\right), \quad q = \frac{C}{m+b}. \tag{3.14}$$

m and b are slope and y-intercept of $\hat{Z}(t)$ for events specified as C. In the case of PDSI this calibration has been done for the most severe dry spell ($C = -4$) from Kansas. However, the sensitivity to precipitation of the index can vary over regions and is not necessarily the same for dry and wet spells. Thus the SC-PDSI calculates two pairs of duration factors for each location, using least square fits for the extreme events ($C_1 = -4, C_2 = 4$). b is further adjusted to match the most extreme event in the reference data. As reference data the same model output for the period 1900-2014 is used as for the SPI and SPEI.

3.3 Rescaling Indices

The drought indices that are used in this thesis provide different scales (Table 3.1 and 3.2). Both scales agree in some of their labels and the indices can be rescaled to a common scale, to make the comparison easier. For the SPI, SPEI and SC-PDSI the 2.3% wettest and 2.3% most dry months of the reference period are considered to be extreme wet or extreme dry by definition. The percentiles are mapped to a common scale from -1 to 1. This means dividing the standardized indices SPI and SPEI by 2 and PDSI and SC-PDSI by 4 leads to a scale that can be used for all four indices in common, where -1 and -0.5 are the thresholds for extreme and moderate drought events. The PDSI categories near normal, incipient wet/dry, slightly wet and mild drought are merged into one category named mild or normal.

Table 3.3: A common scale for drought indices normalized by extreme conditions synthesized from Table 3.2 and 3.1.

SPI	PDSI	Normalized	Label
> 2	> 4	> 1	Extreme wet
1.5 to 2	3 to 4	0.75 to 1	Severe wet
1 to 1.5	2 to 3	0.5 to 0.75	Moderate wet
-1 to 1	-2 to 2	-0.5 to 0.5	Mild or normal
-1.5 to -1	-3 to -2	-0.75 to -0.5	Moderate dry
-2 to -1.5	-4 to -3	-1 to -0.75	Severe dry
< -2	< -4	< -1	Extreme dry

3.4 Applied Drought Metrics

The analysed drought indices are calculated for different future predictions of climate models. In contrast to short-term weather predictions, the chosen ESMs produce long-term climate projections, where weather and other simulated short-term processes are not primarily defined by the initial state of the variables. Precipitation is influenced by complex meteorological processes on spatial and temporal scales that can not be resolved by the used models. The parametrisations used differ from model to model and small changes of the atmospheric state can result in completely different weather patterns. Weather is often referred to as a chaotic system. Therefore, it is expected that future predictions of monthly precipitation over multiple decades is almost uncorrelated for different models. Figure A.1 shows an example of almost independent precipitation and SC-PDSI time series from different datasets. None of the dataset pairs show a significant correlation of SC-PDSI (Figure A.2). Especially normally distributed uncorrelated data like drought indices, which are based on precipitation, loose most of their information when a multi-model mean is applied. Hence, time integrated metrics are used to describe droughts, which can be averaged over regions and models. While correlations are calculated for indices pairwise, trends and event-based characteristics are calculated for each index. Consecutive months with normalized index values below the threshold are considered as a drought event. Multiple of such events may be found in a given period. Event-based characteristics are calculated for the historical (1900-2014) baseline and two future scenarios 2015-2100 for moderate (index < -0.5) and extreme (index < -1) droughts. All time independent metrics, that are used in the analysis are listed below, followed by some information on how they are calculated.

Cross-correlation The Pearson correlation coefficient is used to measure the similarity of the drought indices time series pairwise.

Trend: The slope of a linear fit of a time series of index values is rescaled to time intervals of 50 years.

Mean duration: The durations in months of all events in the period of interest is averaged.

Frequency: The total number of events per year. To link the frequency to the occurrence rate it has to be multiplied by the mean duration.

Mean average Index: The mean of the respective Index during an event, averaged over all events in the period of interest.

The Pearson correlation coefficient r_{XY} can be used to analyse the association between two monthly sampled normal distributed variables X and Y (Lord, Qin, and Geedipally 2021). With s_x (s_y) being the standard deviations and $\bar{x}$ ($\bar{y}$) the mean values of X (Y) their correlation is calculated as

$$r_{XY} = \frac{\mathrm{cov}(X,Y)}{s_X, s_Y} \quad \text{, with } \mathrm{cov}(X,Y) = \frac{\sum_{i=1}^{n}(x_i - \bar{x})(y_i - \bar{y})}{n-1}. \tag{3.15}$$

This association measurements are used in a pairwise comparison of time series for different indices in individual datasets.

A linear regression is used for the calculation of trends. It is provided by the scipy python module (Virtanen et al. 2020). A linear function $f(t) = \beta t + \alpha$ is calculated to minimize the sum of squared distances to the actual indices y_i and their time coordinate t_i. For N samples this cost function can be written as

$$C(\alpha, \beta) = \sum_{i=0}^{N} (\beta t_i + \alpha - y_i)^2 . \tag{3.16}$$

Due to the scale-invariance of the linear regression, the trend β for of the normalized indices can easily be rescaled to their original mapping. For compatibility the long-term trends over 115 years for the historical and 85 years for the future period are converted to index change per 50 years, as it is done by Dai, Trenberth, and Qian (2004).

4. Tools and Data

4.1 ESMValTool

The analysis in this work is done utilizing the latest version 2.4 of the Earth System Model Validation Tool v2.4 (Andela et al. 2021). This community diagnostic and performance metrics tool, targeting routine evaluation of Earth system models participating in CMIP, was first released in 2016 (Eyring et al. 2016b). Since then the software has been developed rapidly. The newest major version two of the tool contains technical improvements to increase performance and usability (Righi et al. 2019) as well as additional large-scale diagnostics to evaluate ESMs (Eyring et al. 2020, diagnostics for emergent constraints and future projections (Lauer et al. 2020), and several more specific diagnostics including extreme events (Weigel et al. 2021). The ESMValTool can be used to reproduce figures from IPCC Fifth Assessment Report (AR5) and is integrated into the infrastructure of the Earth System Grid Federation (ESGF) at the Deutsches Klimarechenzentrum (DKRZ) for the evaluation of CMIP6 models, shortly after their output is published (Eyring et al. 2020; Lauer et al. 2020).

The tool is split into two modules: Firstly the ESMValCore (Andela et al. 2020b), which provides common preprocessing operations including data extraction, filtering and re-gridding. The core module is automatically loaded and used by the other module, the ESMValTool (Andela et al. 2020a). The latter provides many ready to use diagnostics and editable recipes to run analysis and evaluations for different scientific use cases on the preprocessed data. The tool makes it easy for users to run existing diagnostics by creating or modifying recipes. Diagnostics are scripts, that contain the analysis in any of the supported scripting languages. By contrast, the recipes are text files, which contain the list of datasets to use, as well as sets of parameters and configurations for the diagnostics.

As part of this work a diagnostic *diag_scpdsi.py* has been developed to calculate the PDSI and SC-PDSI and *plot_indices.py* to analyse and visualize the result including the calculation of characteristics and comparison with other indices. Methods to calculate the precipitation based indices, SPI and SPEI are already included in the ESMValTool (Weigel et al. 2021). The analysis could be applied to any normalized monthly drought index. Figure 4.1 visualizes the workflow and the interaction of different components in the ESMValTool. The named diagnostics (red) are used in this thesis.

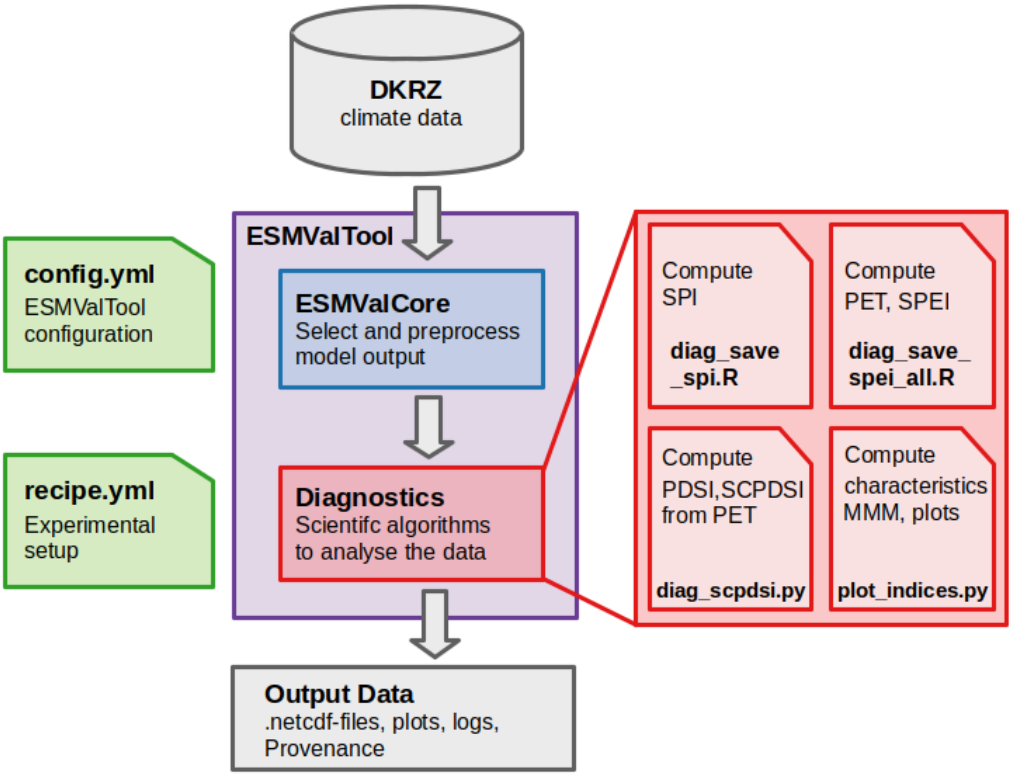

Figure 4.1: Workflow and interaction of different components in the ESMValTool framework.

Existing diagnostics have been modified and used to calculate PET, SPI and SPEI. A new diagnostic (diag_scpdsi.py) has been developed to calculate PDSI and SC-PDSI by applying the algorithms described in 3.2.3 and 3.2.4 to datasets compatible to the Climate Model Output Rewriter (CMOR; Taylor, Doutriaux, and Peterschmitt 2004). This diagnostic makes use of functions from the open source python library *climate_indices* (Adams 2017). All figures and other results in this work are generated using the newly developed *plot_indices.py* diagnostic.

4.2 ScenarioMIP

The Coupled Model Intercomparison Project (CMIP) organized by the World Climate Research Program (WCRP), started with its first phase in 1996 comparing global coupled climate models (Meehl et al. 1997) and has grown to an international climate research activity for different scientific communities. 2016 has the sixth phase of CMIP started (CMIP6; Eyring et al. 2016a). The Diagnostic, Evaluation and Characterization of Klima (DECK) experiments form a baseline for CMIP6 and future phases. The

Table 4.1: Shared Socioeconomic Pathways used in the scenarios in ScenarioMIP. The forcing levels belong to the integrated pathways selected for ScenarioMIP Tier 1. Assumptions and values taken from O'Neill et al. (2016).

SSP	Assumptions	Forcing level in 2100
SSP1	substantial investments in education and health, rapid economic growth, and well-functioning institutions increasing shift toward sustainable practices	2.6 Wm-2
SSP2	central pathway in which trends continue their historical patterns without substantial deviations	4.5 Wm-2
SSP3	little investment in education or health, fast growing population, and increasing inequalities countries prioritize regional security	7.0 Wm-2
SSP4	little investment in education or health, fast growing population, and increasing inequalities large inequalities within and across countries	-
SSP5	substantial investments in education and health, rapid economic growth, and well-functioning institutions & energy intensive, fossil-based economy	8.5 Wm-2

DECK experiments include a historical Atmospheric Intercomparison Project (AMIP) simulation, a pre-industrial control simulation (piControl), a simulation forced by an abrupt quadrupling of CO_2 (abrupt-4xCO2) and a simulation forced by a 1% CO_2 increase per year (Eyring et al. 2016a). These experiments and a historical simulation from 1850 to 2015 are mandatory to perform for any participating model.

Additional experiments targeted at specific scientific questions can be added to the project as a CMIP-Endorsed Model Intercomparison Project (MIP). For CMIP6 one such endorsement is the ScenarioMIP (O'Neill et al. 2016), which defines experiments for eight alternative possible future pathways of anthropogenic drivers like greenhouse gases, chemical reactive gases, aerosols and land use from 2015 to 2100. One of the primary objectives of the ScenarioMIP is to facilitate integrated research on climate impact, which will be important for mitigation and adaptation policy considerations (O'Neill et al., 2016). Future pathways of societal development, the SSPs, have been developed and combined with the Representative Concentration Pathways (RCPs) from CMIP5 (Kriegler et al. 2014; O'Neill et al. 2014; Riahi et al. 2017, Van Vuuren et al. 2014). A short description of each SSP is given in table 4.1.

Four integrated pathways (SSP1-2.6, SSP2-4.5, SSP3-7.0, SSP5-8.5) have been selected from the feasible SSP-RCP combinations to form Tier 1 of ScenarioMIP. It is mandatory for all participating models of this MIP to produce predictions for these scenarios. Contributions to two pathways (SSP2-4.5, SSP5-8.5) by seven models form the data base for this thesis. The contributing models are presented in table 4.2. In figure labels and technical descriptions their identifiers SSP245 and SSP585 are used.

4.3 Datasets

The minimum requirement for a ScenarioMIP contributor to be considered in this thesis is the availability of needed variables, which are precipitation *pr*, monthly minimum temperature *tasmin*, monthly maximum temperature *tasmax*, surface wind speed *sfcWind*, total cloud cover *clt* and sea level pressure *psl*, for the historical, SSP2-4.5 and SSP5-8.5 scenarios in the r1i1p1f1 ensemble. Due to computational limitations, only seven models have been chosen from the list of candidates. Table 4.2 shows a summary of the selected CMIP6 models. The field capacity (capacity of soil to store water) *mrsofc* is taken from the AWI-CM-1-1-MR (2000) model and considered to be constant between 1900 and 2100. It is used for the water balance during PDSI calculation described in Section 3.2.3.

All datasets regardless of their nativ resolution have been re-gridded to a $3^\circ \times 3^\circ$ and oceans have been masked out. The time period from 1900 to 2014 is taken from the historical experiment and combined with different ScenarioMIP contribution of the same model contribution until 2100. The scenario independent historical period (1900-2014) is used as reference period for the SPI, SPEI, PDSI and SC-PDSI calculation. It is also used as historical baseline for the assessment and discussion of changes in drought indices.

Table 4.2: Overview of models contributed to ScenarioMIP, that have been used in this thesis.

Model Name	Institute	Resolution	Notes	Reference
ACCESS-ESM1-5	Commonwealth Scientific and Industrial Research Organisation (CSIRO)	$1.9° \times 1.3°$, 38 levels	interactive carbon cycle (CASA-CNP); atmosphere component (UM); Land surface model (CABLE) with 10 vegetated types + ice, lake and bare ground (Fig. A.3)	Ziehn et al. 2020
AWICM11-MR	Alfred Wegner Institut (AWI)	T127L95	unstructured ocean meshes to locally increase resolution (FESOM); Atmosphere component ECHAM6 from MPI	Semmler et al. 2020
CMCC-ESM2	Euro-Mediterranean Centre on Climate Change (CMCC) Foundation	$0.9° \times 1.25°$, 30 levels	SILVA (land surface and vegetation); included carbon cycle; based on Community Earth System Model (CESM) operated at the National Centre for Atmospheric Research (NCAR)	Cherchi et al. 2019
CanESM5	Canadian Centre for Climate Modelling and Analysis (CCCma)	T63L49 ($\approx 2.8°$)	Fifth version of the Canadian Earth System Model; global coupled Model; fractional land masks for appropriate surface fluxes; sub-daily water balance for 3 soil layers; 4 plant functional types (PFTs); vegetation model; river networks	Swart et al. 2019; Verseghy 2000
MIROC6	cooperatively developed by a Japanese modelling community	T85L81 ($\approx 1.4°$)	atmospheric model based on CCSR-NIES; land-surface model: MATSIRO including river-routing model based on kinematic wave flow	Tatebe et al. 2019
MPI-ESM1-2-LR	Max Planck Institute (MPI) for Meteorology	T63L95 ($\approx 2.8°$)	atmospheric component: ECHAM6.3; land-surface scheme: JSBACH	Gutjahr et al. 2019
MRI-ESM2-0	Meteorological Research Institute (MRI) of the Japan Meteorological Agency	T159L90 ($\approx 1.125°$)	Atmosphere-Land component: MRI-AGCM3.5	Yukimoto et al. 2019

5. Results

In the first part of this section the newly implemented PDSI and SC-PDSI calculating diagnostic is tested and example results are shown and discussed. Metrics and drought characteristics are calculated based on these monthly indices and compared with those based on standardized indices SPI and SPEI, from existing methods. As primary input monthly variables predicted by seven models (ACCESS-ESM1-5, AWI-CM-1-1-MR, CMC-ESM2, CANESM5, MIROC6, MPI-ESM1-2-LR, MRI-ESM2-0) and re-gridded to a 3°x3° resolution are used for all indices. The PET is calculated independently from the indices using the approximation described in Section 3.1. The four drought Indices are normalized in a way that extreme droughts belong to values <-1 and extreme wet spells to values >1 (i.e. SPI and SPEI divided by 2 and PDSI and SC-PDSI divided by 4) to make them easier to compare. Drought index values in the results are given on this normalized common scale (Table 3.3), unless described otherwise.

SPEI and SC-PDSI, which are spatially comparable and consider PET, are chosen in the second part of the results, to discuss the differences of the future scenarios to the historical period and to each other. To do regional characteristics are extracted for the IPCC AR6 WG1 reference regions described in Section 2.4.

5.1 Index Comparison

The *plot_indices.py* diagnostic is able to produce maps for given dates and timelines for given locations and intervals. The plots are created for each dataset and each experiment. Figure 5.1 shows an example map for the PDSI and SC-PDSI in the summer of the last year of the historical period (July 2014) using data produced by the MIROC6 model.

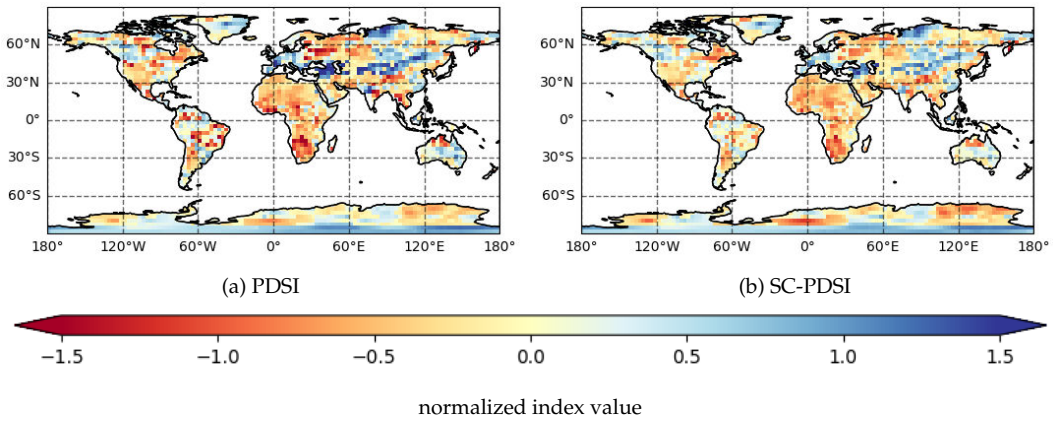

Figure 5.1: PDSI (a) and SC-PDSI (b) for July 2014 plotted globally based on the MIROC6 dataset.

The values in 5.1 are distributed between -1 and 1 with a few exceptions for the PDSI. The PDSI shows a few locations with extreme wet spells (Middle East and Central Asia) and extreme droughts (South Africa, South America). Most regions show a value close to zero which indicates normal or near normal conditions without ongoing droughts or wet spells. Further, one can see that both indices, the original PDSI and the enhanced SC-PDSI, qualitatively agree in their patterns at least for this specific point in time. The main difference is the locally recalibrated characteristic climate, described in section 3.2.4, which leads to a scaling of the calculated index, depending on the location. Parameters that differ between SC-PDSI and PDSI are constant in time, but location dependent. Therefore, the global pattern may differ between this two indices, but the correlation of time lines is expected to be high for any location. Which can also be observed in the next example. Figure 5.2 exemplarily shows a time line for Western Central Europe (WCE) of all four analysed drought indices PDSI, SC-PDSI, SPI and SPEI. Their values are averaged throughout the WCE region and shown with their respective standard deviation. The shape of the WCE region is shown in Figure 2.2. The figure shows the full analysed time span from 1900 to 2100, split into the historical period in the top panel and the SSP2-4.5 future scenario at the bottom.

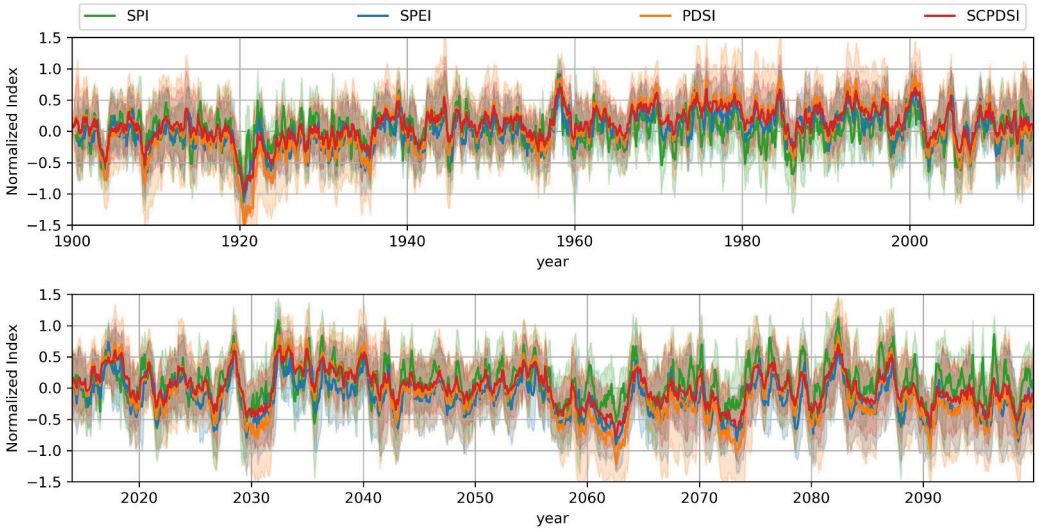

Figure 5.2: Drought Indices calculated based on MIROC6 model output for the CMIP6 historical and ScenarioMIP SSP2-4.5 experiments. The data has been averaged over all cells in the Western Central European reference region WCE. The semitransparent regions indicate the standard deviations of the grid cells for each index. The time series is split into two panels to improve visibility.

One can see a high qualitative agreement of all indices, but some indications for systematic differences can be seen too. The SPI and SPEI, which have a high agreement in the historical phase experiment before 2014, are diverging for WCE in the future. This might be related to the moisture loss by increasing PET, which is part of the SPEI but not of the SPI. In WCE, the purely precipitation based SPI tends towards higher values than the three other PET dependent indices. This is most obvious for the last decades of this century. The SC-PDSI seems to correlate well with the PDSI over the full period in WCE. The SC-PDSI, however, is attenuated compared to the PDSI, which is probably a result of the previously discussed calibration.

To proof the qualitative findings from the examples and quantify the index agreements correlations are calculated pairwise globally and are averaged over all seven datasets. Figure 5.3 shows a multi-model mean of Pearson correlation coefficients between SC-PDSI/PDSI, SC-PDSI/SPI, SC-PDSI/SPEI and SPI/SPEI based on data contributed to the combined historical and SSP2-4.5 experiments. Figure 5.3 (a) confirms the expectation of high correlation between SC-PDSI and PDSI by showing values close to 1 for all regions. Only in North Africa slightly lower coefficients are found by some models, which becomes more visible in the multi-model standard deviations shown in Figure 5.4. In panel (c) and (d) is apparent, that SPEI is almost uncorrelated to SPI and SC-PDSI for North Africa and parts of Central Asia. Apart from that, the correlation coefficients range from 0.6 to 1 for all index combinations and can be considered to be significant. Correlation

maps of PDSI to SPEI and SPI are not shown, as they are similar to those from SC-PDSI.

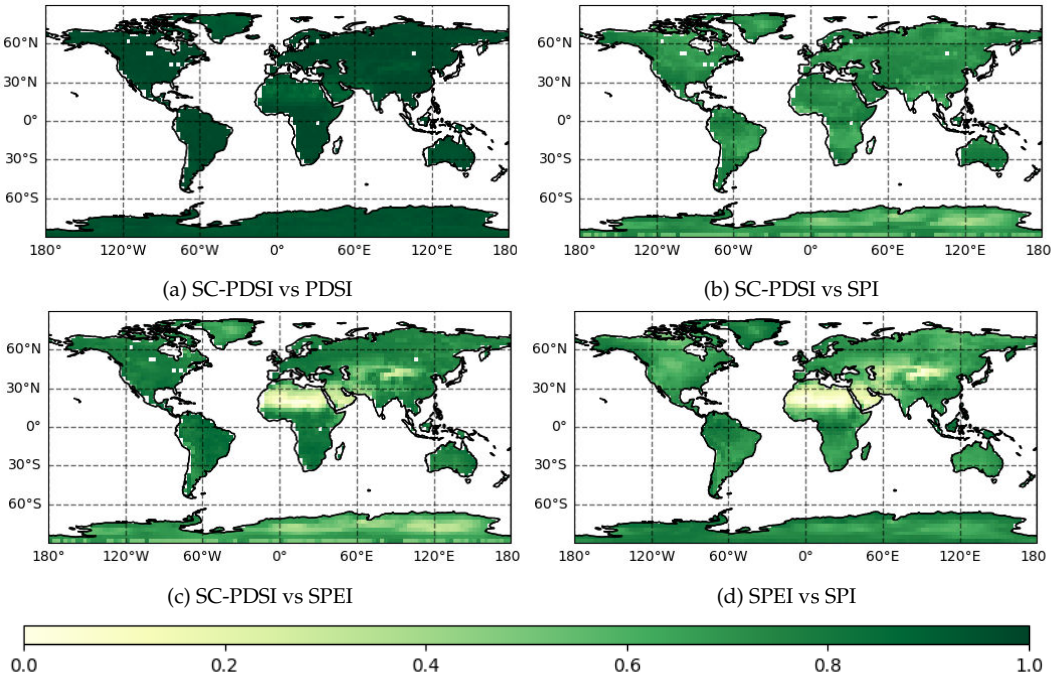

(a) SC-PDSI vs PDSI

(b) SC-PDSI vs SPI

(c) SC-PDSI vs SPEI

(d) SPEI vs SPI

Figure 5.3: Multi-model mean Pearson correlations of four different drought indices calculated for the combined experiment historical-SSP245 over the period 1900-2100.

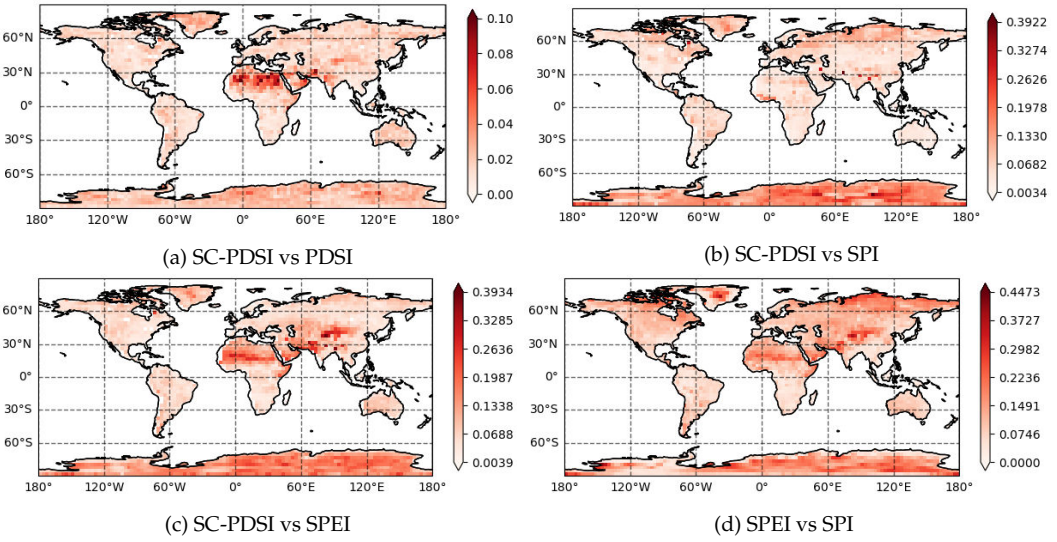

(a) SC-PDSI vs PDSI

(b) SC-PDSI vs SPI

(c) SC-PDSI vs SPEI

(d) SPEI vs SPI

Figure 5.4: Multi-model standard deviations of Pearson correlation coefficients between PDSI and SC-PDSI for the combined experiment historical-SSP245 on a global scale from 1900 to 2100. The right panel shows the standard deviation of the multi-model mean.

To analyse the development towards wetter or dryer climate conditions in future scenarios at any location, trends of the monthly drought indices are calculated over the full period (1900-2100). These Trends are shown as multi-model means in Figure 5.5. Their standard deviations over the different datasets can be found in Figure A.6 in the appendix.

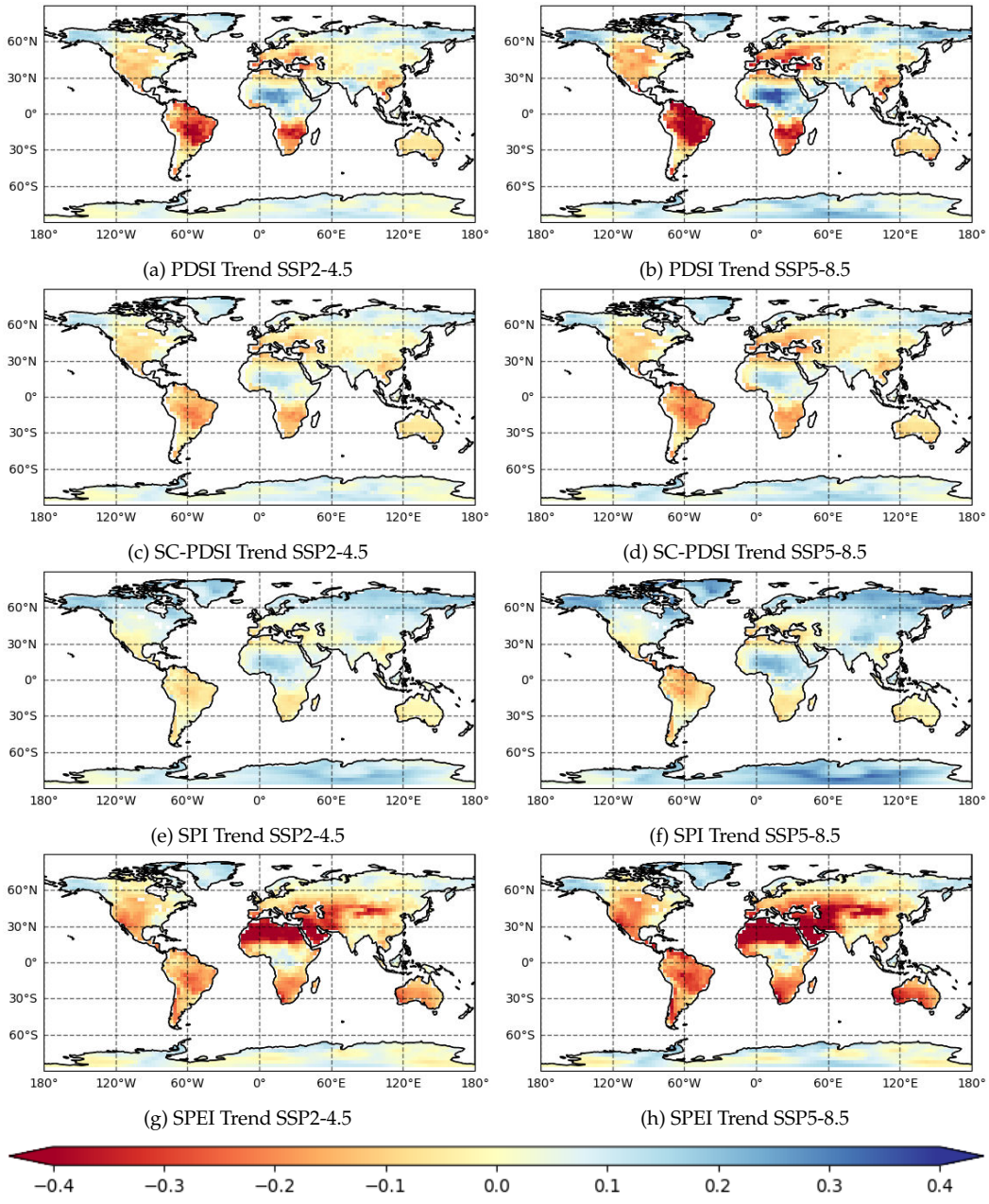

(a) PDSI Trend SSP2-4.5

(b) PDSI Trend SSP5-8.5

(c) SC-PDSI Trend SSP2-4.5

(d) SC-PDSI Trend SSP5-8.5

(e) SPI Trend SSP2-4.5

(f) SPI Trend SSP5-8.5

(g) SPEI Trend SSP2-4.5

(h) SPEI Trend SSP5-8.5

Figure 5.5: Multi-model mean of long term trends (1900-2100) of drought indices in historical experiment combined with SSP2-4.5 and SSP5-8.5 future scenarios. For the SC-PDSI trends for individual scenarios can be found in A.8. Standard deviations of the multi-model mean are shown in Figure A.6.

All four drought indices agree in negative trends indicating generally drier conditions in the northern part of South America and South Africa in both future scenarios SSP2-4.5 and SSP5-8.5. A positive trend towards generally wetter conditions can be found for the Sahara in PDSI, SC-PDSI and SPI values in both Scenarios.

The PDSI shows the most drastic changes for large areas of South America. Index decrease of more than 0.4/50yr can be found in the SSP5-8.5 future scenario in Figure 5.5 (b). The SPEI also shows a strong negative trend of less than -0.5/50yr for the northern part of Africa and slightly less intense for South Africa. The central part of Africa from 0°N up to 15 °N shows almost no trend for the SPEI, weak positive trends for SPI and SC-PDSI and the overall strongest positive trend of more than 0.4/50yr for PDSI in the SSP5-8.5 scenario. Around the Mediterranean Sea negative trends down to -0.1/50yr can be found in Figure 5.5 (a, c, g). This region of drying is pronounced in the SSP5-8.5 scenario and extends over Europe and West Asia. For Central Asia no clear trend is observable over all models in any of the analysed indices. The SPI shows a consistent positive trend between 0.1/50yr and 0.3/50yr in this area, while the SPEI strongly decrease in parts of the same area.

The spatial pattern of the SC-PDSI and the PDSI trends is similar, but the SC-PDSI trend shows less extreme values, as a result of generally lower absolute values in regions with the largest changes. The SPI as an index solely depending on precipitation shows less regions with negative trends and no large differences between the two scenarios. All negative index trends in the SSP5-8.5 scenario are enhanced compared to the SSP2-4.5 scenario. For the PDSI and SPI higher absolute values for the positive trends at Central Africa can be found as well. The trends of the input variables in Figure 5.6 can be used as explanation for some of this differences. The precipitation trends (a) and (b) are similar for both scenarios and its spatial features are comparable to the SPI trends in 5.5. Increasing PET is another effect leading towards smaller SPEI, PDSI and SC-PDSI values. The PET shows only positive trends in Figure 5.6 (e) and (f), due to global warming conditions in the period 1900-2014 (c) and (d). In the SSP5-8.5 future scenario the temperature change is significantly higher resulting in positive PET trends of more than 30 mm s^{-1} per 50 years in subtropical regions around 30°N and 30°S.

Nevertheless, while precipitation plays the primary role in establishment of droughts, the increase of global temperature and therefore PET (Figure 5.6) reinforces agricultural droughts and is responsible for drying conditions in many areas. This can be seen by comparing the SPI, which is solely based on precipitation, with the other PET based indices in Figure 5.5. Long term positive trends in precipitation compensates increasing temperature in some areas especially for central Africa, while they enhance the effect of drying elsewhere i.e. northern South America.

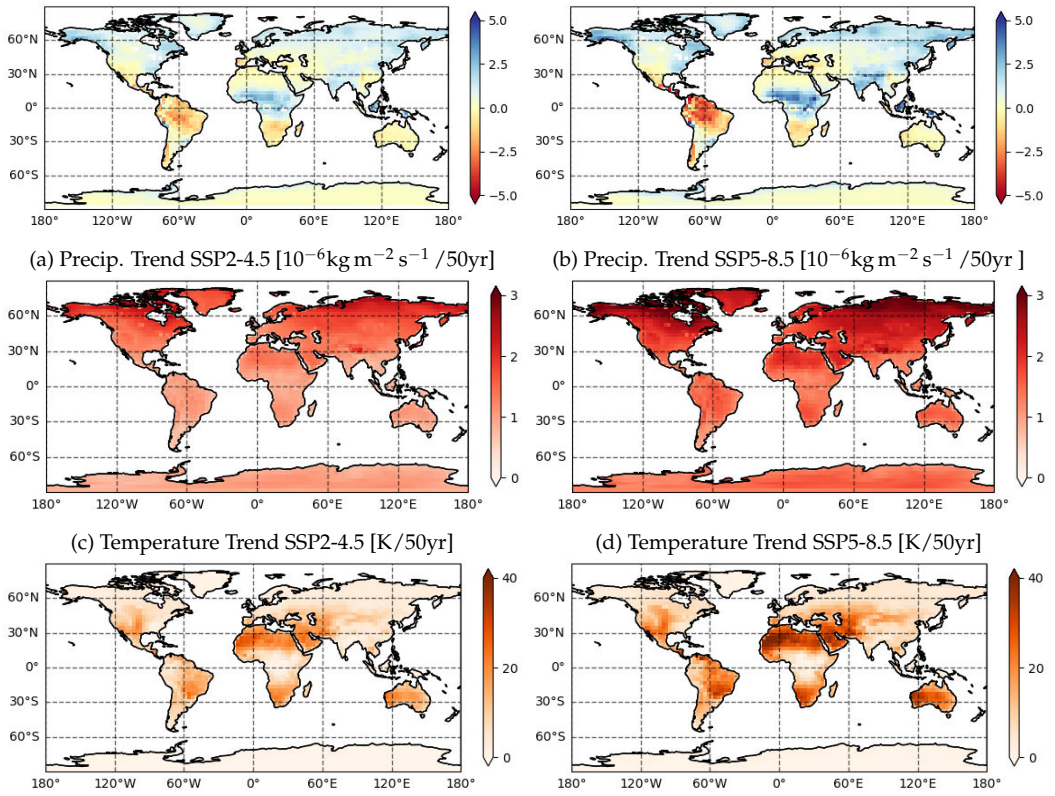

(a) Precip. Trend SSP2-4.5 [10^{-6}kg m^{-2} s^{-1} /50yr]

(b) Precip. Trend SSP5-8.5 [10^{-6}kg m^{-2} s^{-1} /50yr]

(c) Temperature Trend SSP2-4.5 [K/50yr]

(d) Temperature Trend SSP5-8.5 [K/50yr]

(e) PET Trend SSP2-4.5 [mm /month /50yr]

(f) PET Trend SSP5-8.5 [mm /month /50yr]

Figure 5.6: Multi-model mean of long term trends (1900-2100) of drought indicators used for index calculation considering SSP2-4.5 and SSP5-8.5 future scenarios.

However, index trends on its own are not as meaningful for economic impacts of droughts as the changes in characteristics of harmful events. The severity of both extreme dry and wet events could massively increase without changing the trend. Further, slight shifting towards dryer climate may result in the same trends as an increase in extreme droughts. Therefore event based characteristics of droughts are calculated in the next section.

For each index the characteristical frequencies, durations and mean index values are calculated for moderate and extreme drought events as described in Section 3.4. Such events are consecutive months with normalized index values below -0.5 (moderate) or below -1 (extreme). The multi-model mean of the SC-PDSI characteristics for this period is shown in Figure 5.7. Their standard deviations along the different datasets can be found in the Appendix (A.12). Locations without predicted extreme events have a frequency of zero (yellow), which leads to missing values (white) for other characteristics, requiring existing events.

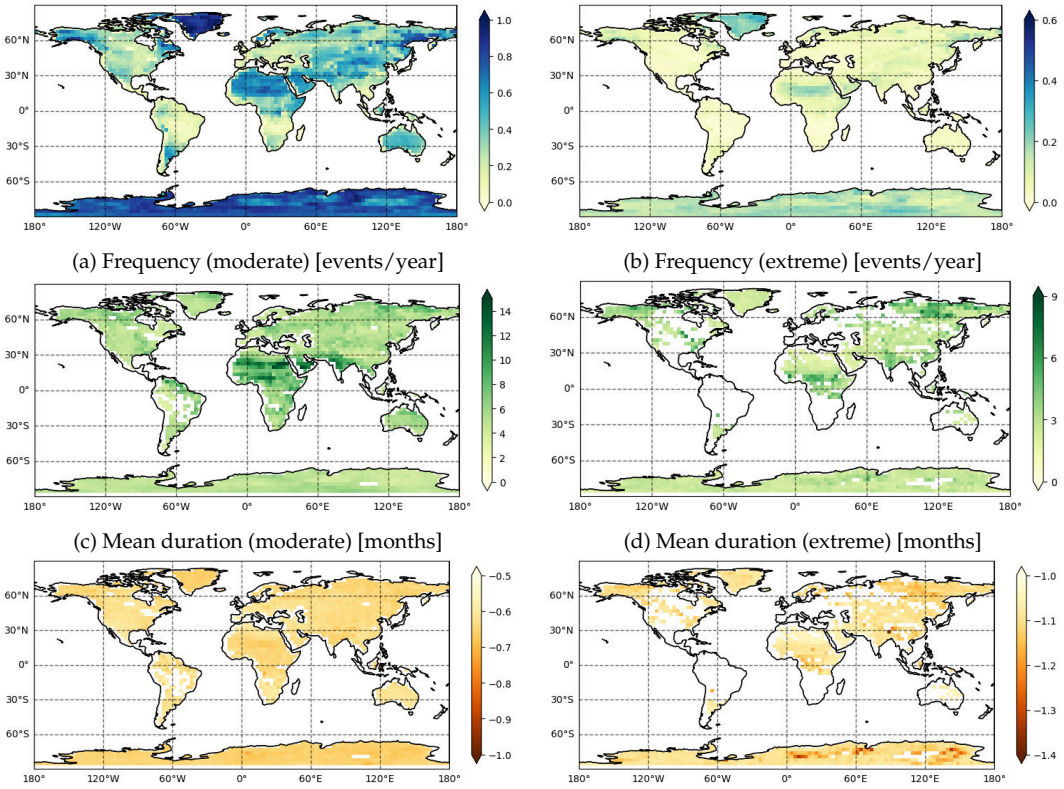

(a) Frequency (moderate) [events/year]

(b) Frequency (extreme) [events/year]

(c) Mean duration (moderate) [months]

(d) Mean duration (extreme) [months]

(e) Averaged Index (moderate)

(f) Averaged Index (extreme)

Figure 5.7: Characteristics based on normalized SC-PDSI calculated globally for the historical period 1900-2014. Sub-figures (a, c, e) consider moderate droughts with an index threshold of -0.5. For extreme droughts (index < -1) characteristics are shown in (b, d, f). Corresponding standard deviations can be found in Figure A.12.

More than one moderate drought every two years can be found in Northern Africa and parts of Asia averaged over the historical period 1900-2014. The average duration of these events is between 4 and 8 months, except some locations in India and North Africa, where events with durations of more than 10 months on average occur. For extreme droughts the frequencies (less than 0.4 events per year) and average durations (less than 5 months) are significantly lower then for moderate droughts. The average index is close to the threshold of -1, while the SC-PDSI during moderates droughts is between -0.6 and -0.7 globally.

The highest variance can be found in the frequencies, where up to 3 events per year are considered as extreme droughts in northern Africa, Antarctica and Greenland. Due to the simple water balance model, which does not consider snow coverage, the resulting Palmer indices are not expected to reliably indicate droughts in polar regions. Since the SC-PDSI distribution has been calibrated along the 2.3%-percentile at SC-PDSI of -1, the low frequencies and durations everywhere else match the expectations. For the future scenarios SSP2-4.5 and SSP5-8.5 the characteristics of the SC-PDSI

are similar, but different compared to the reference period (Figure A.4 and A.5). The regional differences in the characteristics and those between the SSP2-4.5 and SSP5-8.5 future scenarios are evaluated in the next part for the SC-PDSI and the SPEI.

5.2 The Role of SSPs in Agricultural Drought Development

In the first part is shown that the SPI, which is purely based on precipitation, describes meteorological droughts and their response to changing precipitation patterns in future climate scenarios. However, it does not consider thermodynamic processes in the atmosphere, whose significant impact on the establishment and intensity of agricultural droughts are confirmed. Moreover, the PDSI highly correlates with the SC-PDSI, which is adjusted to the local climate. Due to the advantages of the SPEI and SC-PDSI over their predecessors, the following analysis focus on these two indices, while some figures for the PDSI and SPI are provided in the appendix for the interested reader. The previously discussed trend and event based characteristics are averaged over the climatic similar IPCC AR6 WG1 reference regions shown in Figure 2.2 to examine the role of different SSPs in future development of agricultural droughts.

Frequencies, mean duration and mean averaged indices for moderate and extreme droughts are shown in Figure 5.8 and 5.9 for the SSP2-4.5 future scenario. The colours are used to visually support the differences of the values written in the hexagons.

In the SSP2-4.5 future scenario roughly 0.5 $\pm$0.1 moderate drought events per year are predicted by both indices in some regions of Europe, America and Asia (WCE, EEU, WSB, WCA and CNA), while most of the other regions have frequencies between 0 and 0.5 events per year. For the SPEI the hotspot with most moderate droughts in East Central Asia is spread out to the neighbour regions WCA, WSB, ESB and TIB and significant more events are predicted for Western and Eastern Europe such as South America by the SPEI compared to the SC-PDSI. In the subtropics around the Mediterranean (MED, WCA, SAH and ARP) the frequencies of moderate droughts are lower, but their mean duration is increased up to 10 months according to the SC-PDSI and up to more than three years by the SPEI (ARP). For many subtropic regions, especially the arid area from Western Africa up Eastern Central Asia, the SPEI predicts moderate dry conditions for three to six months per year. The SC-PDSI shows similar average moderate drought durations for most parts of the Earth, except the Mediterranean and its surrounding regions. Following the SC-PDSI no moderate droughts lasting for more than a year is predicted in this future scenario. In the regions where SPEI and SC-PDSI differ the most (SAH and ARP) an average index

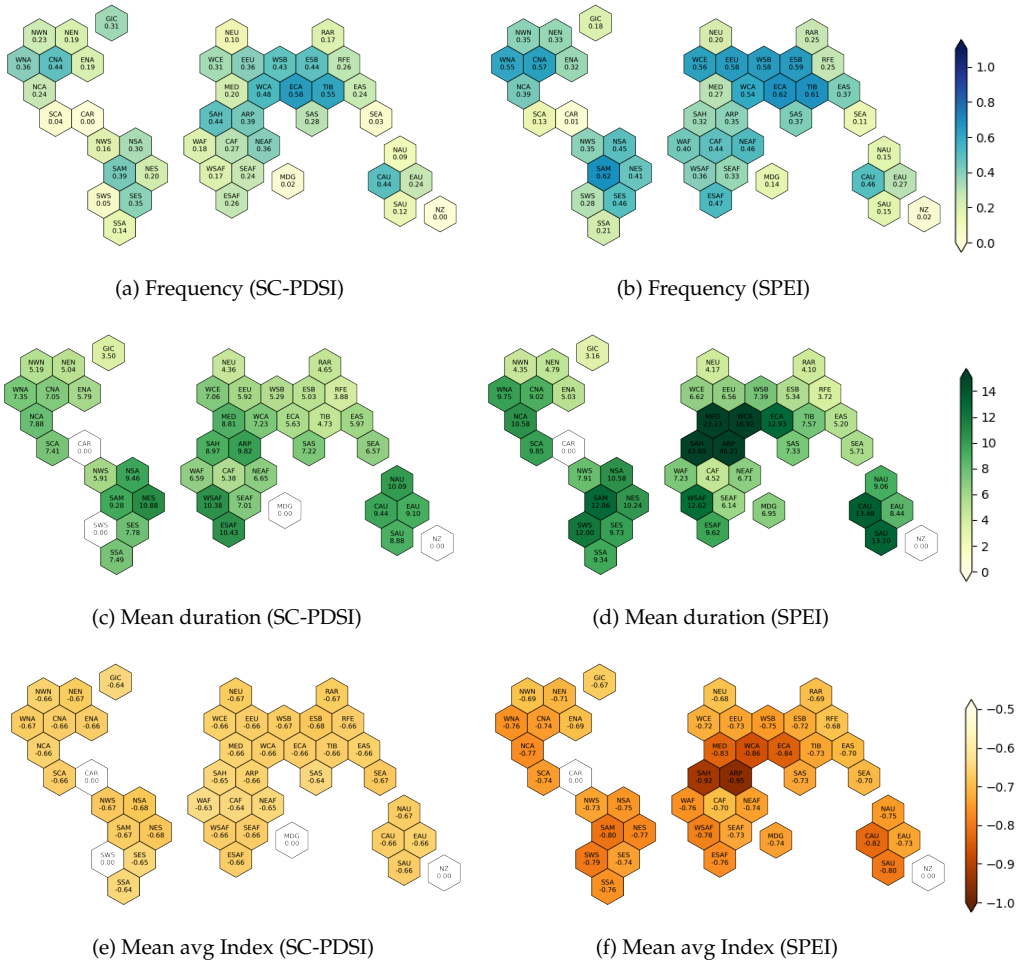

(a) Frequency (SC-PDSI)

(b) Frequency (SPEI)

(c) Mean duration (SC-PDSI)

(d) Mean duration (SPEI)

(e) Mean avg Index (SC-PDSI)

(f) Mean avg Index (SPEI)

Figure 5.8: Characteristics based on different indices for moderate droughts in the SSP2-4.5 projection from 2015 to 2100 . Colours are used to visualise the respective characteristic value of each hexagon. Mean duration is given in months and frequencies in events/year. Severities and indices are unit-less. Values are averaged over AR6 WG1 reference regions and shown in the respective hexagons.

value close to -1 is shown which indicates almost extreme dry conditions for several years. However, this regions are arid and mostly covered by bare ground without trees, crops or grass (Ziehn et al. 2020; Figure A.3). Both indices have known limitations under this conditions. The mean average SC-PDSI over moderate droughts for each region spreads -0.54 and -0.67, which is consistent to the observations for the historical period (1900-2014) in Figure 5.7.

Extreme drought events are consecutive months with index values below -1. They are less frequent than moderate events by definition. Figure 5.9 shows frequencies and mean durations of extreme droughts in the SSP2-4.5 scenario (2015-2100). Both indices agree in the spatial pattern of the frequency. Most events occur in the arid regions SAH, ARP, WCA, ECA and at around

some spots in North and South America (CNA, WNA, SAM). However, the SPEI shows roughly three times more extreme droughts in most regions. Frequencies of 0.53 events per year with an average duration of 7.5 months can be found for Western Central Asia (Fig. 5.9 (b), (d)), which would correspond to roughly one six months lasting extreme drought every two years. The occurrence rate for this region would be 33% which is more than 10 times larger than the 2.3% of the historical baseline (1900-2014). According to the SC-PDSI the occurrence rate for extreme events in Western Central Asia in the SSP2.4-5 scenario is 3.4%. In agreement to moderate droughts the mean event durations differ most in the arid regions.

Only the frequencies based on SPEI reach 0.5 per year and more for extreme droughts in the arid regions SAH, ARP, WCA, ECA. In this regions the SPEI shows also mean durations of 15 for this extreme events. The PDSI shows some long term extreme droughts with more than 10 months in South America as well. The frequencies and or durations and therefore the severities of moderate and extreme droughts based on SC-PDSI and SPEI are higher for most regions in future scenarios compared to the historical reference period.

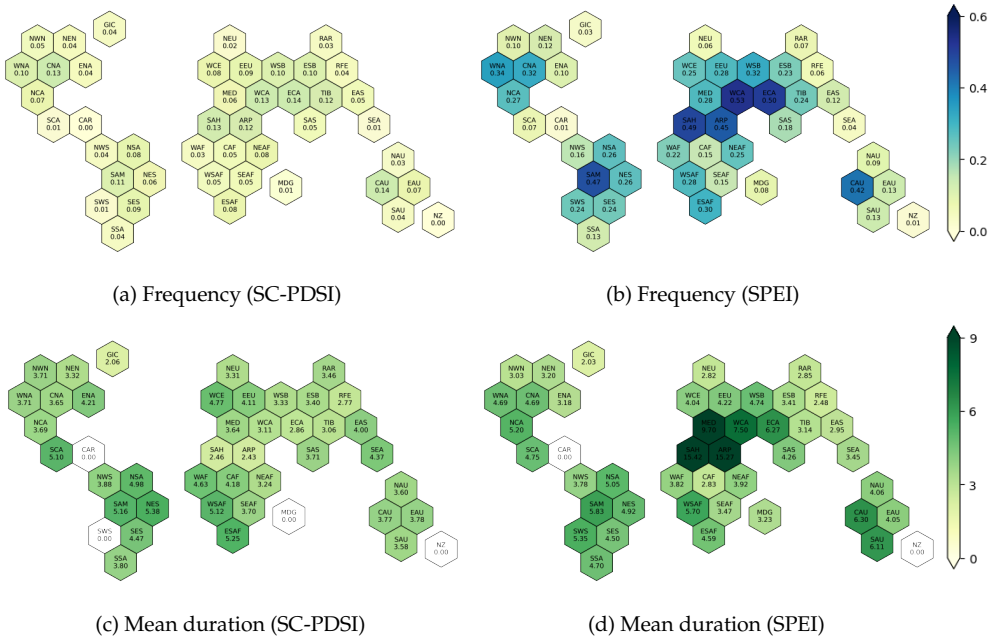

(a) Frequency (SC-PDSI)

(b) Frequency (SPEI)

(c) Mean duration (SC-PDSI)

(d) Mean duration (SPEI)

Figure 5.9: Similar to 5.8, but for extreme droughts in the SSP2-4.5 Scenario.

The SSP5-8.5 future scenario, which represents an anthropogenic forcing of 8.5 Wm^{-2} at the end of the century, showed larger positive temperature trends (Fig. 5.6 c,d) and enhanced positive and negative trends depending on the region (Fig. 5.6 a,b). The global mean temperature is for the historical period and both future scenarios is shown in Figure 5.10. SSP5-8.5 shows a more drastic increase of temperature over the next decades. In 2100, at

the end of the analysed period, a total increase of roughly 5.5 K can be seen, while the temperature in the SSP2-4.5 only rises by roughly 2.5 K.

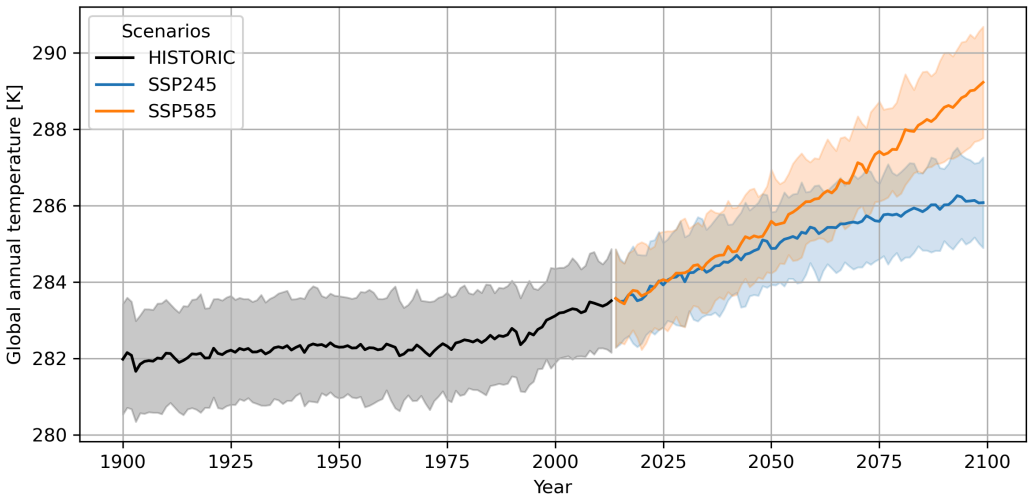

Figure 5.10: The global averaged annual temperature for different scenarios. The filled area around the lines indicate the standard deviation of the multi-model mean. The data have been derived from monthly minimum and maximum temperatures, that have been used for index calculation.

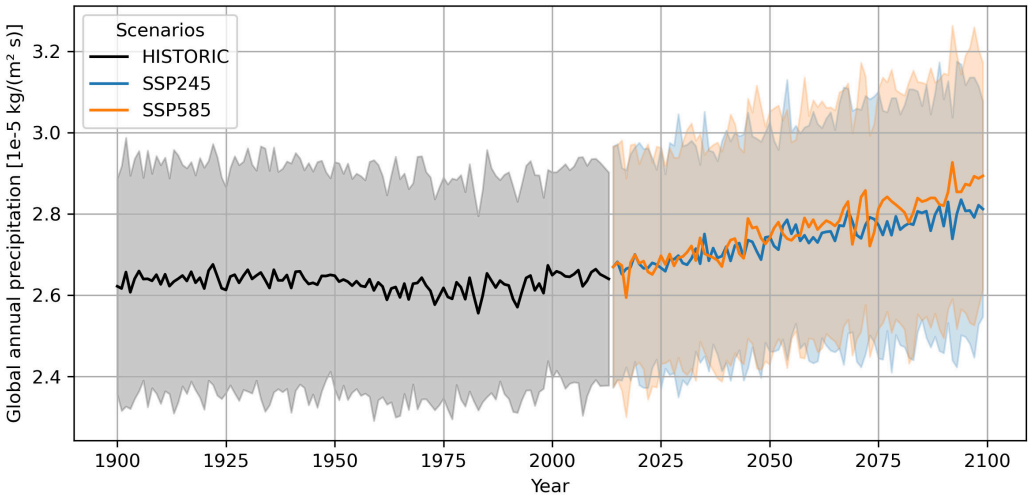

Figure 5.11: The global averaged annual precipitation for different scenarios. The filled area around the lines indicate the standard deviation of the multi-model mean. The data have been derived from monthly precipitation, that have been used for index calculation.

Multi-model standard deviations of the global mean are shown as shaded areas for the respective periods in 5.10 and 5.11. The latter Figure shows global precipitation. For the globally averaged annual precipitation in Figure 5.11 no significant difference can be seen. The slope for multi-model

mean temperature in the SSP5-8.5 scenario is slightly steeper than for SSP2-4.5, but this difference is small considering the multi-model standard deviations of both scenarios, which widely overlap. As already shown previously for trends of the full period, the precipitation change highly depends on the region (Fig. 5.6). That is especially the case for the future periods, whose precipitation trends are appended as Figure A.10.

To see the impact of the different SSPs on the regional frequency and mean duration, Figures 5.8 and 5.9 have been created for the SSP5-8.5 scenario as well (Fig. A.16 and A.17). The spatial differences are much larger than those between the scenarios, therefore difference plots showing the absolute and relative differences between frequency and mean duration of extreme droughts for both scenarios have been created and will be discussed instead.

Figure 5.12a shows several regions (NWN, NSA, EEU, WSB, ESB, TIB, WAF, CAF), where the frequency of extreme droughts differ by one or more event per year for the SC-PDSI. In panel b of Figure 5.12 the frequency is increased by more than one event per year for all regions except GLC, MED, ECA, MED, SAH, WSAF and SAU. Apart from Greenland this exceptions show an increase of mean extreme drought duration by more than 40%. It is likely, that several extreme events in this regions are merged into fewer long lasting super droughts in the SSP5-8.5. Extreme droughts in the SSP5-8.5 are extended in their duration compared to SSP2-4.5 for most of the regions. Greenland/Iceland (GIC) is the only region where less events and a shorter mean extreme droughts are found in the SSP5-8.5 than in the SSP2-4.5 scenario using the SPEI.

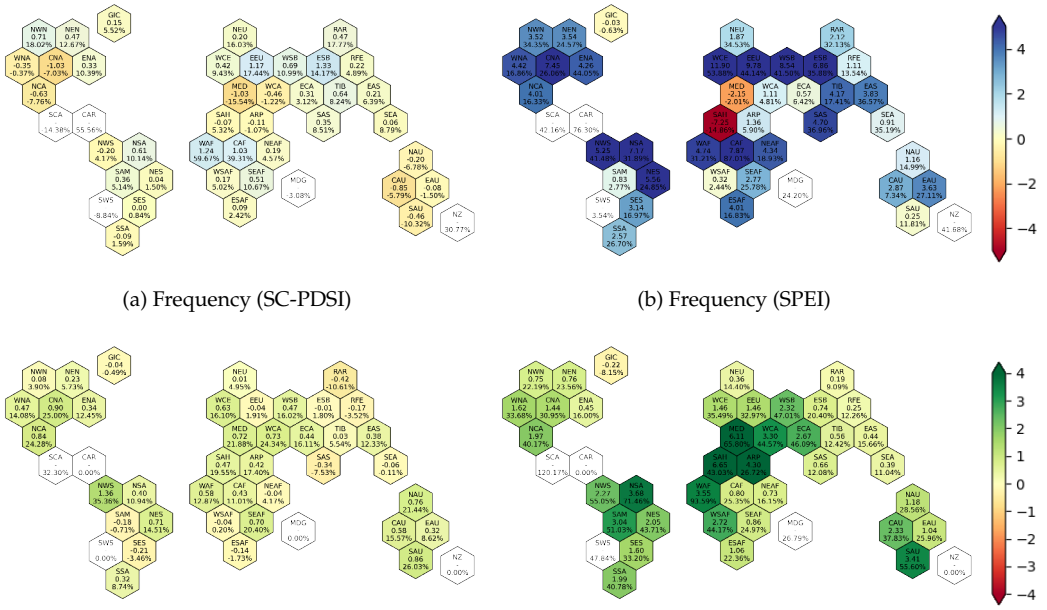

(a) Frequency (SC-PDSI)

(b) Frequency (SPEI)

(c) Mean duration (SC-PDSI)

(d) Mean duration (SPEI)

Figure 5.12: Differences of extreme drought frequency [months/100years] and mean durations [months]. The first number and colour of each hexagon is the absolute difference (SSP5-8.5-SSP2-4.5), while the second number is the difference relative to SSP2-4.5.

For the SC-PDSI and SPEI trends of the future period from 2015 to 2100 in Figure 5.13, one can see a general intensification and expansion of regions with negative trends. Both indices show negative trends during the future period around the Mediterranean, which expands towards Central Europe in the SSP5-8.5 future scenario. These findings agree with those from the long term trends in Figure 5.5, which is expected, since the full period (1900-2100) is just a combination of different future scenarios with the same data for the historical period. Possible causes for the differences between the indices have been discussed already. However, the trend values significantly differ for the future period. In South America, Central North America, South Africa and Australia mainly weak negative trends are found (0 to -0.25 per 50yr) for the SSP2-4.5 scenario, which are stronger in SSP5-8.5 (-0.25 to -0.5 50yr for SC-PDSI and less than -0.5 per 50yr almost anywhere for SPEI). According to the SPEI trend the normal conditions in 2100 are what have been considered as an extreme drought for the baseline period (1900-2014). This results should be treated carefully, since the trends for future scenarios show large differences between the datasets. The multi-model standard deviation for both future scenarios (A.9) is in the same order of magnitude as the calculated trends. Highest standard deviations can be found in the tropics (Central Africa and large parts of Northern South America). Nevertheless, subtracting the trends for the SSP2-4.5 from those

for the SSP5-8.5 scenario and averaging the differences along the reference regions leads to Figure 5.14.

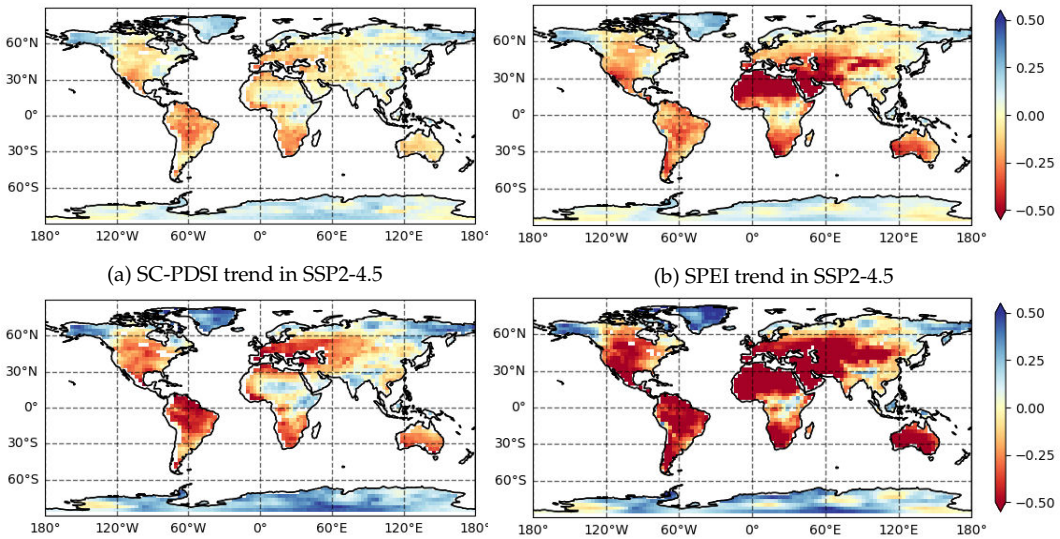

(a) SC-PDSI trend in SSP2-4.5

(b) SPEI trend in SSP2-4.5

(c) SC-PDSI trend in SSP5-8.5

(d) SPEI trend in SSP5-8.5

Figure 5.13: 50 year trend of SC-PDSI and SPEI in two different future scenarios SSP2-4.5 and SSP5-8.5 (2015-2100).

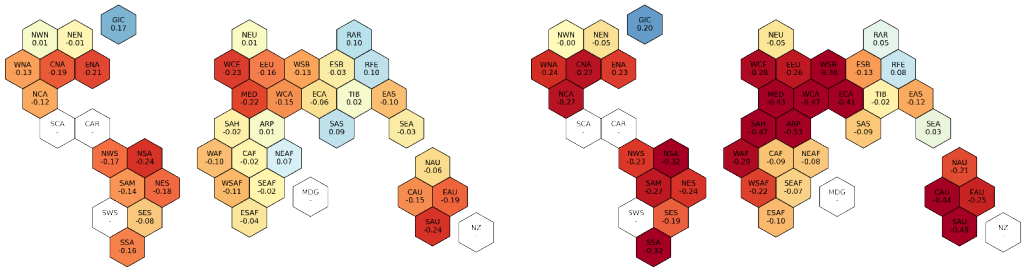

(a) SC-PDSI

(b) SPEI

Figure 5.14: The absolute difference between the multi-model mean 50yr trends for two future scenarios (SSP5-8.5-SSP2-4.5). The trends have been calculated for SC-PDSI and SPEI based on seven models for the period 2015-2100. Red (blue) colours indicate regions, where the SSP5-8.5 scenario shows lower (higher) trends. Yellow indicates similar trends and regions coloured white, provide not enough values to compare.

In Figure 5.14 only a few regions (GLC, RAR and RFE) show a positive trend difference, which means higher (or less negative) trends in the SSP5-8.5 compared to SSP2-4.5. For this regions, positive trends are found for both indices in Figure 5.13, meaning the regions are expected to change towards wetter climate in the future. The differences of SPEI trends in contrast to the

SC-PDSI trend differences show generally more and higher negative values. Comparing 5.14 with 5.13 one can conclude, that the indices change toward dryer conditions in arid regions, drought index trends found in SSP2-4.5 are intensified in SSP5.8-5 and the SPEI shows stronger trends and changes of the trends than the SC-PDSI. These agrees with the previously analysed event characteristics, showing more or longer extreme droughts with higher differences between the scenarios in the regions with negative trends.

To summarize the regional trends and changes of moderate and extreme droughts the statistical distribution of the SC-PDSI and SPEI is compared between the historical period (1900-2014) and the future scenarios SSP2-4.5 and SSP5-8.5 (2015-2100).

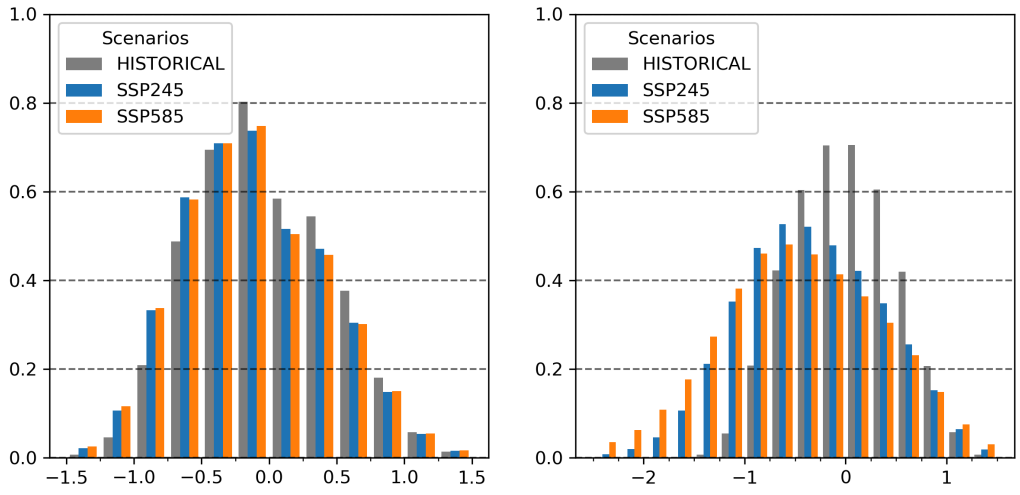

(a) SC-PDSI

(b) SPEI

Figure 5.15: Histograms of SC-PDSI and SPEI for the region between 60°S and 60°N. Indices collected over all seven datasets. The historical group shows index values from 1950 to 2014. SSP2-4.5 and SSP5-8.5 contain values from 2015 to 2100.

Figure 5.15 shows the statistical density distribution of index values derived from seven datasets as histograms for the region 60°S to 60°N in intervals of 0.25. Polar regions have been excluded because of two reasons. On one hand, they contain more outliers especially for the SC-PDSI, which does not consider snow coverage. On the other hand, Figure 5.15 is created without weighting the values by the area of their grid cells. The grey bars show the index values for the baseline period used to calibrate them. For the SC-PDSI, parameters are adjusted, so that 2% of previously approximated PDSI are above and below 1 and -1. For the standardized SPEI in contrast one can see the historical values following the exact symmetric normal distribution. Most SC-PDSI values are found between 0 and -0.25 for all periods and scenarios. One can see a general widening of the SC-PDSI distribution in the future. For both scenarios the peak is slightly lower and significant more

values below -0.5 are found and twice as much below -1, which means that the occurrence of moderate and extreme droughts around the globe will be significantly higher in the period from 2014 to 2100 predicted according to the SC-PDSI in both future scenarios. For the SSP5.8-5 scenario the occurrence of extreme droughts is even higher than for the SSP2-4.5 scenario. A general shift of less than 0.25 towards dryer conditions in the future can be found for SC-PDSI. This is small compared to the shift of the SPEIs mode from 0 in the historical period to roughly -0.75 in future scenarios. A mode of -0.75 means that moderate drought would be the most common or normal condition between 60°S to 60°N from 2014 to 2100. Overall the SPEI and SC-PDSI indices agree in a shift towards dryer conditions in both future scenarios, while the SSP5-8.5 with higher radiative forcing at the end of this century shows a significant higher occurrence of extreme droughts compared to the SSP2-4.5. The effect of drying by due to increasing PET is more dominant for the SPEI than the SC-PDSI resulting in larger differences of the scenarios especially for arid regions in the subtropics.

6. Discussion

For this thesis new diagnostics have been implemented to the ESMValTool to calculate PDSI and SC-PDSI based on CMIP6 data. The calculation time especially for the SC-PDSI, where an computational expensive calibration is required, can become a limitation. For 200 years of monthly data from seven datasets, it was necessary to reduce the resolution of the data to $3^\circ \times 3^\circ$, to keep the calculation time of SC-PDSI values below one day. Even if technical optimizations could reduce the calculation time, it is notable a disadvantage of the SC-PDSI. Event based characteristics especially for extreme events require a high temporal and spatial resolution. Agricultural droughts with spatial extends of more than 500km and durations of at least months can be found with the methods and data used in this thesis, but smaller events are possibly not resolved. Further, the quantitative results for the characteristics might depend on the resolution of the data.

However, resulting PDSI and SC-PDSI timelines have been shown to closely correlate with SPI and SPEI for the historical period. The order of magnitude of the indices converted back from normalization agrees with those in the literature (Dai, Trenberth, and Qian 2004). SC-PDSI trends based on observational data and reanalysis from 1950 to 2008 have been calculated by Dai (2011) using different PET approximations (Figure A.7). Comparing the trends of SC-PDSI based on the Penman-Monteith approximation for the PET considering temperature change from their Figure A.7d with the trends calculated in this thesis for the same time period based on model contributions to the CMIP6 historical experiment (Figure A.8b) shows agreement in some regions, but also some major differences. For his comparison the normalized SC-PDSI values are multiplied by 4 to match the original scale. In some regions of South America negative trends between 0 and -2 per 50yr can be found in both figures. The same accounts for Europe, South Africa and eastern Asia. In other parts of Asia trends between -1 and +1 per 50yr dominate. This study was not able to find the strong negative trends with less than -3/50yr as one can see in Figure A.7d in areas of North America central Africa and at the east coast of Asia. For central Africa positive trends have been calculated in this work. For the USA small absolute trends less than 2/50yr have been found in both studies, but again with different signs. Beside the input data, they used different reference periods and spatial resolution, which makes it difficult to address the discrepancies.

Findings of this thesis for drought occurrence change in future scenarios based on SPEI agree with recent publications. Balting et al. (2021) found

significant drought intensification in dry regions for the SSP2-4.5 and SSP5-8.5 future scenario of CMIP6 data. In contrast to this thesis, Balting et al. focused on the Northern Hemisphere during summer (June, July and August). They compared model projections for the historical baseline (1971-2000) to a future period (2071-2100) based on SSP1-2.6, SSP2-4.5 and SSP8-5.8. The resulting SPEI difference is shown in Figure A.18, where panel b and c show the same spatial pattern as long term trends (1900-2100) of the SPEI (Fig. 5.5 g and h) calculated for this thesis. The strong trend towards lower SPEI values agree with the regions around the Mediterranean of high differences between the historical and future periods in Figure A.18 for SSP2-4.5 and SSP5-8.5. Similar negative trends at the South-West coast of North America and small positive trends in some regions in the North of Asia and North America can be found in both studies too. To compare the absolute difference between two periods with 100 years distance with the normalized (by 2) 50 year trend of this thesis. The trend values have to multiplied by four. In the Center of North America Figure A.18 shows SPEI differences from 0 to -1 for the SSP2-4.5 and -0.5 to -1.5 for the SSP5-8.5 scenario. The rescaled SPEI trends for corresponding regions are between 0 and -0.8 (Fig. 5.5 g) and -0.4 and -1.2 (h). The regional changes of the SPEI agree in their pattern and quantities. The drought occurrence rates found by Balting et al. cannot be exactly confirmed by this thesis, since different thresholds and different sets of models have been used throughout the studies. However, a general stronger increase of frequency and duration 5.12 and a general shift towards more intense droughts for the SSP5-8.5 scenario compared to SSP2-4.5, have been found as well.

Understanding of drought indices, their differences and their ability to consider changing climate conditions, is an intermediate goal of this thesis. An effect of drying caused by increased PET, as a result of global warming is described in the literature and confirmed by the results. While the SC-PDSI correlated well with the SPI for the reference period, one can see stronger trends towards negative indices and hence a tendency to stronger or more frequent droughts in the three indices involving PET. PDSI and SC-PDSI rely on the same physical approach of a water balance model in contrast to the SPEI. Considering PET is advisable in research about the impact of changing climate to drought characteristics (Vicente-Serrano, Beguería, and López-Moreno 2010). This does not hold the other way around. The consideration of PET does not automatically improve an index. The effect of PET may be under- or overestimated and should be validated on reliable soil moisture data under warming conditions. This problem have been proposed for the SPEI by Rehana and Monish (2021).

Overall, a global tendency towards more severe and frequent agricultural droughts can be concluded from the results in agreement with the assessments for atmospheric-based drought indices of the IPCC AR6 (Seneviratne

et al. 2021). According to Seneviratne et al. (2021), the spatial extent of droughts predicted by atmospheric-based drought indices is expanded to most of North America, Europe, Africa, Central and East Asia and southern Australia. The differences between trends and characteristics for SPI and the PET-based indices agree partly, but have not been analysed for future projections explicitly, within this thesis. The comparison of the SSP2-4.5 and SSP5-8.5 showed an increase in frequency of extreme drought events in future projections, which is even stronger in SSP5-8.5, the scenario with the higher forcing level. This agrees with the conclusion of Seneviratne et al. (2021), that the probability of drought hazards is rising with increasing forcing levels of different future scenarios. An important spread of PDSI-PM and SPEI-PM exists in future projections among different models (Seneviratne et al. 2021, Cook et al. 2014). This spread also exists for the SC-PDSI and SPEI among the seven models used in this thesis. The multi-model standard deviations of trends in future scenarios (Fig. A.9) is of the same magnitude as the multi-model means (Fig. 5.13)).

The results as a whole can facilitate to the superior goal of understanding the impact of a changing climate on characteristics and trends of droughts on the global scale. IPCC AR6 summarized, that different drought types respond differently to increasing greenhouse gas concentrations and can be associated with different impacts (Seneviratne et al. 2021). A lack of sufficient soil moisture, due to precipitation deficit or evaporation, sometimes amplified by increased atmospheric evaporative demand, result in agricultural and ecological drought (Chen et al. 2021). Further IPCC AR6 found high confidence in thermodynamic processes being the main driver of drought changes under human-induced climate change (Seneviratne et al. 2021). This agrees with the results of the index comparison in this thesis. The SPI which does not directly consider the thermodynamic processes was not able to detected drying trends in several regions, predicted by the other indices, based on PET.

Strengths and weaknesses of the evaluated indices for application to future projections and climate change research that stood out during this thesis are summarized in Table 6.1. The SPI is comparably easy to calculate and solely based on precipitation which is widely available in simulation output and observations. Changes in climate are only indirectly considered by this index in the way they affect the precipitation. Effects that lead to drying by evaporation and transpiration are not included and therefore the index is not suited for research in changes in agricultural droughts. The PDSI, in contrast, is based on PET in addition to precipitation and therefore aware of temperature changes and it involves a physical water balance model, which can further differentiate between temporal variability in precipitation. The results and the literature showed that its spatial comparability is very limited and therefore the SC-PDSI should be considered instead, especially for

global studies. Its water balance model, based on physical properties of the soil and atmosphere, considers several direct and indirect influences of a changing climate, but requires significantly more computation time and additional input variables. Some components, that may become important when discussing changes in droughts are not considered by the SC-PDSI, i.e. water storage, streamflow, snowfall land-use and change of vegetation (Dai, Trenberth, and Qian 2004).

Table 6.1: Advantages and disadvantages of the SPI, SPEI, PDSI and SC-PDSI for application in climate change research based on model predictions.

Index	Advantages	Disadvantages
SPI	requires only precipitation; low computational effort	no consideration of temperature; not suited for agricultural droughts
SPEI	considers PET; widely used in drought research	might overestimate impact of PET
PDSI	physical simulation of soil; widely used in the USA; considers PET for water balance	not comparable across regions; complex calculation
SC-PDSI	physical simulation of soil; considers PET for water balance	even more complex calculation

The SPEI is primarily based on the statistical distribution of precipitation, but also accounts for temperature changes through PET, in contrast to the SPI. Compared to the PDSI, the SPEI is more sensitive to PET (Seneviratne et al. 2021; Cook et al. 2014; Vicente-Serrano et al. 2015), which agrees with the findings of this thesis, that differences between the SC-PDSI and SPEI trends are higher regions with strong PET trends. It is likely, that SPEI overestimates PET in arid regions (Rehana and Monish 2021), which promotes the SC-PDSI over the SPEI for this regions.

Anthropogenic influence to the changes in drought could be analysed based on the results to some extend. The reference period starts several decades after the beginning of the industrial revolution and anthropogenic impacts are already considered in the determination of the climatic appropriate precipitation. The differences in characteristics for different future scenarios, however, are directly linked to the socioeconomic pathways. The results are not sufficient to be used in political decision making, as they are purely based on physical processes. To link the droughts to their ecological consequences or food or fresh water security for humans is beyond the scope of this study. The term agricultural drought may indicate direct impacts on agricultural industry and food security, but in the scope of this work is purely used to describe a specific type or category of droughts. The actual crop yield highly depend on the type of crop and its state of growth. To

face this type of research question soil and atmospheric properties and several other circumstances i.e. the possibility of irrigation must be taken into account on a regional level.

7. Summary and Outlook

To compare the most widely used drought indices SPI, SPEI, PDSI and SC-PDSI, two diagnostics have been developed for the ESMValTool v2. One for calculating the PDSI and SC-PDSI values and another to apply different metrics and characteristics to normalised monthly drought indices (including SPI and SPEI). Required monthly input variables for each index are taken from the same CMIP6 models (ACCESS-ESM1-5, AWI-CM-1-1-MR, CMC-ESM2, CANESM5, MIROC6, MPI-ESM1-2-LR, MRI-ESM2-0). The once calculated PET is reused by the SPEI, PDSI and SC-PDSI. The period 1900-2014 is used as baseline to calibrate all indices and two future scenarios SSP2-4.5 and SSP5-8.5 are analysed for the period 2015-2100.

For the seven CMIP6 models analysed in this thesis, the PDSI and SC-PDSI qualitatively agree and are highly correlated everywhere as expected. The original PDSI makes use of constants, that have been experimentally determined for locations within the USA based on observational data available in 1965, which leads to systematic under- or overestimations in regions with different climate. The SC-PDSI overcomes this problem by recalculating such constant based on reference data for each location. The produced results for SC-PDSI generally agree with those for SPEI except for arid areas of North Africa, Middle East and Central Asia. The overestimate of the PETs drying effect by SPEI for arid regions could be related to this. The applicability of the SC-PDSIs underlying water balance model to simulate extreme arid regions is still uncertain and makes the SC-PDSI less reliable for this regions.

To avoid loosing information about drought events in spatial, temporal or multi-model means, trends and characteristical properties of the occurring events in a given period of time for moderate and extreme droughts have been calculated. This includes the frequency, duration, severity and average index of events below the thresholds -0.5 and -1 for normalized indices. These characteristics are cumulated and multi-model means have been applied globally. Spatial averages over the IPCC WG1 reference regions have been calculated to visualize regional timelines and simplify comparing between scenarios and with the synthesis in the AR6.

For the analysed period 1900 to 2100 a dominating drying trend could be found for the SPEI strongest in arid regions from the Sahara over the Middle East to Central Asia. This large area experiences SPEI trends of less than -1 per 50yr (rescaled from normalization in the figures). The SC-PDSI shows

generally less extreme trends to PDSI and SPEI, while the spatial characteristics of both other indices can be affirmed. The areas with positive and negative trends are roughly balanced for the SC-PDSI and negative trends are dominant for the SPI. The causes for the most extreme trends and the differences between the indices could be linked to changes in the most important input variables.

Roughly 0.5 moderate drought events per year could be found for all indices in parts of Europe and Asia in the SSP2-4.5 future scenario and less in most of other regions. Extreme droughts are rare with typically less than 0.2 events per year. Only the SPEI shows frequencies of more than 0.5/yr with mean durations of more than a year. The frequencies or durations of drought events increase in the SSP2-4.5 and SSP5-8.5 future scenarios according to SC-PDSI and SPEI.

Both future scenarios (2015-2100) show more total number of months with moderate or extreme drought conditions according to the SPEI and SC-PDSI, than the reference period (1900-2014). Frequency or duration of drought events is significantly increased, compared to the reference period. For the SSP5-8.5 scenario the probability of extreme drought is higher than for SSP2-4.5, which agrees with recent literature Balting et al. 2021. While this holds for the SC-PDSI and the SPEI, the effect is significantly stronger for the SPEI compared to the SC-PDSI. This is especially the case in arid regions around the Mediterranean, where the largest negative trends have been found and linked to increasing PET. The huge differences are likely due to different implementations of PET between SPEI and SC-PDSI. The SC-PDSI limits the amount of water that can evaporate in a certain time with the amount of water in the upper soil layer. SPEI might overestimate the impact of PET, since it has no limitation like that. However, an underestimation of role of PET might be an other reason. Further evaluation of the change of input variables could be done for the arid regions to understand the processes causing the differences.

The presented results could be extended by CMIP6 models, scenarios and other monthly drought indices using the existing methods. A huge part of evaluation is designed to be applied to a regional selection of the data. This could be used to recreate some of the results explicitly for specific regions with more datasets and higher spatial resolution. The results have shown very different index behaviours and large multi-model standard deviations for tropical regions mainly covered by deserts. Further scientific research focusing on these regions may provide a deeper understanding, that may be transferred back to the global scale. From a technical perspective the created diagnostic could be optimised for parallel computing to consider more than seven CMIP6 models or increase the spatial resolution at the same computation time. While the results have been compared to literature and other findings based on CMIP6 simulations, the input variables have not been

evaluated in this thesis. A comparison of the historical simulation with variables and derived drought indices from observational or reanalysis data for the same period, would be a useful follow up study to provide insights into the performance of individual models and the multi-model mean.

The results have been shown to be highly dependent on the PET, where only one of many available approximation methods have been used. Many assumptions have been done i.e. the crop height, which impact the resulting PET and therefore the index values. McColl proposed 2020 an alternative to the Penman-Monteith evapotranspiration to overcome an conceptual error of the Penman-Monteith equation. ESMs provide PET as predicted variable, which probably make use of internal model components and data that is not included in most of the traditional approximations. This way actual simulated data from a coupled biospheric model could be used to account for changes in plant types. Further research could be done including different types of PET approximations or model predictions. Rehana and Monish (2021) further proposed a method to restructure the SPEI to use estimations of actual evapotranspiration instead of PET for water-limited areas.

One motivation for developing precipitation and temperature based drought indices over the last decades are the sparse measurements of evaporation and soil moisture in observational data. However, this is not necessarily the case for datasets produced by ESMs, which often simulate dense hydrological data. Several of the CMIP6 contributing models calculate soil moisture for multiple layers. Soil moisture anomaly is an indicator for agricultural droughts. Its correlation with the PDSI have been globally examined by Dai, Trenberth, and Qian (2004). They found a significant correlation between 0.5 and 0.8 with highest values in the late summer under warm conditions and low impact of melting snow, which is not accounted by the PDSI. Using soil moisture anomaly or soil moisture based indices could overcome some of the mentioned limitations of the PDSI and SC-PDSI (Dai, Trenberth, and Qian 2004). This work could be continued by including soil moisture anomaly based on the reference period and comparing this to the existing indices.

A. Additional Figures

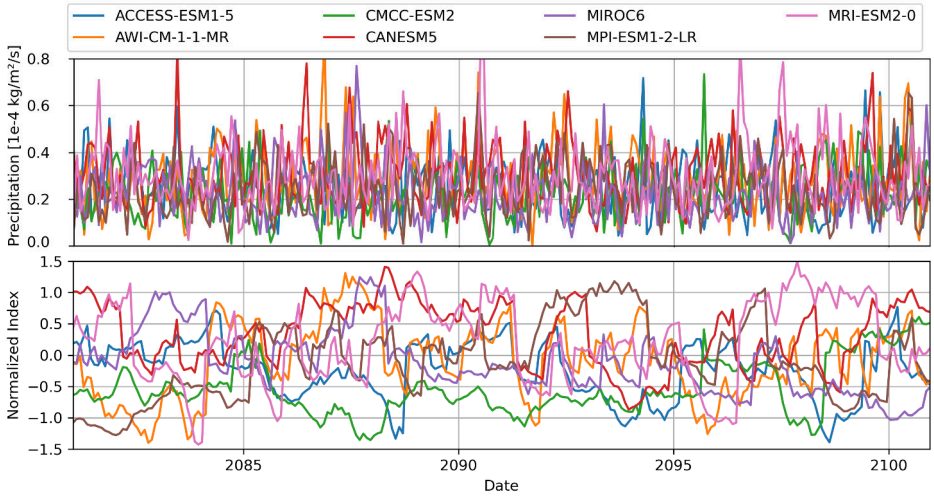

Figure A.1: Precipitation and normalized SC-PDSI based on seven different CMIP6 models for the last 20 years of the SSP2-4.5 future projection (2080-2100) on a shared time axis at a location close to Moscow.

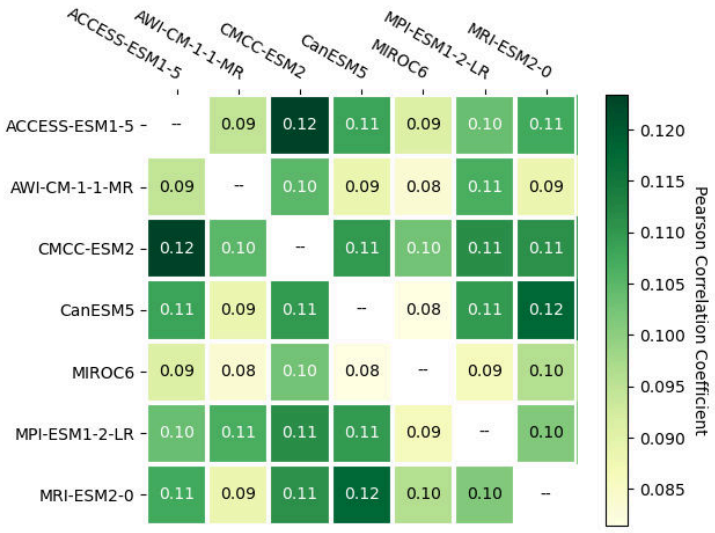

Figure A.2: Globally averaged cross correlations of SC-PDSI values between all analysed datasets in the combined historical-SSP2-4.5 scenario (1900-2100).

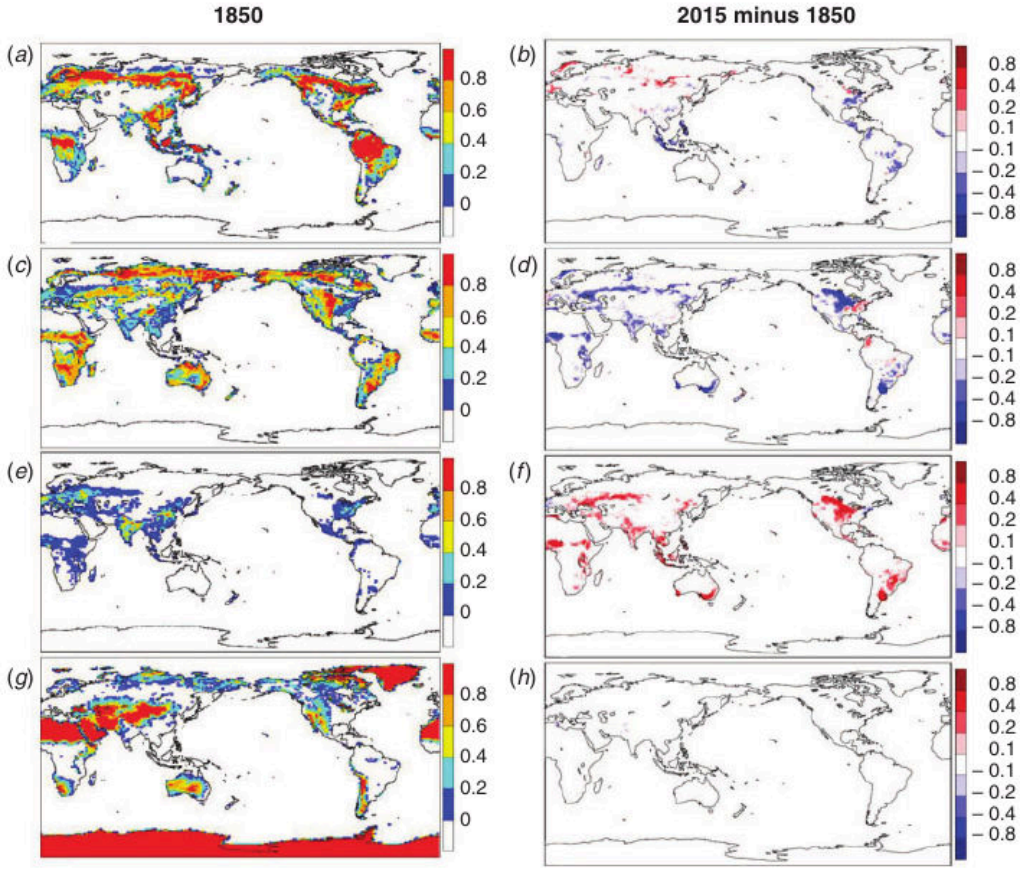

Figure A.3: Grid-cell fraction of (a) trees, (c) grass and shrubs, (e) crops and (g) lakes, ice and bare ground for 1850 and the change in grid-cell fraction between 2015 and 1850 for (b) trees, (d) grass and shrubs, (f) crops and (h) lakes, ice and bare ground. (taken from Ziehn et al. 2020)

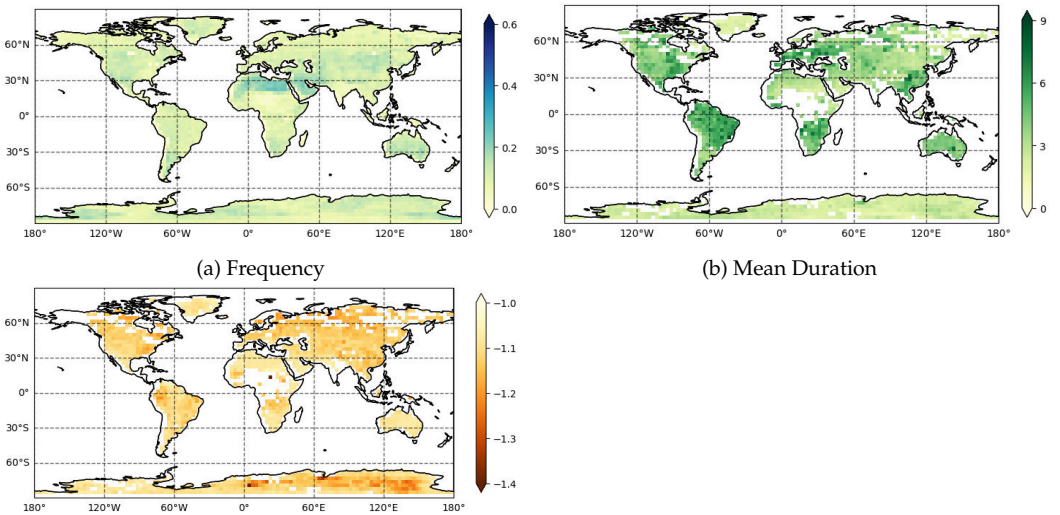

(a) Frequency

(b) Mean Duration

(c) Averaged Index

Figure A.4: SC-PDSI characteristics calculated globally for the SSP5-8.5 (2014-2100).

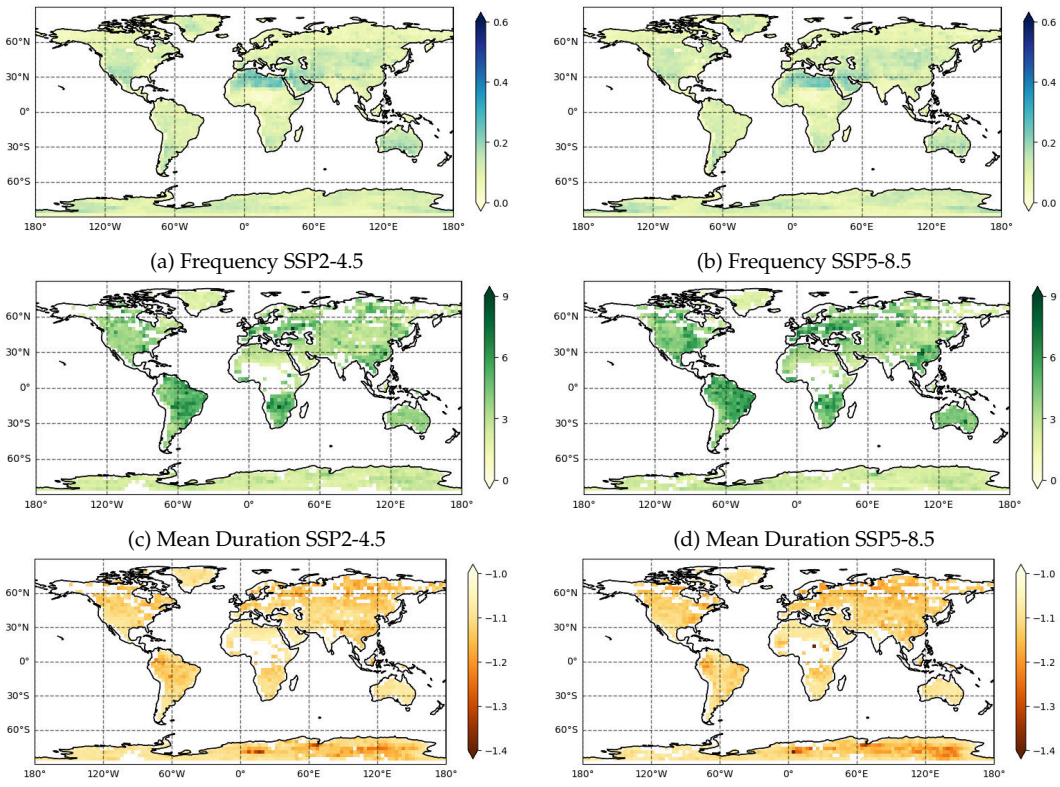

(a) Frequency SSP2-4.5

(b) Frequency SSP5-8.5

(c) Mean Duration SSP2-4.5

(d) Mean Duration SSP5-8.5

(e) Averaged Index SSP2-4.5

(f) Averaged Index SSP5-8.5

Figure A.5: Characteristics based on normalized SC-PDSI calculated globally for two experiments SSP2-4.5 and SSP5-8.5 (2014-2100).

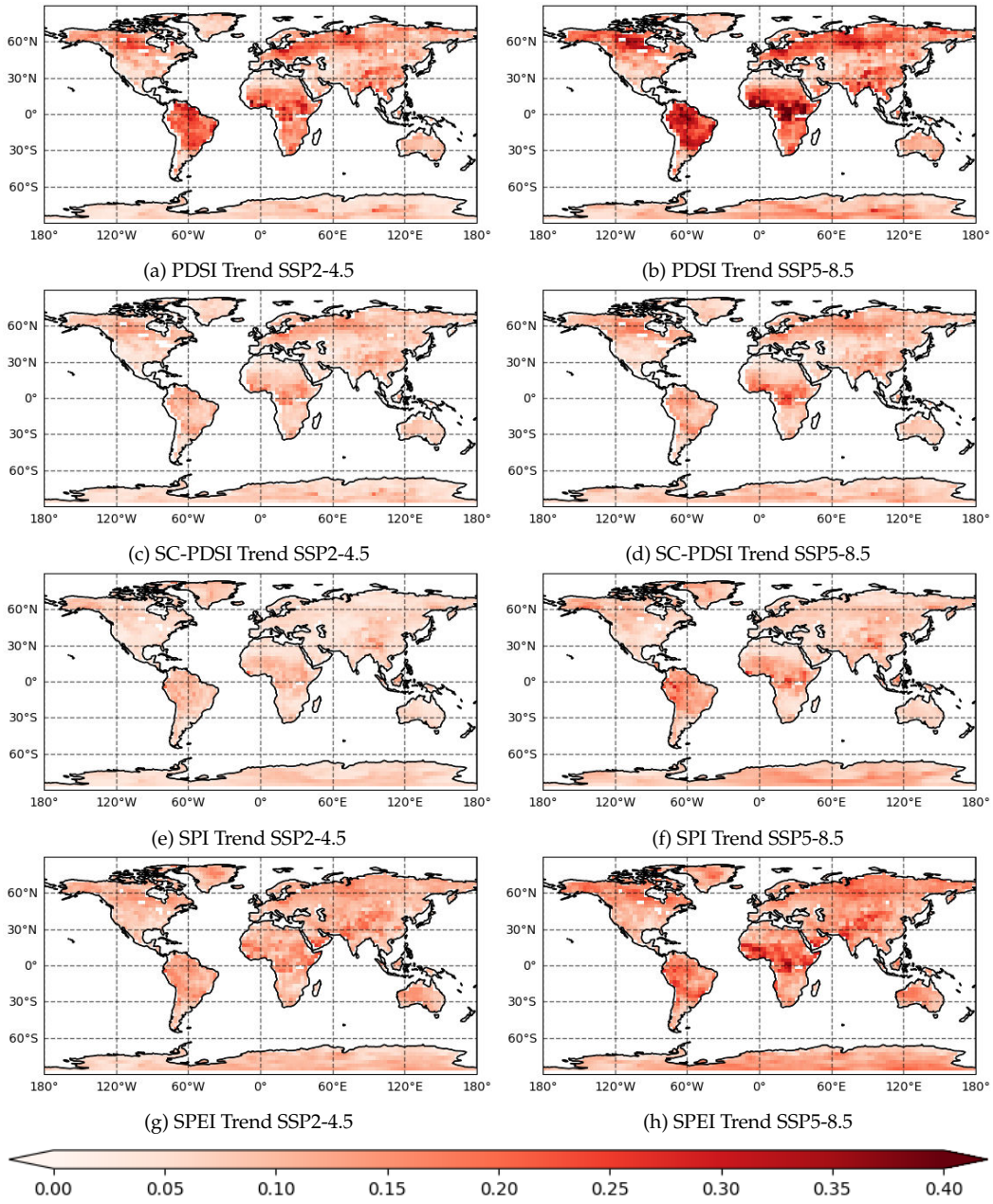

(a) PDSI Trend SSP2-4.5

(b) PDSI Trend SSP5-8.5

(c) SC-PDSI Trend SSP2-4.5

(d) SC-PDSI Trend SSP5-8.5

(e) SPI Trend SSP2-4.5

(f) SPI Trend SSP5-8.5

(g) SPEI Trend SSP2-4.5

(h) SPEI Trend SSP5-8.5

Figure A.6: Multi-model standard deviations of long term trends (1900-2100) of drought indices in historical experiment combined with SSP2-4.5 and SSP5-8.5 future scenarios.

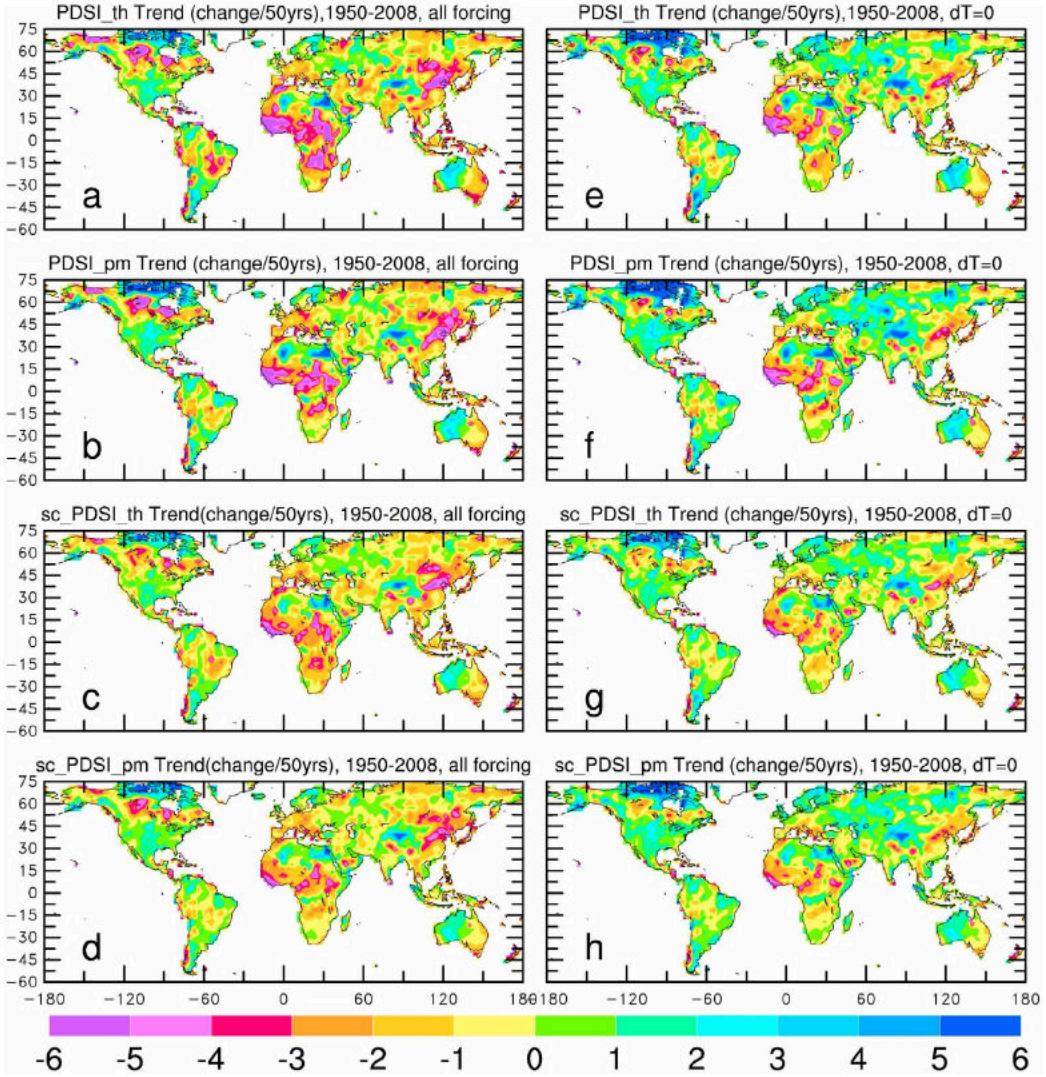

Figure A.7: Trend maps (red, drying, change per 50 years) in the four forms of the annual PDSI from 1900 to 2014 computed using (a, b, c, d) all forcing data and (e, f, g, h) all but no temperature changes for PDSI_th (a, e), PDSI_pm (b, f), SC-PDSI_th (c, g), and SC-PDSI_pm (d, h). Figure taken from Dai 2011.

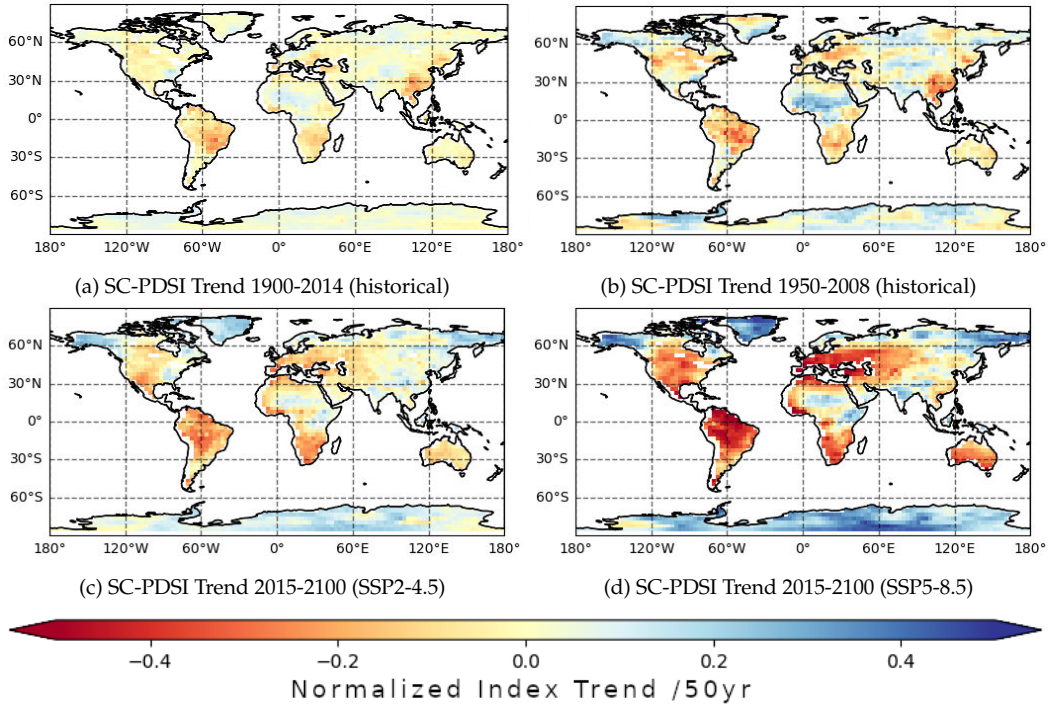

(a) SC-PDSI Trend 1900-2014 (historical)

(b) SC-PDSI Trend 1950-2008 (historical)

(c) SC-PDSI Trend 2015-2100 (SSP2-4.5)

(d) SC-PDSI Trend 2015-2100 (SSP5-8.5)

Figure A.8: SC-PDSI trends for the reference period and two future scenarios. The period 1950-2008 have been included for comparison with literature.

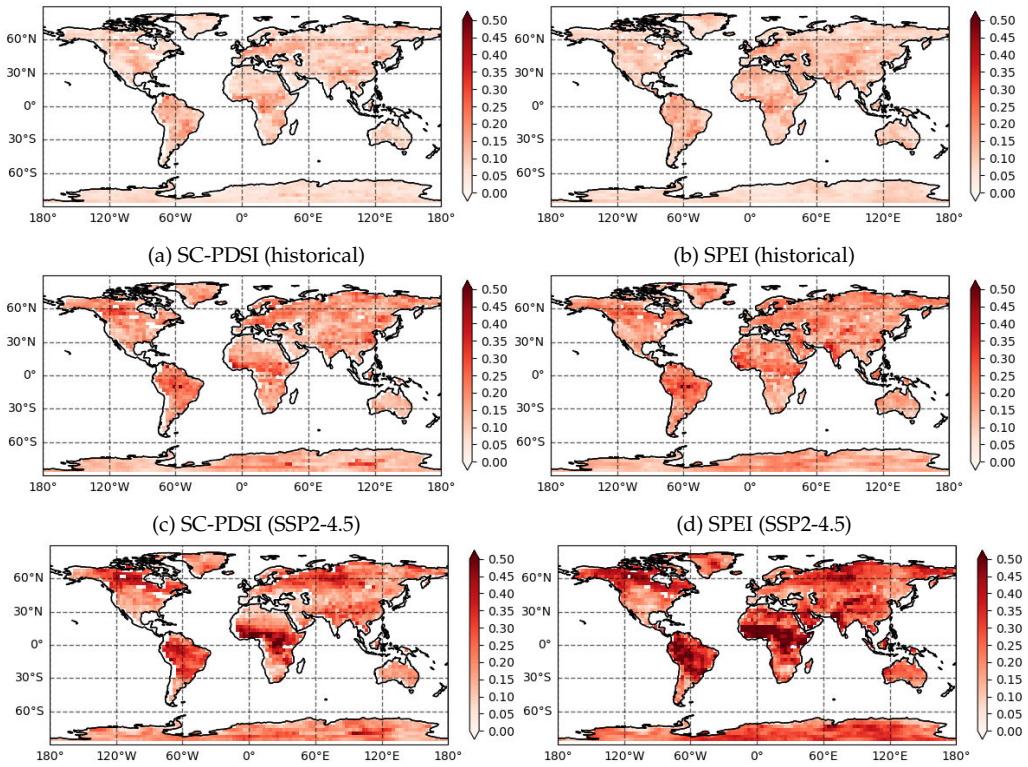

(a) SC-PDSI (historical)

(b) SPEI (historical)

(c) SC-PDSI (SSP2-4.5)

(d) SPEI (SSP2-4.5)

(e) SC-PDSI (SSP5-8.5)

(f) SPEI (SSP5-8.5)

Figure A.9: Multi-model standard deviations of SC-PDSI and SPEI trends in the historical period (1900-2014) and future scenarios (2014-2100).

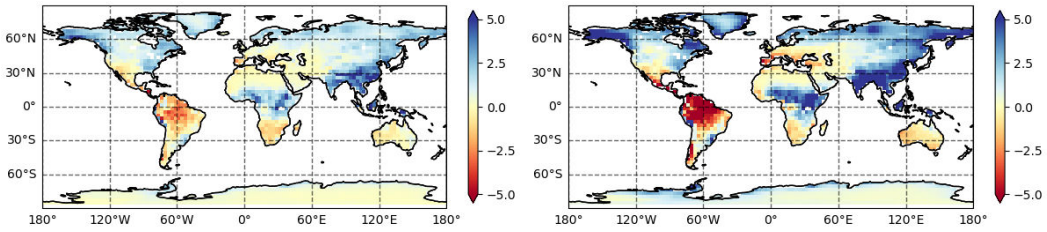

(a) Future scenario SSP2-4.5

(b) Future scenario SSP5-8.5

Figure A.10: Precipitation trend of the period 2015-2100 for two scenarios SSP2-4.5 and SSP5-8.5. The values are given in $10^{-6}\,\mathrm{kg\,m^{-2}\,s^{-1}/50yr}$

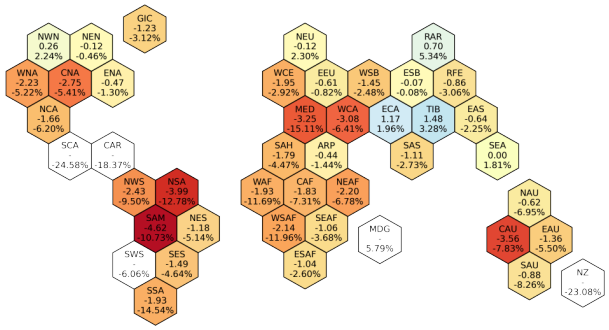

Figure A.11: Difference of moderate drought frequency in events per century for each reference region. The first number and colour of each hexagon is the absolute difference (SSP5-8.5-SSP2-4.5), while the second number is the difference relative to SSP2-4.5.

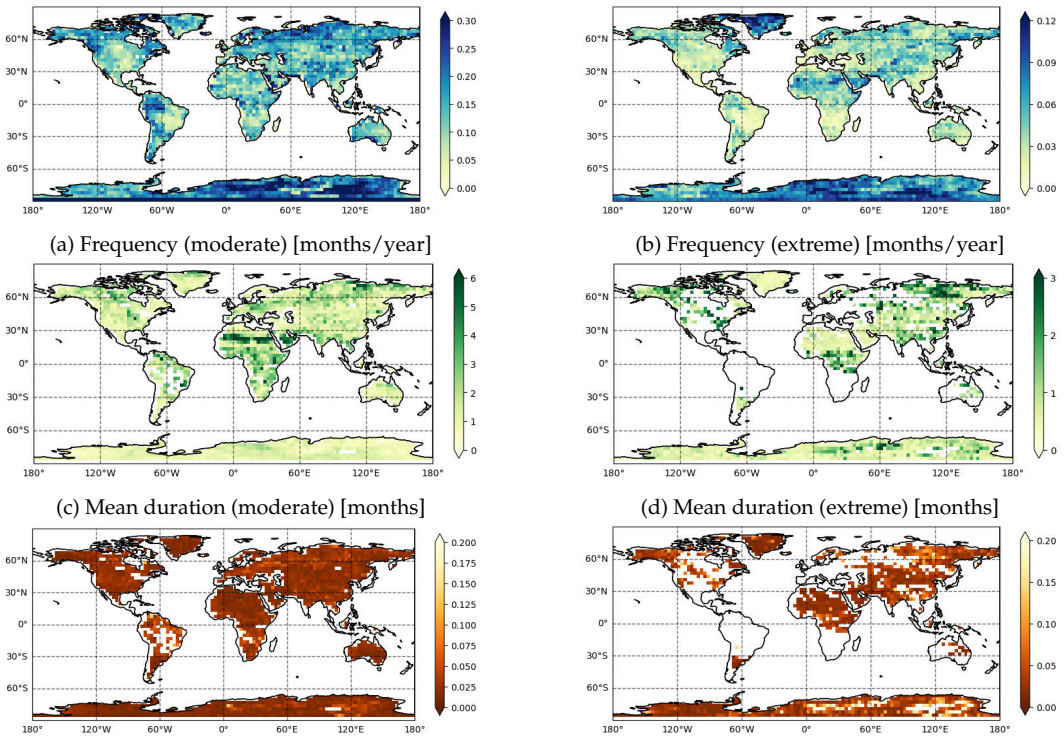

(a) Frequency (moderate) [months/year]

(b) Frequency (extreme) [months/year]

(c) Mean duration (moderate) [months]

(d) Mean duration (extreme) [months]

(e) Averaged Index (moderate)

(f) Averaged Index (extreme)

Figure A.12: Multi-model standard deviations of characteristics based on normalized SC-PDSI for the historical period 1900-2014.

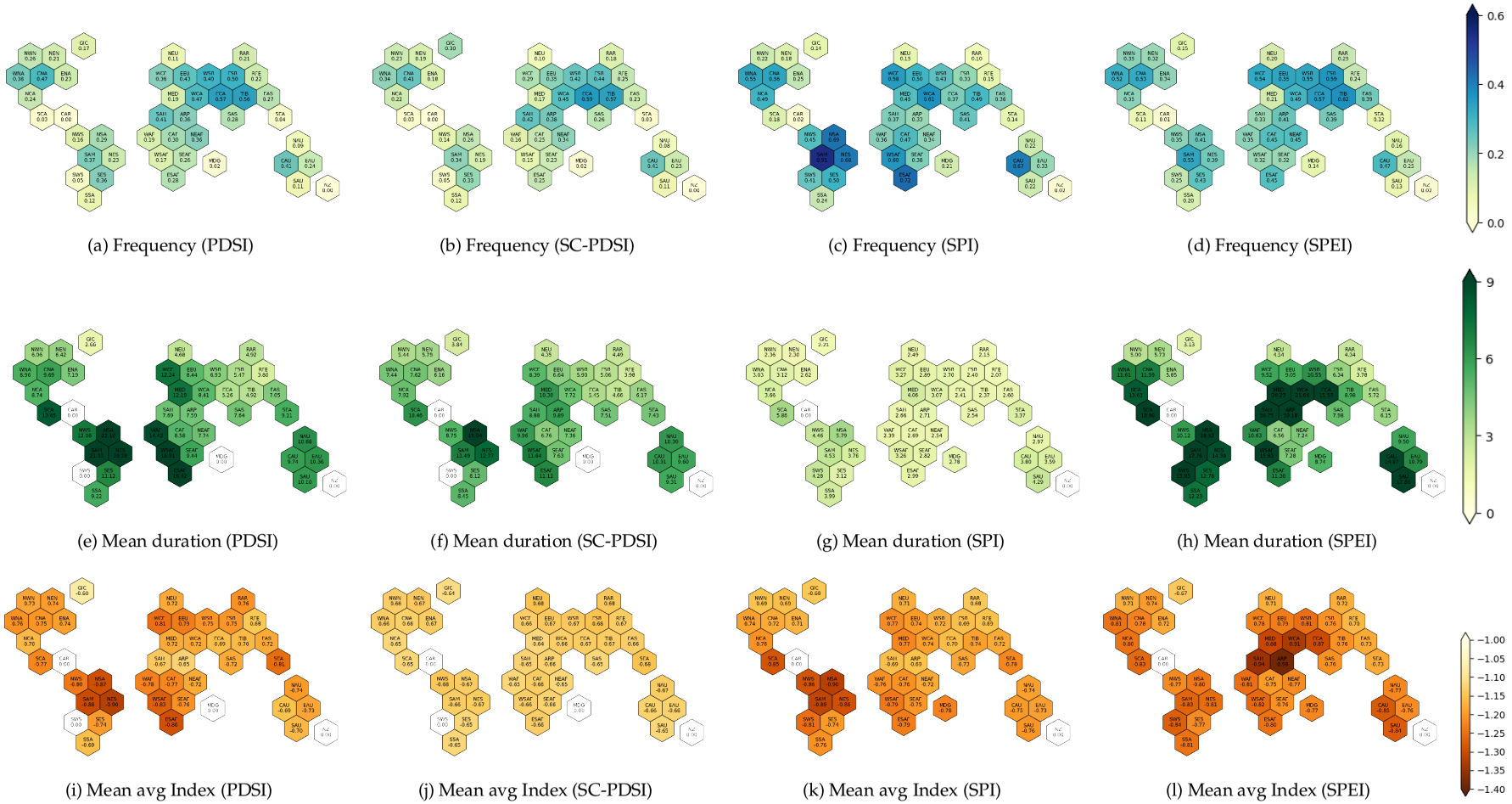

(a) Frequency (PDSI) (b) Frequency (SC-PDSI) (c) Frequency (SPI) (d) Frequency (SPEI)

(e) Mean duration (PDSI) (f) Mean duration (SC-PDSI) (g) Mean duration (SPI) (h) Mean duration (SPEI)

(i) Mean avg Index (PDSI) (j) Mean avg Index (SC-PDSI) (k) Mean avg Index (SPI) (l) Mean avg Index (SPEI)

Figure A.13: Characteristics for moderate droughts (normalized indices below -0.5) in the SSP5-8.5 projection (2015-2100). Mean duration is given in months and frequencies in months/year.

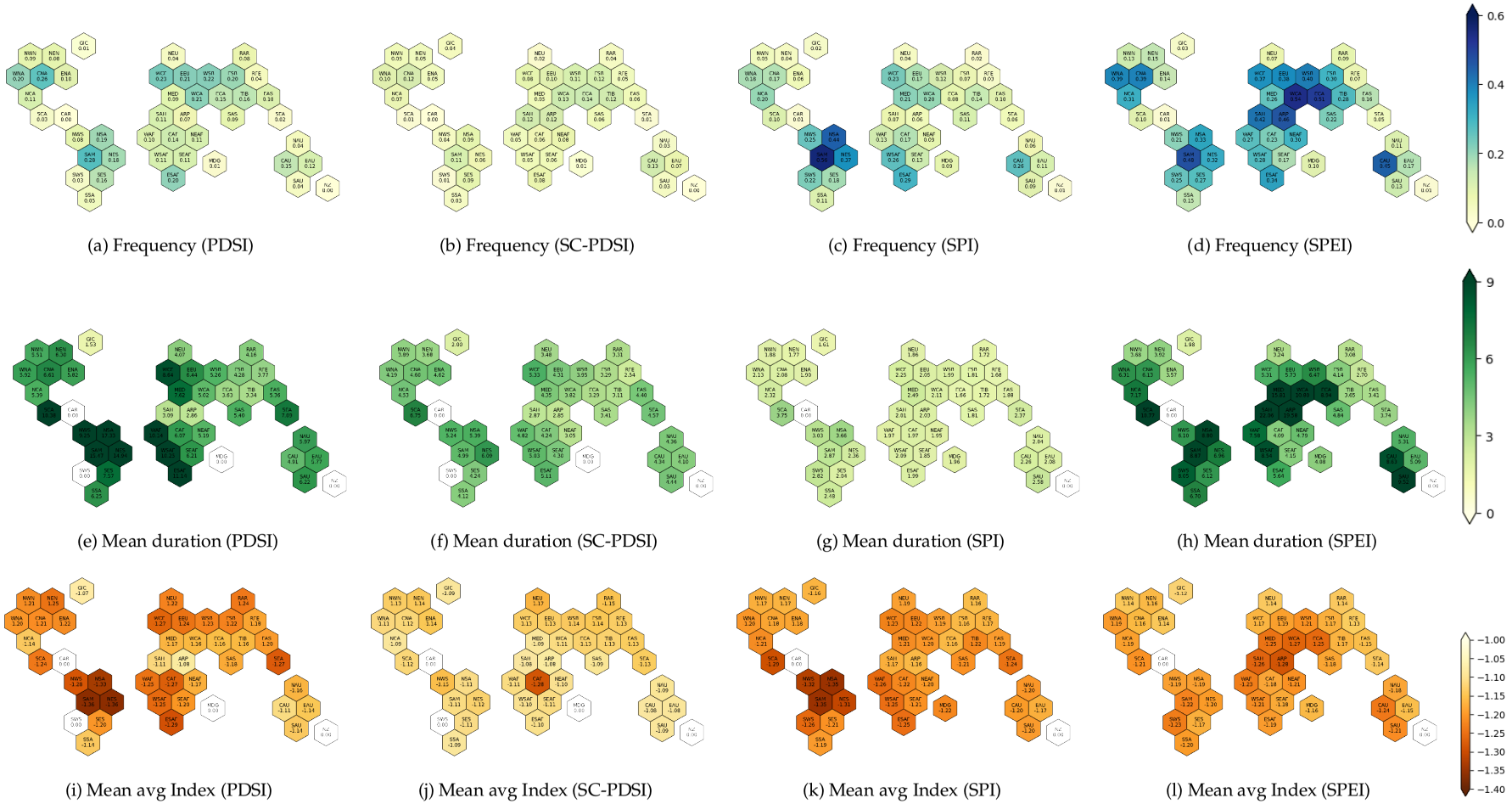

(a) Frequency (PDSI) (b) Frequency (SC-PDSI) (c) Frequency (SPI) (d) Frequency (SPEI)

(e) Mean duration (PDSI) (f) Mean duration (SC-PDSI) (g) Mean duration (SPI) (h) Mean duration (SPEI)

(i) Mean avg Index (PDSI) (j) Mean avg Index (SC-PDSI) (k) Mean avg Index (SPI) (l) Mean avg Index (SPEI)

Figure A.14: Characteristics for extreme droughts (2% driest months 1900-2014) in the SSP5-8.5 projection (2015-2100). Mean duration is given in months and frequencies in months/year.

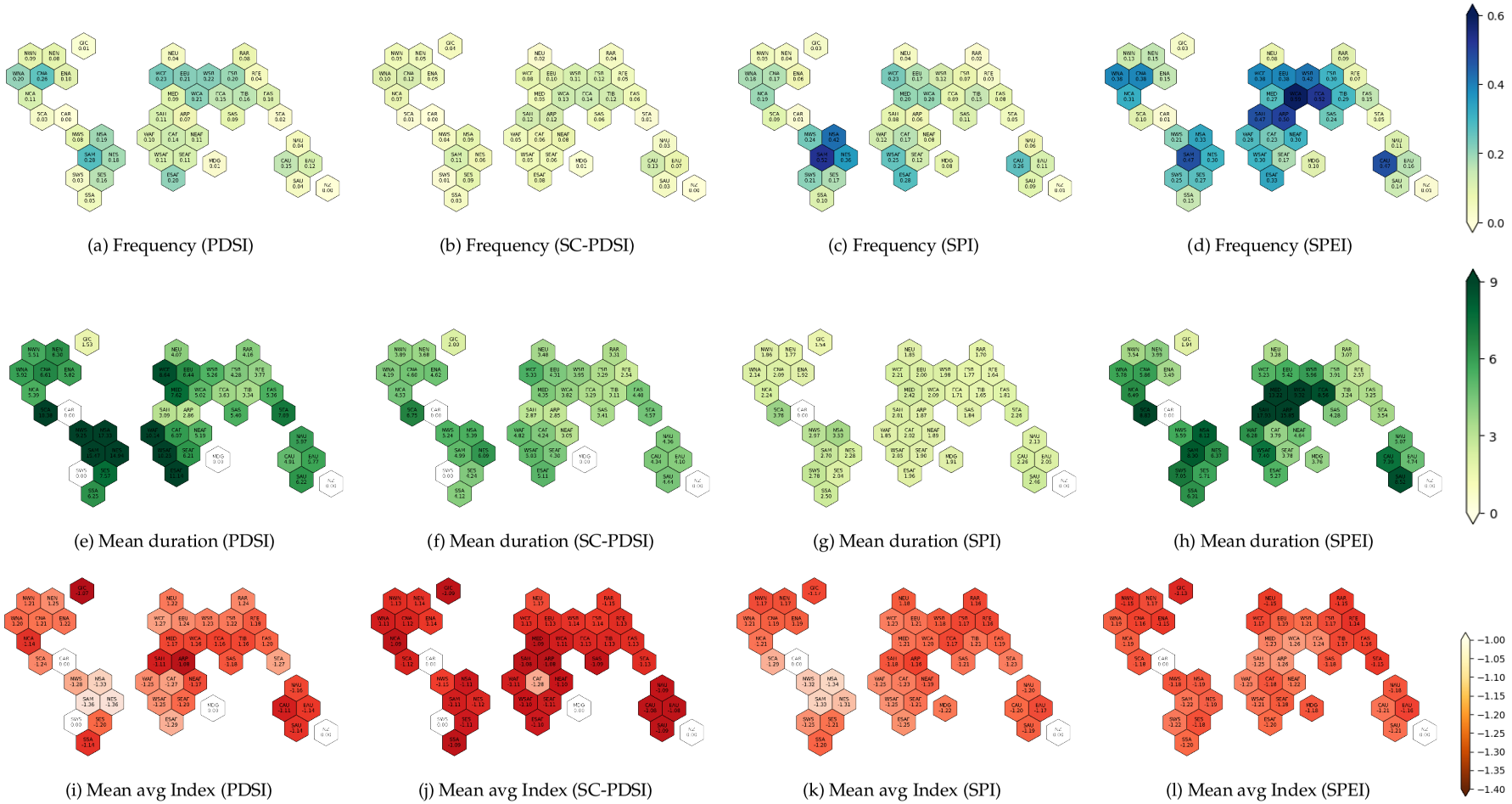

(a) Frequency (PDSI) (b) Frequency (SC-PDSI) (c) Frequency (SPI) (d) Frequency (SPEI)

(e) Mean duration (PDSI) (f) Mean duration (SC-PDSI) (g) Mean duration (SPI) (h) Mean duration (SPEI)

(i) Mean avg Index (PDSI) (j) Mean avg Index (SC-PDSI) (k) Mean avg Index (SPI) (l) Mean avg Index (SPEI)

Figure A.15: Multi-model standard deviations of characteristics for extreme droughts (2% driest months 1900-2014) in the SSP5-8.5 projection (2015-2100). Mean duration is given in months and frequencies in months/year.

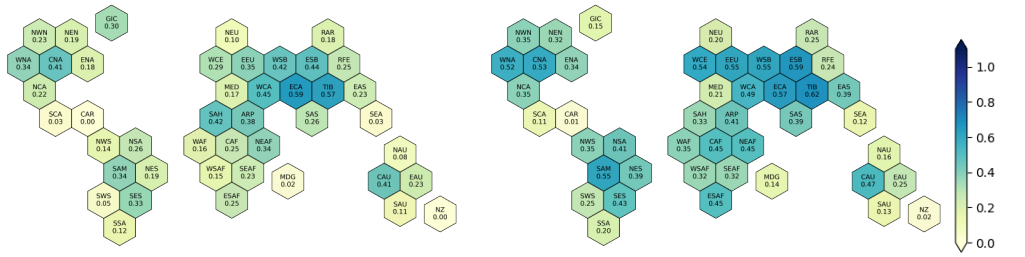

(a) Frequency (SC-PDSI)

(b) Frequency (SPEI)

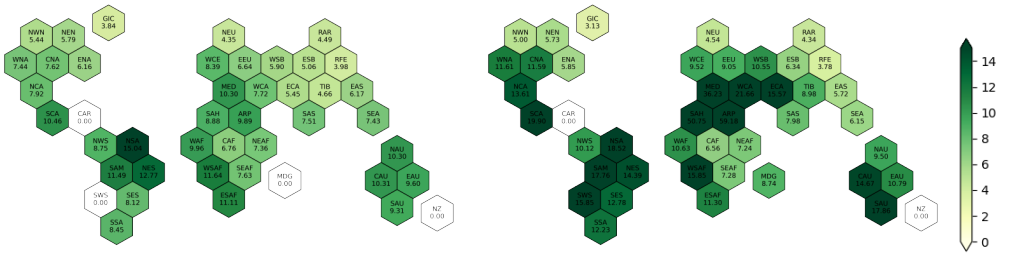

(c) Mean duration (SC-PDSI)

(d) Mean duration (SPEI)

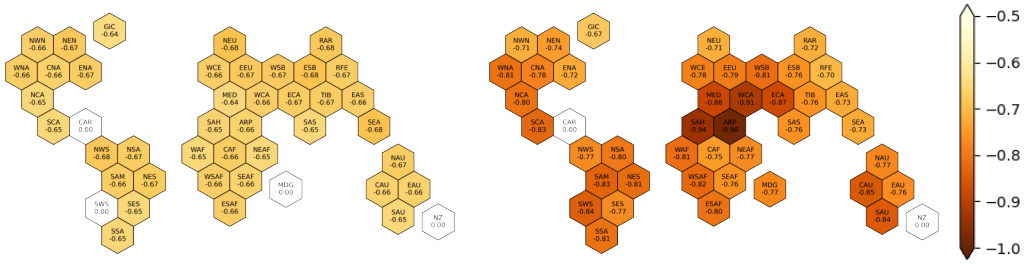

(e) Mean avg Index (SC-PDSI)

(f) Mean avg Index (SPEI)

Figure A.16: Similar to 5.8, but for moderate droughts in the SSP5-8.5 Scenario.

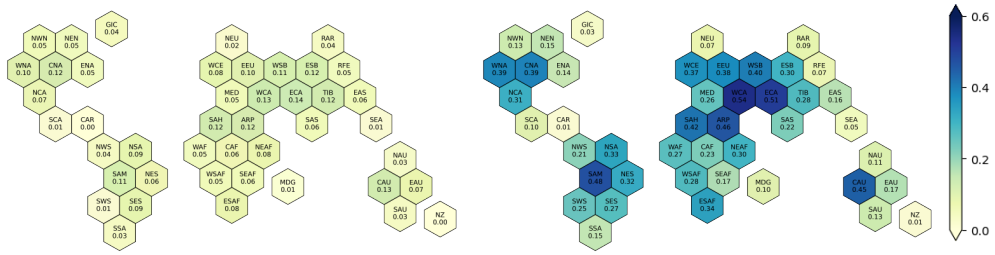

(a) Frequency (SC-PDSI) (b) Frequency (SPEI)

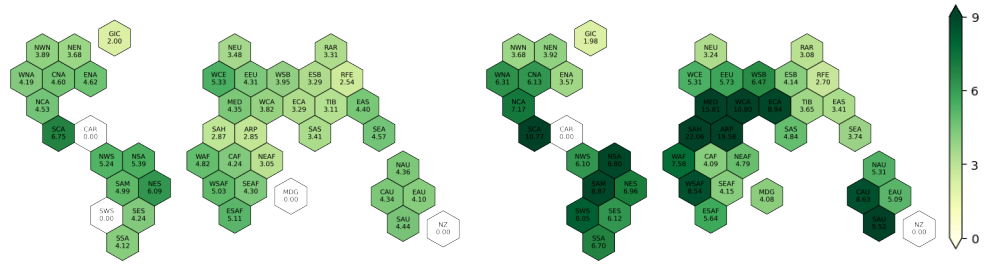

(c) Mean duration (SC-PDSI) (d) Mean duration (SPEI)

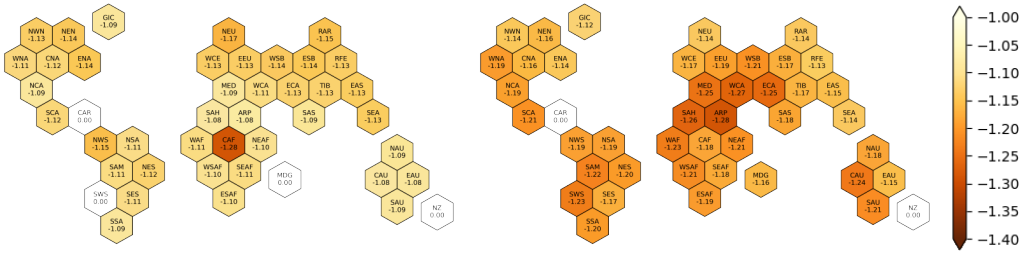

(e) Mean avg Index (SC-PDSI) (f) Mean avg Index (SPEI)

Figure A.17: Similar to 5.8, but for extreme droughts in the SSP5-8.5 Scenario.

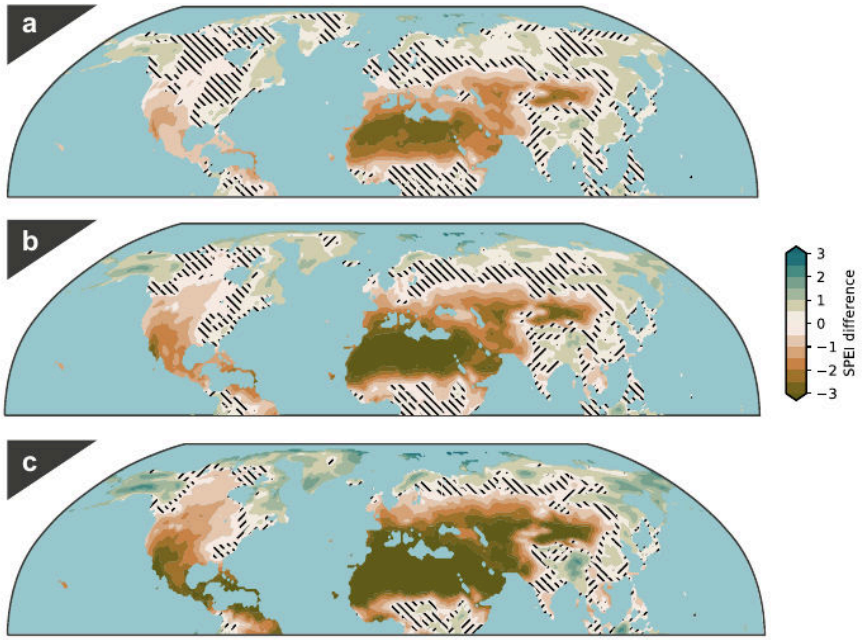

Figure A.18: Changes to summer drought conditions under SSP1-2.6, SSP2-4.5 and SSP5-8.5. ac Averaged anomalies of summer droughts under SSP1-2.6 (a) and SSP2-4.5 (b) and SSP5-8.5 (c) in the Northern Hemisphere for the period 20712100 relative to the baseline period of 19712000. The hatched areas in all three subfigures indicate areas with insignificant changes according to the two-sided Students t test ($p < 0.05$). (Fig. 6 from Balting et al. 2021)

Bibliography

Adams, James (2017). *Climate_indices, an Open Source Python Library Providing Reference Implementations of Commonly Used Climate Indices*. URL: https://github.com/monocongo/climate_indices.

Adeniyi, Kemisola Esther (Aug. 2019). "Changes in Drought Characteristics in Earth System Model Simulations of the Past and Future". PhD thesis.

Allen, Richard G, Luis S Pereira, Dirk Raes, and Martin Smith (1998). *Crop Evapotranspiration - Guidelines for Computing Crop Water Requirements*. Ed. by R. G. Allen and Food and Agriculture Organization of the United Nations. FAO Irrigation and Drainage Paper 56. Rome: Food and Agriculture Organization of the United Nations.

Alley, William M. (July 1984). "The Palmer Drought Severity Index: Limitations and Assumptions". In: *Journal of Climate and Applied Meteorology* 23.7, pp. 1100–1109. ISSN: 0733-3021. DOI: 10.1175/1520-0450(1984)023<1100:TPDSIL>2.0.CO;2. URL: https://journals.ametsoc.org/doi/abs/10.1175/1520-0450%281984%29023%3C1100%3ATPDSIL%3E2.0.CO%3B2 (visited on 01/07/2020).

Andela, Bouwe, Bjoern Broetz, Lee de Mora, Niels Drost, Veronika Eyring, Nikolay Koldunov, Axel Lauer, Benjamin Mueller, Valeriu Predoi, Mattia Righi, Manuel Schlund, Javier Vegas-Regidor, Klaus Zimmermann, Kemisola Adeniyi, Enrico Arnone, Omar Bellprat, Peter Berg, Lisa Bock, Louis-Philippe Caron, Nuno Carvalhais, Irene Cionni, Nicola Cortesi, Susanna Corti, Bas Crezee, Edouard Leopold Davin, Paolo Davini, Clara Deser, Faruk Diblen, David Docquier, Laura Dreyer, Carsten Ehbrecht, Paul Earnshaw, Bettina Gier, Nube Gonzalez-Reviriego, Paul Goodman, Stefan Hagemann, Jost von Hardenberg, Birgit Hassler, Alasdair Hunter, Christopher Kadow, Stephan Kindermann, Sujan Koirala, Llorenç Lledó, Quentin Lejeune, Valerio Lembo, Bill Little, Saskia Loosveldt Tomas, Ruth Lorenz, Tomas Lovato, Valerio Lucarini, François Massonnet, Christian Wilhelm Mohr, Pandde Amarjiit, Núria Pérez-Zanón, Adam Phillips, Joellen Russell, Marit Sandstad, Alistair Sellar, Daniel Senftleben, Federico Serva, Jana Sillmann, Tobias Stacke, Ranjini Swaminathan, Verónica Torralba, and Katja Weigel (2020a). "ESMValTool v2.0.0". In: DOI: 10.5281/zenodo.3970975.

Andela, Bouwe, Bjoern Broetz, Lee de Mora, Niels Drost, Veronika Eyring, Nikolay Koldunov, Axel Lauer, Benjamin Mueller, Valeriu Predoi, Mattia Righi, Manuel Schlund, Javier Vegas-Regidor, Klaus Zimmermann, Kemisola Adeniyi, Enrico Arnone, Omar Bellprat, Peter Berg, Lisa Bock, Louis-Philippe Caron, Nuno Carvalhais, Irene Cionni, Nicola Cortesi,

Susanna Corti, Bas Crezee, Edouard Leopold Davin, Paolo Davini, Clara Deser, Faruk Diblen, David Docquier, Laura Dreyer, Carsten Ehbrecht, Paul Earnshaw, Bettina Gier, Nube Gonzalez-Reviriego, Paul Goodman, Stefan Hagemann, Jost von Hardenberg, Birgit Hassler, Alasdair Hunter, Christopher Kadow, Stephan Kindermann, Sujan Koirala, Llorenç Lledó, Quentin Lejeune, Valerio Lembo, Bill Little, Saskia Loosveldt-Tomas, Ruth Lorenz, Tomas Lovato, Valerio Lucarini, François Massonnet, Christian Wilhelm Mohr, Eduardo Moreno-Chamarro, Pandde Amarjiit, Núria Pérez-Zanón, Adam Phillips, Joellen Russell, Marit Sandstad, Alistair Sellar, Daniel Senftleben, Federico Serva, Jana Sillmann, Tobias Stacke, Ranjini Swaminathan, Verónica Torralba, and Katja Weigel (Nov. 2021). *ESMValTool*. Zenodo. DOI: 10.5281/zenodo.5658385. URL: https://zenodo.org/record/5658385 (visited on 12/13/2021).

Andela, Bouwe, Bjoern Broetz, Lee de Mora, Niels Drost, Veronika Eyring, Nikolay Koldunov, Axel Lauer, Valeriu Predoi, Mattia Righi, Manuel Schlund, Javier Vegas-Regidor, Klaus Zimmermann, Lisa Bock, Faruk Diblen, Laura Dreyer, Paul Earnshaw, Birgit Hassler, Bill Little, and Saskia Loosveldt Tomas (2020b). "ESMValCore v2.0.0". In:

Balting, Daniel F., Amir AghaKouchak, Gerrit Lohmann, and Monica Ionita (2021). "Northern Hemisphere Drought Risk in a Warming Climate". In: *npj Climate and Atmospheric Science* 4.1, pp. 1–13. ISSN: 2397-3722. DOI: 10.1038/s41612-021-00218-2. URL: https://www.nature.com/articles/s41612-021-00218-2 (visited on 03/08/2022).

Beguería, Santiago, Sergio M. Vicente-Serrano, Fergus Reig, and Borja Latorre (2014). "Standardized Precipitation Evapotranspiration Index (SPEI) Revisited: Parameter Fitting, Evapotranspiration Models, Tools, Datasets and Drought Monitoring". In: *International Journal of Climatology* 34.10, pp. 3001–3023. ISSN: 0899-8418. DOI: 10.1002/joc.3887. URL: https://dx.doi.org/10.1002/joc.3887.

Burton, Ian, R.W. Kates, and G.F. White (1978). *The Environment as Hazard*. Oxford University Press. ISBN: 978-0-19-502221-6. URL: https://books.google.de/books?id=HrYPAQAAIAAJ.

Chen, D., M. Rojas, B.H. Samset, K. Cobb, A. Diongue Niang, S. Edwards, S. Emori, S.H. Faria, E. Hawkins, P. Hope, P. Huybrechts, M. Meinshausen, S.K. Mustafa, G.-K. Plattner, and A.-M. Treguier (2021). "IPCC, 2021: Framing, Context, and Methods". In: *Climate Change 2021: The Physical Science Basis. Contribution of Working Group I to the Sixth Assessment Report of the Intergovernmental Panel on Climate Change* [MassonDelmotte, V., P. Zhai, A. Pirani, S.L. Connors, C. Péan, S. Berger, N. Caud, Y. Chen, L. Goldfarb, M.I. Gomis, M. Huang, K. Leitzell, E. Lonnoy, J.B.R. Matthews, T.K. Maycock, T. Waterfield, O. Yelekçi, R. Yu, and B. Zhou (eds.)] URL: https://www.ipcc.ch/report/ar6/wg1/downloads/report/IPCC_AR6_WGI_Chapter_01.pdf (visited on 01/19/2022).

Cherchi, A., P. G. Fogli, T. Lovato, D. Peano, D. Iovino, S. Gualdi, S. Masina, E. Scoccimarro, S. Materia, A. Bellucci, and A. Navarra (2019). "Global Mean Climate and Main Patterns of Variability in the CMCC-CM2 Coupled Model". In: *Journal of Advances in Modeling Earth Systems* 11.1, pp. 185–209. ISSN: 1942-2466. DOI: 10.1029/2018MS001369. URL: https://onlinelibrary.wiley.com/doi/abs/10.1029/2018MS001369 (visited on 01/13/2022).

Collins, Matthew, Reto Knutti, Julie Arblaster, Jean-Louis Dufresne, Thierry Fichefet, Pierre Friedlingstein, Xuejie Gao, William J. Gutowski, Tim Johns, and Gerhard Krinner (2013). "Long-Term Climate Change: Projections, Commitments and Irreversibility". In: *Climate Change 2013-The Physical Science Basis: Contribution of Working Group I to the Fifth Assessment Report of the Intergovernmental Panel on Climate Change*. Cambridge University Press, pp. 1029–1136.

Cook, Benjamin I., Jason E. Smerdon, Richard Seager, and Sloan Coats (Nov. 2014). "Global Warming and 21st Century Drying". In: *Climate Dynamics* 43.9, pp. 2607–2627. ISSN: 1432-0894. DOI: 10.1007/s00382-014-2075-y. URL: https://doi.org/10.1007/s00382-014-2075-y (visited on 03/24/2022).

Dai, Aiguo (June 2011). "Characteristics and Trends in Various Forms of the Palmer Drought Severity Index during 1900–2008". In: *Journal of Geophysical Research* 116.D12, p. D12115. ISSN: 0148-0227. DOI: 10.1029/2010JD015541. URL: http://doi.wiley.com/10.1029/2010JD015541 (visited on 01/06/2020).

Dai, Aiguo, Kevin E. Trenberth, and Taotao Qian (Dec. 2004). "A Global Dataset of Palmer Drought Severity Index for 1870–2002: Relationship with Soil Moisture and Effects of Surface Warming". In: *Journal of Hydrometeorology* 5.6, pp. 1117–1130. ISSN: 1525-755X, 1525-7541. DOI: 10.1175/JHM-386.1. URL: http://journals.ametsoc.org/doi/abs/10.1175/JHM-386.1 (visited on 01/06/2020).

Dai, Aiguo and Tianbao Zhao (Oct. 2017). "Uncertainties in Historical Changes and Future Projections of Drought. Part I: Estimates of Historical Drought Changes". In: *Climatic Change* 144.3, pp. 519–533. ISSN: 1573-1480. DOI: 10.1007/s10584-016-1705-2. URL: https://doi.org/10.1007/s10584-016-1705-2 (visited on 01/18/2022).

Dennis, Cain/NWS (2019). *Water Cycle | National Oceanic and Atmospheric Administration*. URL: https://www.noaa.gov/education/resource-collections/freshwater/water-cycle (visited on 02/24/2022).

Eyring, Veronika, Lisa Bock, Axel Lauer, Mattia Righi, Manuel Schlund, Bouwe Andela, Enrico Arnone, Omar Bellprat, Björn Brötz, Louis-Philippe Caron, Nuno Carvalhais, Irene Cionni, Nicola Cortesi, Bas Crezee, Edouard L. Davin, Paolo Davini, Kevin Debeire, Lee De Mora, Clara Deser, David Docquier, Paul Earnshaw, Carsten Ehbrecht, Bettina K. Gier, Nube Gonzalez-Reviriego, Paul Goodman, Stefan Hagemann, Steven Hardiman, Birgit Hassler, Alasdair Hunter, Christopher Kadow,

Stephan Kindermann, Sujan Koirala, Nikolay Koldunov, Quentin Lejeune, Valerio Lembo, Tomas Lovato, Valerio Lucarini, François Massonnet, Benjamin Müller, Amarjiit Pandde, Núria Pérez-Zanón, Adam Phillips, Valeriu Predoi, Joellen Russell, Alistair Sellar, Federico Serva, Tobias Stacke, Ranjini Swaminathan, Verónica Torralba, Javier Vegas-Regidor, Jost Von Hardenberg, Katja Weigel, and Klaus Zimmermann (2020). "Earth System Model Evaluation Tool (ESMValTool) v2.0 – an Extended Set of Large-Scale Diagnostics for Quasi-Operational and Comprehensive Evaluation of Earth System Models in CMIP". In: *Geoscientific Model Development* 13.7, pp. 3383–3438. ISSN: 1991-9603. DOI: 10.5194/gmd-13-3383-2020. URL: https://dx.doi.org/10.5194/gmd-13-3383-2020.

Eyring, Veronika, Sandrine Bony, Gerald A. Meehl, Catherine A. Senior, Bjorn Stevens, Ronald J. Stouffer, and Karl E. Taylor (May 2016a). "Overview of the Coupled Model Intercomparison Project Phase 6 (CMIP6) Experimental Design and Organization". In: *Geoscientific Model Development* 9.5, pp. 1937–1958. ISSN: 1991-9603. DOI: 10.5194/gmd-9-1937-2016. URL: https://www.geosci-model-dev.net/9/1937/2016/ (visited on 01/06/2020).

Eyring, Veronika, Mattia Righi, Axel Lauer, Martin Evaldsson, Sabrina Wenzel, Colin Jones, Alessandro Anav, Oliver Andrews, Irene Cionni, Edouard L. Davin, Clara Deser, Carsten Ehbrecht, Pierre Friedlingstein, Peter Gleckler, Klaus-Dirk Gottschaldt, Stefan Hagemann, Martin Juckes, Stephan Kindermann, John Krasting, Dominik Kunert, Richard Levine, Alexander Loew, Jarmo Mäkelä, Gill Martin, Erik Mason, Adam S. Phillips, Simon Read, Catherine Rio, Romain Roehrig, Daniel Senftleben, Andreas Sterl, Lambertus H. van Ulft, Jeremy Walton, Shiyu Wang, and Keith D. Williams (May 2016b). "ESMValTool (v1.0) – a Community Diagnostic and Performance Metrics Tool for Routine Evaluation of Earth System Models in CMIP". In: *Geoscientific Model Development* 9.5, pp. 1747–1802. ISSN: 1991-9603. DOI: 10.5194/gmd-9-1747-2016. URL: https://www.geosci-model-dev.net/9/1747/2016/ (visited on 01/06/2020).

Fischer, E. M., U. Beyerle, and R. Knutti (Dec. 2013). "Robust Spatially Aggregated Projections of Climate Extremes". In: *Nature Climate Change* 3.12, pp. 1033–1038. ISSN: 1758-6798. DOI: 10.1038/nclimate2051. URL: https://www.nature.com/articles/nclimate2051 (visited on 01/19/2022).

García-Herrera, Ricardo, Jose M. Garrido-Perez, David Barriopedro, Carlos Ordóñez, Sergio M. Vicente-Serrano, Raquel Nieto, Luis Gimeno, Rogert Sorí, and Pascal Yiou (June 2019a). "The European 2016/17 Drought". In: *Journal of Climate* 32.11, pp. 3169–3187. ISSN: 0894-8755, 1520-0442. DOI: 10.1175/JCLI-D-18-0331.1. URL: https://journals.ametsoc.org/view/journals/clim/32/11/jcli-d-18-0331.1.xml (visited on 02/11/2022).

García-Herrera, Ricardo, Jose M. Garrido-Perez, David Barriopedro, Carlos Ordóñez, Sergio M. Vicente-Serrano, Raquel Nieto, Luis Gimeno, Rogert Sorí, and Pascal Yiou (June 2019b). "The European 2016/17 Drought". In: *Journal of Climate* 32.11, pp. 3169–3187. ISSN: 0894-8755, 1520-0442. DOI: 10.1175/JCLI-D-18-0331.1. URL: http://journals.ametsoc.org/doi/10.1175/JCLI-D-18-0331.1 (visited on 01/06/2020).

Greve, Peter, Lukas Gudmundsson, and Sonia I. Seneviratne (Mar. 2018). "Regional Scaling of Annual Mean Precipitation and Water Availability with Global Temperature Change". In: *Earth System Dynamics* 9.1, pp. 227–240. ISSN: 2190-4979. DOI: 10.5194/esd-9-227-2018. URL: https://esd.copernicus.org/articles/9/227/2018/ (visited on 02/23/2022).

Greve, Peter, Boris Orlowsky, Brigitte Mueller, Justin Sheffield, Markus Reichstein, and Sonia I. Seneviratne (Oct. 2014). "Global Assessment of Trends in Wetting and Drying over Land". In: *Nature Geoscience* 7.10, pp. 716–721. ISSN: 1752-0894, 1752-0908. DOI: 10.1038/ngeo2247. URL: http://www.nature.com/articles/ngeo2247 (visited on 01/06/2020).

Guenang, Guy Merlin and F. Mkankam Kamga (2014). "Computation of the Standardized Precipitation Index (SPI) and Its Use to Assess Drought Occurrences in Cameroon over Recent Decades". In: *Journal of Applied Meteorology and Climatology* 53.10, pp. 2310–2324. ISSN: 1558-8424. DOI: 10.1175/jamc-d-14-0032.1. URL: https://dx.doi.org/10.1175/jamc-d-14-0032.1.

Gulev, S.K., P.W. Thorne, J. Ahn, F.J. Dentener, C.M. Domingues, S. Gerland, D. Gong, H.C. Nnamchi, J. Quaas, and J.A. Rivera (2021). "Changing State of the Climate System". In: *Climate Change 2021: The Physical Science Basis. Contribution of Working Group I to the Sixth Assessment Report of the Intergovernmental Panel on Climate Change* [MassonDelmotte, V., P. Zhai, A. Pirani, S.L. Connors, C. Péan, S. Berger, N. Caud, Y. Chen, L. Goldfarb, M.I. Gomis, M. Huang, K. Leitzell, E. Lonnoy, J.B.R. Matthews, T.K. Maycock, T. Waterfield, O. Yelekçi, R. Yu, and B. Zhou (eds.)] URL: https://www.ipcc.ch/report/ar6/wg1/downloads/report/IPCC_AR6_WGI_Chapter_02.pdf (visited on 02/23/2022).

Gutjahr, Oliver, Dian Putrasahan, Katja Lohmann, Johann H. Jungclaus, Jin-Song von Storch, Nils Brüggemann, Helmuth Haak, and Achim Stössel (July 2019). "Max Planck Institute Earth System Model (MPI-ESM1.2) for the High-Resolution Model Intercomparison Project (HighResMIP)". In: *Geoscientific Model Development* 12.7, pp. 3241–3281. ISSN: 1991-9603. DOI: 10.5194/gmd-12-3241-2019. URL: https://gmd.copernicus.org/articles/12/3241/2019/ (visited on 01/13/2022).

Guttman, Nathaniel B. (Feb. 1998). "COMPARING THE PALMER DROUGHT INDEX AND THE STANDARDIZED PRECIPITATION INDEX". In: *Journal of the American Water Resources Association* 34.1, pp. 113–121. ISSN: 1093-474X, 1752-1688. DOI: 10.1111/j.1752-

1688.1998.tb05964.x. URL: http://doi.wiley.com/10.1111/j.1752-1688.1998.tb05964.x (visited on 01/06/2020).

Hagman, G, H Beer, M Bendz, and A Wijkman (1984). *Prevention Better than Cure. Report on Human and Environmental Disasters in the Third World. 2. Ed.* Tech. rep. URL: https://scholar.google.com/scholar_lookup?title=Prevention+better+than+cure.+Report+on+human+and+environmental+disasters+in+the+Third+World.+2.+ed.&author=Hagman+G.&publication_year=1984 (visited on 02/10/2022).

Hamon, W Russell (1963). "Computation of Direct Runoff Amounts from Storm Rainfall". In: *International Association of Scientific Hydrology Publication* 63, pp. 52–62.

Hargreaves, George H and Zohrab A Samani (1985). "Reference Crop Evapotranspiration from Temperature". In: *Applied engineering in agriculture* 1.2, pp. 96–99.

Hauser, Mathias, Aaron Spring, Julius Busecke, and Martin van Driel (Sept. 2021). *Regionmask/Regionmask: Version 0.8.0*. Zenodo. DOI: 10.5281/zenodo.5532848. URL: https://zenodo.org/record/5532848 (visited on 12/23/2021).

Hayes, Michael, Luiz Cavalcanti, and Anne Steinemann (Mar. 2005). "Drought Indicators and Triggers". In: *Drought and Water Crises*. Ed. by Donald Wilhite. Vol. 107. CRC Press, pp. 71–92. ISBN: 978-0-8247-2771-0 978-1-4200-2838-6. DOI: 10.1201/9781420028386.ch4. URL: http://www.crcnetbase.com/doi/abs/10.1201/9781420028386.ch4 (visited on 01/18/2022).

Heddinghaus, Thomas R. and Paul Sabol (1991). "A Review of the Palmer Drought Severity Index and Where Do We Go From Here". In: *Proc. 7th Conf. On Applied Climatol, American Meteorological Society*.

Hunt, B. G. (2011). "Global Characteristics of Pluvial and Dry Multi-year Episodes, with Emphasis on Megadroughts". In: *International Journal of Climatology* 31.10, pp. 1425–1439.

IPCC (2021). *Climate Change 2021: The Physical Science Basis. Contribution of Working Group I to the Sixth Assessment Report of the Intergovernmental Panel on Climate Change*. Vol. [Masson-Delmotte, V., P. Zhai, A. Pirani, S.L. Connors, C. Péan, S. Berger, N. Caud, Y. Chen, L. Goldfarb, M.I. Gomis, M. Huang, K. Leitzell, E. Lonnoy, J.B.R. Matthews, T.K. Maycock, T. Waterfield, O. Yelekçi, R. Yu, and B. Zhou (eds.)]. Cambridge University Press. In Press.

Iturbide, Maialen, José M. Gutiérrez, Lincoln M. Alves, Joaquín Bedia, Ruth Cerezo-Mota, Ezequiel Cimadevilla, Antonio S. Cofiño, Alejandro Di Luca, Sergio Henrique Faria, Irina V. Gorodetskaya, Mathias Hauser, Sixto Herrera, Kevin Hennessy, Helene T. Hewitt, Richard G. Jones, Svitlana Krakovska, Rodrigo Manzanas, Daniel Martínez-Castro, Gemma T. Narisma, Intan S. Nurhati, Izidine Pinto, Sonia I. Seneviratne, Bart van den Hurk, and Carolina S. Vera (Nov. 2020). "An Update of IPCC Climate Reference Regions for Subcontinental Analysis of Climate Model

Data: Definition and Aggregated Datasets". In: *Earth System Science Data* 12.4, pp. 2959–2970. ISSN: 1866-3508. DOI: 10.5194/essd-12-2959-2020. URL: https://essd.copernicus.org/articles/12/2959/2020/ (visited on 12/23/2021).

Karl, Thomas R. (Aug. 1983). "Some Spatial Characteristics of Drought Duration in the United States". In: *Journal of Applied Meteorology and Climatology* 22.8, pp. 1356–1366. ISSN: 1520-0450. DOI: 10.1175/1520-0450(1983)022<1356:SSCODD>2.0.CO;2. URL: https://journals.ametsoc.org/view/journals/apme/22/8/1520-0450_1983_022_1356_sscodd_2_0_co_2.xml (visited on 01/05/2022).

Kriegler, Elmar, Jae Edmonds, Stéphane Hallegatte, Kristie L. Ebi, Tom Kram, Keywan Riahi, Harald Winkler, and Detlef P. Van Vuuren (2014). "A New Scenario Framework for Climate Change Research: The Concept of Shared Climate Policy Assumptions". In: *Climatic Change* 122.3, pp. 401–414. ISSN: 0165-0009. DOI: 10.1007/s10584-013-0971-5. URL: https://dx.doi.org/10.1007/s10584-013-0971-5.

Lauer, Axel, Veronika Eyring, Omar Bellprat, Lisa Bock, Bettina K. Gier, Alasdair Hunter, Ruth Lorenz, Núria Pérez-Zanón, Mattia Righi, Manuel Schlund, Daniel Senftleben, Katja Weigel, and Sabrina Zechlau (2020). "Earth System Model Evaluation Tool (ESMValTool) v2.0 – Diagnostics for Emergent Constraints and Future Projections from Earth System Models in CMIP". In: *Geoscientific Model Development* 13.9, pp. 4205–4228. ISSN: 1991-9603. DOI: 10.5194/gmd-13-4205-2020. URL: https://dx.doi.org/10.5194/gmd-13-4205-2020.

Le, Hung Manh, Gerald Corzo, Vicente Medina, Vitali Diaz, Bang Luong Nguyen, and Dimitri P. Solomatine (2019). "7 - A Comparison of Spatial–Temporal Scale Between Multiscalar Drought Indices in the South Central Region of Vietnam". In: *Spatiotemporal Analysis of Extreme Hydrological Events*. Ed. by Gerald Corzo and Emmanouil A. Varouchakis. Elsevier, pp. 143–169. ISBN: 978-0-12-811689-0. DOI: 10.1016/B978-0-12-811689-0.00007-0. URL: http://www.sciencedirect.com/science/article/pii/B9780128116890000070.

Lord, Dominique, Xiao Qin, and Srinivas R. Geedipally (Jan. 2021). "Chapter 5 - Exploratory Analyses of Safety Data". In: *Highway Safety Analytics and Modeling*. Ed. by Dominique Lord, Xiao Qin, and Srinivas R. Geedipally. Elsevier, pp. 135–177. ISBN: 978-0-12-816818-9. DOI: 10.1016/B978-0-12-816818-9.00015-9. URL: https://www.sciencedirect.com/science/article/pii/B9780128168189000159 (visited on 01/20/2022).

Martin, E. R. (Nov. 2018). "Future Projections of Global Pluvial and Drought Event Characteristics". In: *Geophysical Research Letters* 45.21, pp. 11,913–11,920. ISSN: 00948276. DOI: 10.1029/2018GL079807. URL: http://doi.wiley.com/10.1029/2018GL079807 (visited on 01/06/2020).

Masson-Delmotte, V., P. Zhai, A. Pirani, S.L. Connors, C. Péan, S. Berger, N. Caud, Y. Chen, L. Goldfarb, M.I. Gomis, M. Huang, K. Leitzell, E. Lonnoy, J.B.R. Matthews, T.K. Maycock, T. Waterfield, O. Yelekçi, R. Yu, and

B. Zhou (2021). "Summary for Policymakers". In: *Climate Change 2021: The Physical Science Basis. Contribution of Working Group I to the Sixth Assessment Report of the Intergovernmental Panel on Climate Change* [Masson-Delmotte, V., P. Zhai, A. Pirani, S.L. Connors, C. Péan, S. Berger, N. Caud, Y. Chen, L. Goldfarb, M.I. Gomis, M. Huang, K. Leitzell, E. Lonnoy, J.B.R. Matthews, T.K. Maycock, T. Waterfield, O. Yelekçi, R. Yu, and B. Zhou (eds.)] URL: https://www.ipcc.ch/report/ar6/wg1/downloads/report/IPCC_AR6_WGI_SPM_final.pdf (visited on 12/08/2021).

McColl, Kaighin A. (June 2020). "Practical and Theoretical Benefits of an Alternative to the Penman-Monteith Evapotranspiration Equation". In: *Water Resources Research* 56.6. ISSN: 0043-1397, 1944-7973. DOI: 10.1029/2020WR027106. URL: https://onlinelibrary.wiley.com/doi/10.1029/2020WR027106 (visited on 10/22/2021).

McEvoy, Daniel J., Justin L. Huntington, John T. Abatzoglou, and Laura M. Edwards (Dec. 2012). "An Evaluation of Multiscalar Drought Indices in Nevada and Eastern California". In: *Earth Interactions* 16.18, pp. 1–18. ISSN: 1087-3562. DOI: 10.1175/2012EI000447.1. URL: https://journals.ametsoc.org/ei/article/16/18/1/481/An-Evaluation-of-Multiscalar-Drought-Indices-in (visited on 08/04/2020).

McKee, Thomas B, Nolan J Doesken, and John Kleist (1993). "THE RELATIONSHIP OF DROUGHT FREQUENCY AND DURATION TO TIME SCALES". In: p. 6.

Meehl, Gerald A., George J. Boer, Curt Covey, Mojib Latif, and Ronald J. Stouffer (1997). "Intercomparison Makes for a Better Climate Model". In: *Eos, Transactions American Geophysical Union* 78.41, p. 445. ISSN: 0096-3941. DOI: 10.1029/97eo00276. URL: https://dx.doi.org/10.1029/97eo00276.

Monteith, John L (1965). "Evaporation and Environment". In: *Symposia of the Society for Experimental Biology*. Vol. 19. Cambridge University Press (CUP) Cambridge, pp. 205–234.

O'Neill, Brian C., Elmar Kriegler, Keywan Riahi, Kristie L. Ebi, Stephane Hallegatte, Timothy R. Carter, Ritu Mathur, and Detlef P. Van Vuuren (2014). "A New Scenario Framework for Climate Change Research: The Concept of Shared Socioeconomic Pathways". In: *Climatic Change* 122.3, pp. 387–400. ISSN: 0165-0009. DOI: 10.1007/s10584-013-0905-2. URL: https://dx.doi.org/10.1007/s10584-013-0905-2.

O'Neill, Brian C., Claudia Tebaldi, Detlef P. van Vuuren, Veronika Eyring, Pierre Friedlingstein, George Hurtt, Reto Knutti, Elmar Kriegler, Jean-Francois Lamarque, Jason Lowe, Gerald A. Meehl, Richard Moss, Keywan Riahi, and Benjamin M. Sanderson (Sept. 2016). "The Scenario Model Intercomparison Project (ScenarioMIP) for CMIP6". In: *Geoscientific Model Development* 9.9, pp. 3461–3482. ISSN: 1991-9603. DOI: 10.5194/gmd-9-3461-2016. URL: https://www.geosci-model-dev.net/9/3461/2016/ (visited on 01/28/2020).

Otkin, Jason A., Martha C. Anderson, Christopher Hain, Mark Svoboda, David Johnson, Richard Mueller, Tsegaye Tadesse, Brian Wardlow, and Jesslyn Brown (Mar. 2016). "Assessing the Evolution of Soil Moisture and Vegetation Conditions during the 2012 United States Flash Drought". In: *Agricultural and Forest Meteorology* 218–219, pp. 230–242. ISSN: 0168-1923. DOI: 10.1016/j.agrformet.2015.12.065. URL: https://www.sciencedirect.com/science/article/pii/S0168192315300265 (visited on 02/11/2022).

Oudin, Ludovic, Frédéric Hervieu, Claude Michel, Charles Perrin, Vazken Andréassian, François Anctil, and Cécile Loumagne (2005). "Which Potential Evapotranspiration Input for a Lumped Rainfall–Runoff Model?" In: *Journal of Hydrology* 303.1-4, pp. 290–306. ISSN: 0022-1694. DOI: 10.1016/j.jhydrol.2004.08.026. URL: https://dx.doi.org/10.1016/j.jhydrol.2004.08.026.

Padrón, Ryan S., Lukas Gudmundsson, Bertrand Decharme, Agnès Ducharne, David M. Lawrence, Jiafu Mao, Daniele Peano, Gerhard Krinner, Hyungjun Kim, and Sonia I. Seneviratne (July 2020). "Observed Changes in Dry-Season Water Availability Attributed to Human-Induced Climate Change". In: *Nature Geoscience* 13.7, pp. 477–481. ISSN: 1752-0894, 1752-0908. DOI: 10.1038/s41561-020-0594-1. URL: http://www.nature.com/articles/s41561-020-0594-1 (visited on 03/27/2022).

Palmer, Wayne C (1965). *Meteorological Drought*. Tech. rep.

Penman, Howard Latimer (1948). "Natural Evaporation from Open Water, Bare Soil and Grass". In: *Proceedings of the Royal Society of London. Series A. Mathematical and Physical Sciences* 193.1032, pp. 120–145. ISSN: 0080-4630.

Pereira, Luis S., Richard G. Allen, Martin Smith, and Dirk Raes (Jan. 2015). "Crop Evapotranspiration Estimation with FAO56: Past and Future". In: *Agricultural Water Management* 147, pp. 4–20. ISSN: 03783774. DOI: 10.1016/j.agwat.2014.07.031. URL: https://linkinghub.elsevier.com/retrieve/pii/S0378377414002315 (visited on 01/14/2022).

Peters, Everson J (2014). "Measuring the Severity of Dry Seasons in the Grenadines". In: p. 9.

Redmond, Kelly T. (2002). "The Depiction of Drought: A Commentary". In: *Bulletin of the American Meteorological Society* 83.8, pp. 1143–1148. ISSN: 0003-0007. DOI: 10.1175/1520-0477-83.8.1143. URL: https://doi.org/10.1175/1520-0477-83.8.1143 (visited on 11/06/2020).

Rehana, S. and N. T. Monish (Apr. 2021). "Impact of Potential and Actual Evapotranspiration on Drought Phenomena over Water and Energy-Limited Regions". In: *Theoretical and Applied Climatology* 144.1, pp. 215–238. ISSN: 1434-4483. DOI: 10.1007/s00704-021-03521-3. URL: https://doi.org/10.1007/s00704-021-03521-3 (visited on 02/10/2022).

Riahi, Keywan, Detlef P. Van Vuuren, Elmar Kriegler, Jae Edmonds, Brian C. O'Neill, Shinichiro Fujimori, Nico Bauer, Katherine Calvin, Rob Dellink,

Oliver Fricko, Wolfgang Lutz, Alexander Popp, Jesus Crespo Cuaresma, Samir Kc, Marian Leimbach, Leiwen Jiang, Tom Kram, Shilpa Rao, Johannes Emmerling, Kristie Ebi, Tomoko Hasegawa, Petr Havlik, Florian Humpenöder, Lara Aleluia Da Silva, Steve Smith, Elke Stehfest, Valentina Bosetti, Jiyong Eom, David Gernaat, Toshihiko Masui, Joeri Rogelj, Jessica Strefler, Laurent Drouet, Volker Krey, Gunnar Luderer, Mathijs Harmsen, Kiyoshi Takahashi, Lavinia Baumstark, Jonathan C. Doelman, Mikiko Kainuma, Zbigniew Klimont, Giacomo Marangoni, Hermann Lotze-Campen, Michael Obersteiner, Andrzej Tabeau, and Massimo Tavoni (2017). "The Shared Socioeconomic Pathways and Their Energy, Land Use, and Greenhouse Gas Emissions Implications: An Overview". In: *Global Environmental Change* 42, pp. 153–168. ISSN: 0959-3780. DOI: 10.1016/j.gloenvcha.2016.05.009. URL: https://dx.doi.org/10.1016/j.gloenvcha.2016.05.009.

Righi, Mattia, Bouwe Andela, Veronika Eyring, Axel Lauer, Valeriu Predoi, Manuel Schlund, Javier Vegas-Regidor, Lisa Bock, Björn Brötz, Lee de Mora, Faruk Diblen, Laura Dreyer, Niels Drost, Paul Earnshaw, Birgit Hassler, Nikolay Koldunov, Bill Little, Saskia Loosveldt Tomas, and Klaus Zimmermann (Sept. 2019). *ESMValTool v2.0 - Technical Overview*. Preprint. Climate and Earth System Modeling. DOI: 10.5194/gmd-2019-226. URL: https://www.geosci-model-dev-discuss.net/gmd-2019-226/ (visited on 01/27/2020).

Schulze, E. D., O. L. Lange, L. Kappen, U. Buschbom, and M. Evenari (Mar. 1973). "Stomatal Responses to Changes in Temperature at Increasing Water Stress". In: *Planta* 110.1, pp. 29–42. ISSN: 1432-2048. DOI: 10.1007/BF00386920. URL: https://doi.org/10.1007/BF00386920 (visited on 02/22/2022).

Semmler, Tido, Sergey Danilov, Paul Gierz, Helge F. Goessling, Jan Hegewald, Claudia Hinrichs, Nikolay Koldunov, Narges Khosravi, Longjiang Mu, Thomas Rackow, Dmitry V. Sein, Dmitry Sidorenko, Qiang Wang, and Thomas Jung (2020). "Simulations for CMIP6 With the AWI Climate Model AWI-CM-1-1". In: *Journal of Advances in Modeling Earth Systems* 12.9, e2019MS002009. ISSN: 1942-2466. DOI: 10.1029/2019MS002009. URL: https://onlinelibrary.wiley.com/doi/abs/10.1029/2019MS002009 (visited on 12/14/2021).

Seneviratne, S.I., X. Zhang, M. Adnan, W. Badi, C. Dereczynski, A. Di Luca, S. Ghosh, I. Iskandar, J. Kossin, S. Lewis, S. Otto, I. Pinto, M. Satoh, S.M. Vicente-Serrano, M. Wehner, and B. Zhou (2021). "Weather and Climate Extreme Events in a Changing Climate". In: *Climate Change 2021: The Physical Science Basis. Contribution of Working Group I to the Sixth Assessment Report of the Intergovernmental Panel on Climate Change* [MassonDelmotte, V., P. Zhai, A. Pirani, S.L. Connors, C. Péan, S. Berger, N. Caud, Y. Chen, L. Goldfarb, M.I. Gomis, M. Huang, K. Leitzell, E. Lonnoy, J.B.R. Matthews, T.K. Maycock, T. Waterfield, O. Yelekçi, R. Yu, and B. Zhou (eds.)] Cambridge University Press. In Press.

Shaw, Stephen B. and Susan J. Riha (Apr. 2011). "Assessing Temperature-Based PET Equations under a Changing Climate in Temperate, Deciduous Forests". In: *Hydrological Processes* 25.9, pp. 1466–1478. ISSN: 08856087. DOI: 10.1002/hyp.7913. URL: http://doi.wiley.com/10.1002/hyp.7913 (visited on 08/04/2020).

Spinoni, Jonathan, Paulo Barbosa, Alfred De Jager, Niall McCormick, Gustavo Naumann, Jürgen V. Vogt, Diego Magni, Dario Masante, and Marco Mazzeschi (Apr. 2019). "A New Global Database of Meteorological Drought Events from 1951 to 2016". In: *Journal of Hydrology: Regional Studies* 22, p. 100593. ISSN: 22145818. DOI: 10.1016/j.ejrh.2019.100593. URL: https://linkinghub.elsevier.com/retrieve/pii/S2214581818303136 (visited on 03/27/2022).

Swart, Neil C., Jason N. S. Cole, Viatcheslav V. Kharin, Mike Lazare, John F. Scinocca, Nathan P. Gillett, James Anstey, Vivek Arora, James R. Christian, Sarah Hanna, Yanjun Jiao, Warren G. Lee, Fouad Majaess, Oleg A. Saenko, Christian Seiler, Clint Seinen, Andrew Shao, Michael Sigmond, Larry Solheim, Knut von Salzen, Duo Yang, and Barbara Winter (Nov. 2019). "The Canadian Earth System Model Version 5 (CanESM5.0.3)". In: *Geoscientific Model Development* 12.11, pp. 4823–4873. ISSN: 1991-9603. DOI: 10.5194/gmd-12-4823-2019. URL: https://gmd.copernicus.org/articles/12/4823/2019/ (visited on 12/13/2021).

Tatebe, H., T. Ogura, T. Nitta, Y. Komuro, K. Ogochi, T. Takemura, K. Sudo, M. Sekiguchi, M. Abe, F. Saito, M. Chikira, S. Watanabe, M. Mori, N. Hirota, Y. Kawatani, T. Mochizuki, K. Yoshimura, K. Takata, R. O'Ishi, D. Yamazaki, T. Suzuki, M. Kurogi, T. Kataoka, M. Watanabe, and M. Kimoto (2019). "Description and Basic Evaluation of Simulated Mean State, Internal Variability, and Climate Sensitivity in MIROC6". In: *Geosci. Model Dev.* 12.7, pp. 2727–2765. ISSN: 1991-9603. DOI: 10.5194/gmd-12-2727-2019. URL: https://gmd.copernicus.org/articles/12/2727/2019/.

Taylor, K., Charles Doutriaux, and J. Peterschmitt (2004). "Climate Model Output Rewriter (CMOR)". In: DOI: 10.2172/15014202.

Tebaldi, C., K. Debeire, V. Eyring, E. Fischer, J. Fyfe, P. Friedlingstein, R. Knutti, J. Lowe, B. O'Neill, B. Sanderson, D. van Vuuren, K. Riahi, M. Meinshausen, Z. Nicholls, K. B. Tokarska, G. Hurtt, E. Kriegler, J.-F. Lamarque, G. Meehl, R. Moss, S. E. Bauer, O. Boucher, V. Brovkin, Y.-H. Byun, M. Dix, S. Gualdi, H. Guo, J. G. John, S. Kharin, Y. Kim, T. Koshiro, L. Ma, D. Olivié, S. Panickal, F. Qiao, X. Rong, N. Rosenbloom, M. Schupfner, R. Séférian, A. Sellar, T. Semmler, X. Shi, Z. Song, C. Steger, R. Stouffer, N. Swart, K. Tachiiri, Q. Tang, H. Tatebe, A. Voldoire, E. Volodin, K. Wyser, X. Xin, S. Yang, Y. Yu, and T. Ziehn (Mar. 2021). "Climate Model Projections from the Scenario Model Intercomparison Project (ScenarioMIP) of CMIP6". In: *Earth Syst. Dynam.* 12.1, pp. 253–293. ISSN: 2190-4987. DOI: 10.5194/esd-12-253-2021. URL: https://esd.copernicus.org/articles/12/253/2021/.

Thornthwaite, C. W. (1948). "An Approach toward a Rational Classification of Climate". In: *Geographical Review* 38.1, p. 55. ISSN: 0016-7428. DOI: 10.2307/210739. URL: https://dx.doi.org/10.2307/210739.

Touma, Danielle, Moetasim Ashfaq, Munir A. Nayak, Shih-Chieh Kao, and Noah S. Diffenbaugh (2015). "A Multi-Model and Multi-Index Evaluation of Drought Characteristics in the 21st Century". In: *Journal of Hydrology* 526, pp. 196–207.

Van Vuuren, Detlef P, Elmar Kriegler, Brian C. O'Neill, Kristie L. Ebi, Keywan Riahi, Timothy R. Carter, Jae Edmonds, Stephane Hallegatte, Tom Kram, Ritu Mathur, and Harald Winkler (2014). "A New Scenario Framework for Climate Change Research: Scenario Matrix Architecture". In: *Climatic Change* 122.3, pp. 373–386. ISSN: 0165-0009. DOI: 10.1007/s10584-013-0906-1. URL: https://dx.doi.org/10.1007/s10584-013-0906-1.

Verseghy, Diana L. (Mar. 2000). "The Canadian Land Surface Scheme (CLASS): Its History and Future". In: *Atmosphere-Ocean* 38.1, pp. 1–13. ISSN: 0705-5900, 1480-9214. DOI: 10.1080/07055900.2000.9649637. URL: http://www.tandfonline.com/doi/abs/10.1080/07055900.2000.9649637 (visited on 12/13/2021).

Vicente-Serrano, Sergio M., Santiago Beguería, and Juan I. López-Moreno (Apr. 2010). "A Multiscalar Drought Index Sensitive to Global Warming: The Standardized Precipitation Evapotranspiration Index". In: *Journal of Climate* 23.7, pp. 1696–1718. ISSN: 0894-8755, 1520-0442. DOI: 10.1175/2009JCLI2909.1. URL: http://journals.ametsoc.org/doi/10.1175/2009JCLI2909.1 (visited on 01/06/2020).

Vicente-Serrano, Sergio M., Gerard Van der Schrier, Santiago Beguería, Cesar Azorin-Molina, and Juan-I. Lopez-Moreno (July 2015). "Contribution of Precipitation and Reference Evapotranspiration to Drought Indices under Different Climates". In: *Journal of Hydrology* 526, pp. 42–54. ISSN: 00221694. DOI: 10.1016/j.jhydrol.2014.11.025. URL: https://linkinghub.elsevier.com/retrieve/pii/S0022169414009305 (visited on 03/27/2022).

Virtanen, Pauli, Ralf Gommers, Travis E. Oliphant, Matt Haberland, Tyler Reddy, David Cournapeau, Evgeni Burovski, Pearu Peterson, Warren Weckesser, Jonathan Bright, Stéfan J. van der Walt, Matthew Brett, Joshua Wilson, K. Jarrod Millman, Nikolay Mayorov, Andrew R. J. Nelson, Eric Jones, Robert Kern, Eric Larson, C J Carey, İlhan Polat, Yu Feng, Eric W. Moore, Jake VanderPlas, Denis Laxalde, Josef Perktold, Robert Cimrman, Ian Henriksen, E. A. Quintero, Charles R. Harris, Anne M. Archibald, Antônio H. Ribeiro, Fabian Pedregosa, Paul van Mulbregt, and SciPy 1.0 Contributors (2020). "SciPy 1.0: Fundamental Algorithms for Scientific Computing in Python". In: *Nature Methods* 17, pp. 261–272. DOI: 10.1038/s41592-019-0686-2.

Wartenburger, Richard, Martin Hirschi, Markus G. Donat, Peter Greve, Andy J. Pitman, and Sonia I. Seneviratne (2017). "Changes in Regional

Climate Extremes as a Function of Global Mean Temperature: An Interactive Plotting Framework". In: *Geoscientific Model Development* 10.9, pp. 3609–3634.

Weigel, Katja, Lisa Bock, Bettina K. Gier, Axel Lauer, Mattia Righi, Manuel Schlund, Kemisola Adeniyi, Bouwe Andela, Enrico Arnone, Peter Berg, Louis-Philippe Caron, Irene Cionni, Susanna Corti, Niels Drost, Alasdair Hunter, Llorenç Lledó, Christian Wilhelm Mohr, Aytaç Paçal, Núria Pérez-Zanón, Valeriu Predoi, Marit Sandstad, Jana Sillmann, Andreas Sterl, Javier Vegas-Regidor, Jost Von Hardenberg, and Veronika Eyring (2021). "Earth System Model Evaluation Tool (ESMValTool) v2.0 – Diagnostics for Extreme Events, Regional and Impact Evaluation and Analysis of Earth System Models in CMIP". In: DOI: 10.5194/gmd-2020-244. URL: https://dx.doi.org/10.5194/gmd-2020-244.

Wells, Nathan, Steve Goddard, and Michael J Hayes (2004). "A Self-Calibrating Palmer Drought Severity Index". In: *JOURNAL OF CLIMATE* 17, p. 17.

Wilhite, Donald (Jan. 2000). "Chapter 1 Drought as a Natural Hazard: Concepts and Definitions". In: *Drought Mitigation Center Faculty Publications*. URL: https://digitalcommons.unl.edu/droughtfacpub/69.

Wilhite, Donald A and Michael H Glantz (1985). "Understanding: The Drought Phenomenon: The Role of Definitions". In: *Water International*, p. 11.

Williams, A. Park, Edward R. Cook, Jason E. Smerdon, Benjamin I. Cook, John T. Abatzoglou, Kasey Bolles, Seung H. Baek, Andrew M. Badger, and Ben Livneh (Apr. 2020). "Large Contribution from Anthropogenic Warming to an Emerging North American Megadrought". In: *Science* 368.6488, pp. 314–318. ISSN: 0036-8075, 1095-9203. DOI: 10.1126/science.aaz9600. URL: https://www.science.org/doi/10.1126/science.aaz9600 (visited on 03/27/2022).

Xu, Lei, Nengcheng Chen, and Xiang Zhang (2019). "Global Drought Trends under 1.5 and 2 C Warming". In: *International Journal of Climatology* 39.4, pp. 2375–2385.

Yukimoto, Seiji, Hideaki Kawai, Tsuyoshi Koshiro, Naga Oshima, Kohei Yoshida, Shogo Urakawa, Hiroyuki Tsujino, Makoto Deushi, Taichu Tanaka, Masahiro Hosaka, Shokichi Yabu, Hiromasa Yoshimura, Eiki Shindo, Ryo Mizuta, Atsushi Obata, Yukimasa Adachi, and Masayoshi Ishii (2019). "The Meteorological Research Institute Earth System Model Version 2.0, MRI-ESM2.0: Description and Basic Evaluation of the Physical Component". In: *Journal of the Meteorological Society of Japan. Ser. II* 97.5, pp. 931–965. ISSN: 0026-1165, 2186-9057. DOI: 10.2151/jmsj.2019-051. URL: https://www.jstage.jst.go.jp/article/jmsj/97/5/97_2019-051/_article (visited on 01/14/2022).

Ziehn, Tilo, Matthew A. Chamberlain, Rachel M. Law, Andrew Lenton, Roger W. Bodman, Martin Dix, Lauren Stevens, Ying-Ping Wang, and Jhan Srbinovsky (Aug. 2020). "The Australian Earth System Model:

ACCESS-ESM1.5". In: *Journal of Southern Hemisphere Earth Systems Science* 70.1, pp. 193–214. ISSN: 2206-5865. DOI: 10.1071/ES19035. URL: https://www.publish.csiro.au/es/ES19035 (visited on 01/13/2022).

Zotarelli, Lincoln, Michael D Dukes, Consuelo C Romero, and Kati W Migliaccio (2010). "Step by Step Calculation of the Penman-Monteith Evapotranspiration (FAO-56 Method)". In: p. 10.

Universität Bremen

Nachname **Ruhe** Matrikelnr. **2725124**

Vorname/n **Lukas**

A) Eigenständigkeitserklärung

Ich versichere, dass ich die vorliegende Arbeit selbstständig verfasst und keine anderen als die angegebenen Quellen und Hilfsmittel verwendet habe.
Alle Teile meiner Arbeit, die wortwörtlich oder dem Sinn nach anderen Werken entnommen sind, wurden unter Angabe der Quelle kenntlich gemacht. Gleiches gilt auch für Zeichnungen, Skizzen, bildliche Darstellungen sowie für Quellen aus dem Internet.
Die Arbeit wurde in gleicher oder ähnlicher Form noch nicht als Prüfungsleistung eingereicht.
Die elektronische Fassung der Arbeit stimmt mit der gedruckten Version überein.
Mir ist bewusst, dass wahrheitswidrige Angaben als Täuschung behandelt werden.

B) Erklärung zur Veröffentlichung von Bachelor- oder Masterarbeiten

Die Abschlussarbeit wird zwei Jahre nach Studienabschluss dem Archiv der Universität Bremen zur dauerhaften Archivierung angeboten. Archiviert werden:

1) Masterarbeiten mit lokalem oder regionalem Bezug sowie pro Studienfach und Studienjahr 10 % aller Abschlussarbeiten
2) Bachelorarbeiten des jeweils ersten und letzten Bachelorabschlusses pro Studienfach u. Jahr.

☑ Ich bin damit einverstanden, dass meine Abschlussarbeit im Universitätsarchiv für wissenschaftliche Zwecke von Dritten eingesehen werden darf.

☐ Ich bin damit einverstanden, dass meine Abschlussarbeit nach 30 Jahren (gem. §7 Abs. 2 BremArchivG) im Universitätsarchiv für wissenschaftliche Zwecke von Dritten eingesehen werden darf.

☐ Ich bin nicht damit einverstanden, dass meine Abschlussarbeit im Universitätsarchiv für wissenschaftliche Zwecke von Dritten eingesehen werden darf.

C) Einverständniserklärung über die Bereitstellung und Nutzung der Bachelorarbeit / Masterarbeit / Hausarbeit in elektronischer Form zur Überprüfung durch Plagiatssoftware

Eingereichte Arbeiten können mit der Software *Plagscan* auf einen hauseigenen Server auf Übereinstimmung mit externen Quellen und der institutionseigenen Datenbank untersucht werden.
Zum Zweck des Abgleichs mit zukünftig zu überprüfenden Studien- und Prüfungsarbeiten kann die Arbeit dauerhaft in der institutionseigenen Datenbank der Universität Bremen gespeichert werden.

☐ Ich bin damit einverstanden, dass die von mir vorgelegte und verfasste Arbeit zum Zweck der Überprüfung auf Plagiate auf den *Plagscan*-Server der Universität Bremen hochgeladen wird.
Ich bin ebenfalls damit einverstanden, dass die von mir vorgelegte und verfasste Arbeit zum o.g. Zweck auf
☐ dem *Plagscan*-Server der Universität Bremen hochgeladen u. dauerhaft auf dem *Plagscan*-Server gespeichert wird.

☑ Ich bin nicht damit einverstanden, dass die von mir vorgelegte u. verfasste Arbeit zum o.g. Zweck auf dem *Plagscan*-Server der Universität Bremen hochgeladen u. dauerhaft gespeichert wird.

Mit meiner Unterschrift versichere ich, dass ich die oben stehenden Erklärungen gelesen und verstanden habe.
Mit meiner Unterschrift bestätige ich die Richtigkeit der oben gemachten Angaben.

28.02.2022

Datum Unterschrift